ORGANO BORONATES, PHOSPHATES, AND SULFATES SYNTHESIZED BY FLUORIDE EXCHANGE REACTION AND THEIR TRANSESTERIFICATION REACTIONS IN ETHYLENE-VINYL ALCOHOL VITRIMERS

by

YUTIAN KE

(Under the Direction of Jason Locklin)

ABSTRACT

The second-generation click chemistry, sulfur-fluoride exchange (SuFEx) reaction was established on the silicon centers can activate the exchange of S-F bonds for S-O bonds. We found phosphorus-fluoride and boron-fluoride bonds are reactive as well. This work first proved boron-fluoride exchange reaction (BorFEx) by a set of small molecule studies. Difluoroborane (R-BF_2), generated *via in situ* from trifluoroborates (R-BF_3K), was able to react with bis silyl ethers and form stable cyclic boronic esters. Then we found one particular application for BorFEx in polymer synthesis. Vitrimer is nowadays a hot topic in polymeric research area. Thermosets usually have a better mechanical property and solvent, thermal resistance rather than thermoplastics. Conversely, thermoplastics have the recyclability to be deformed and processed multiple times. We used BorFEx to design a vitrimer with cyclic boronic esters on the backbone and proved it has great mechanical properties and reprocessability as well. Coincidentally, transesterification reaction on

dialkyl phosphite was found to be another excellent dynamic covalent exchange reaction catalyzed by organic bases, while we explored the possibility of the phosphorus-fluoride exchange reaction. Herein, we introduce dialkyl phosphite as a dynamic cross-linker in the polymeric network, which performs the exchange reaction with hydroxyl groups on poly(ethylene-co-vinyl alcohol) (EVOH) backbone through nucleophilic substitution transesterification. The vitrimer samples were proved to be thermally stable, and certain blends of EVOH and vitrimer successfully melt-processed in an extruder on a large scale.

INDEX WORDS: SuFEx, Click Chemistry, BorFEx, Vitrimer, Dynamic Cross-linked Network, EVOH, Dialkyl Phosphite, Transesterification reaction, Extrusion.

ORGANO BORONATES, PHOSPHATES AND SULFATES SYNTHESIZED BY FLUORIDE EXCHANGE REACTION AND THEIR TRANSESTERIFICATION REACTIONS IN ETHYLENE VINYL ALCOHOL VITRIMERS

by

YUTIAN KE

BS, SHANGHAI JIAOTONG UNIVERSITY, CHINA, 2013

MS, UNIVERISITY OF AKRON, 2015

A Dissertation Submitted to the Graduate Faculty of the University of Georgia in Partial Fulfillment of the Requirements for the Degree

DOCTOR OF PHILOSOPHY

ATHENS, GEORGIA

2021

ORGANO BORONATES, PHOSPHATES AND SULFATES SYNTHESIZED BY FLUORIDE EXCHANGE REACTION AND THEIR TRANSESTERIFICATION REACTIONS IN ETHYLENE VINYL ALCOHOL VITRIMERS

by

YUTIAN KE

Major Professor: Jason Locklin

Committee: Robert S. Phillips
Vladimir Popik

Electronic Version Approved:

Ron Walcott
Dean of the Graduate School
The University of Georgia
August 2021

ACKNOWLEDGEMENTS

I would like to thank Dr. Locklin. He is not only an academic advisor but also a friend. He encouraged and supported me in exploring the chemistry world freely. His enthusiasm for scientific research is infectious and inspires everyone to overcome obstacles. I also want to thank my committee members, Dr. Robert S. Phillips, and Dr. Vladimir Popik. They broadened my sight on considering questions and helped me to find other ways to solve problems. I also want to thank all my former and current group members, Dr. Jeremy Yatvin, Dr. Anandi Roy, Dr. Jing Gao, Dr. Karson Brooks, Dr. Li Chen, Dr. Qiaohong Liu, Dr. Apisata Holt, Tim Henkel, Dr. Evan White, Dr. Scott Tull, Dr. Jessica Bramhall, Grant Crane, Jessica Horn, Demichael Winfield, Caitlin Cato, Joshua Bledsoe, Ethan Stinchcomb, Ryan Maynard, Michael Broich, Virginia Weber, Jarod Wolffis, Jessica Drewke. You all helped me a lot. It was a pleasure to work with all of you. Finally, I want to thank my girlfriend Chen Zhao, we both can do it!

TABLE OF CONTENT

Page

LIST OF SCHEMES

Page

LIST OF FIGURES

Page

LIST OF TABLES

Page

CHAPTER 1

INTRODUCTION OF SUFEX

1.01 Recent developed click chemistry

Click Chemistry (CC) is a term invented by K. B. Sharpless in 2001. Reactions with ultra-high yield and super-rapid rate can be defined as CC. CC has had a dominant impact on modern chemistry and is widely used in the conjugation of biological substrates with specific biomolecules. [1]

"Reactivity isn't everything; it's the only thing" ---K. B. Sharpless

Recently, the ultra-high reactivity of CC has accelerated the synthesis of new pharmaceuticals. The discovery of new CC gives more possibilities for molecule building, which is a goal for many chemists. Actually, CC is governed by a fundamental rule: *"all searches must be restricted to molecules that are easy to make."* Nature creates the biomolecules by bond formation between carbon-heteroatom or heteroatom–heteroatom, which gives us the most important hint to finding fast and affective reactions.

Cu(I) catalyzed azide-alkyne cycloaddition (CUAAC)[2] is one of the greatest discoveries in this century, not only in chemistry but also in biology and pharmacy. The two building blocks of CUAAC are a terminal alkyne and an organic azide, which react

quickly when catalyzed by Cu(I) catalyst under a moderate environment. Finally, it forms a 1,4-triazole linkage and combines into one molecule (Scheme 1.01A). The metal catalyst is essential in CUAAC, which potentially limits this reaction's application in biology and drug discovery.

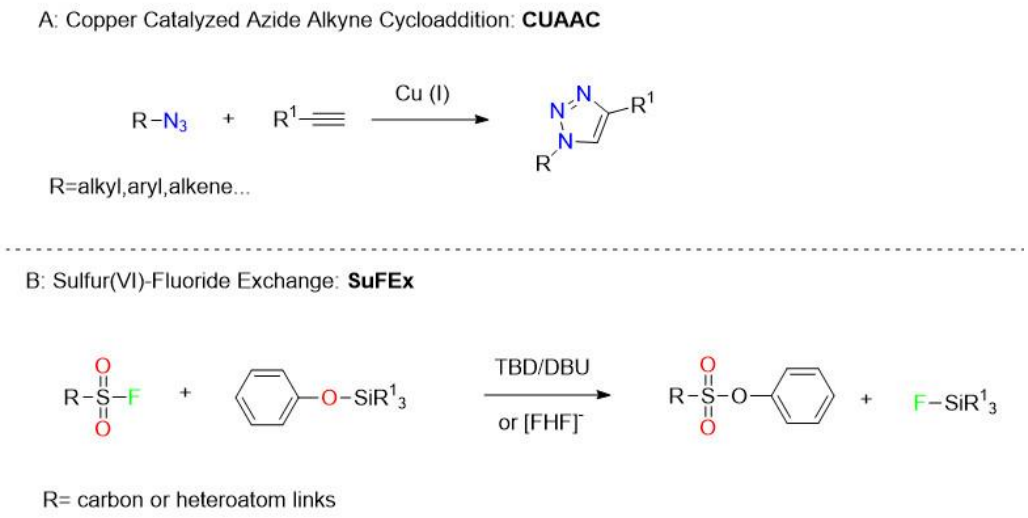

Scheme 1.01. (A) Copper-Catalyzed Azide-Alkyne Cycloaddition (CUAAC); (B) Sulfur(VI)-Fluoride Exchange (SuFEx)

Sulfur (VI)-Fluoride Exchange (SuFEx) was discovered by Sharpless and his co-workers in 2014, and since then, much work has been done to analyze organosulfur fluorides. Surprisingly, S–F bonds are more stable than common S-Cl bonds, even under harsh conditions, like high temperature or super moisture. However, the reactivity of nucleophilic S–F exchange is ultra-fast with proper controls (Scheme 1.01B). Aromatic silyl ethers and S-F bond can be activated by a nitrogen-containing strong base (TBD, DBU,

etc.) or a bifluoride anion $[FHF]^-$ catalyst to form a sulfonate ester as the desired product and a super stable Si-F bond containing compound as the side product. The bond energy of Si-F is very high, which is the possible driving force for the reaction and potentially the reason for such incredible reactivity. The reaction mechanisms behind SuFEx catalysis are not fully understood, though SuFEx reactions are widely used and look straightforward. Compared to CUAAC, metal-free SuFEx has a significant advantage in biological applications.

1.02. SuFEx building blocks and recent research focuses

A widely used reaction should have easy-to-make starting materials. Aromatic silyl ethers are common in chemistry. However, S-F bond-containing compounds are rarely seen in nature. Actually, sulfonyl fluorides and fluorosulfates are easy to synthesize within several steps. Researchers are now focusing on finding various ways to synthesize unique SuFEx building blocks, which contain S-F bonds.

Sulfonyl fluorides (R-SO_2F) Both aryl and alkyl sulfonyl fluorides rapidly undergo SuFEx reactions. Sulfonyl chloride synthesized from sodium sulfate salt is ubiquitous in organic chemistry. Organic sodium sulfate salts (**2**) can be efficiently reacted with thionyl chloride or phosphorus pentachloride at reflux temperature. The most common synthesis of sulfonyl fluorides is through the direct exchange of a sulfonyl chloride with a proper fluoride source (Scheme 1.02). A diphase of a protic solvent, such as acetonitrile or

acetone, and saturated potassium hydrogen bifluoride (KFHF) in water, can easily convert sulfonyl chlorides (**3**) to sulfonyl fluorides (**1**).[3]

By Cl-F exchanging of 2-chloroethenesulfonyl chloride (**4**) and dehydrochlorination of 2-chloroethanesulfonyl fluoride (**5**), Ethene sulfonyl fluoride (ESF) (**6**) can be prepared on a kilogram scale. ESF (**6**) is one of the best building blocks in SuFEx because it offers two different kinds of reactivity. In addition to the sulfonyl fluoride group, ESF (**6**) provides another connection with phenols, alcohols, and amines by Michael addition in mild conditions. Sharpless claims it as *"the most perfect Michael acceptor ever found"* .[4]

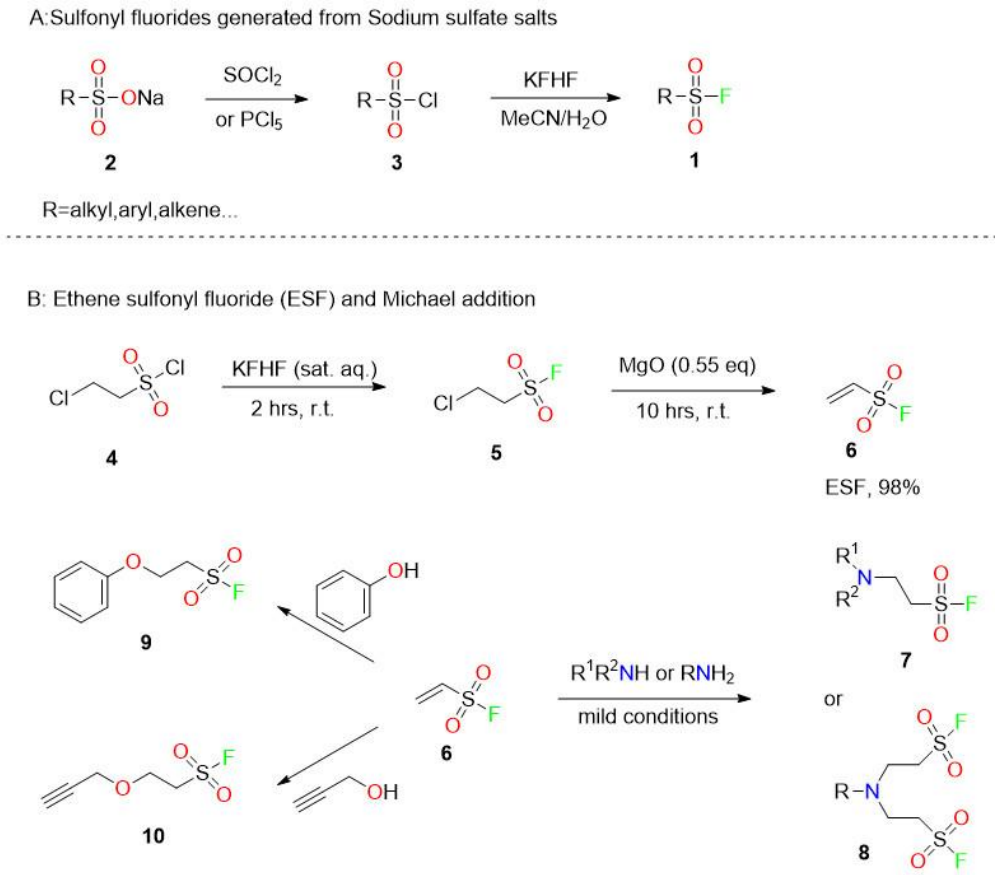

Scheme 1.02. (A) Sulfonyl fluorides synthesized from organic sodium sulfate salts (B)

Ethene sulfonyl fluoride (ESF) synthesis and Michael addition

Besides ESF (**6**), there are a lot of recent works focusing on bifunctional click reagents, such as 1-Bromoethene-1-sulfonyl fluoride (BESF)[5] and 2-Azidoethane-1-sulfonylfluoride (ASF)[6], are not going to be discussed detailly here.

Fluorosulfates (Ar-OSO_2F) Fluorosulfates (**13**) are usually synthesized by a diphase reaction between sulfuryl fluoride (SO_2F_2) gas (**12**) and phenol (**11**) solution with a tertiary amine (Scheme 1.03A). SO_2F_2 is a colorless, odorless gas at room temperature, which is commonly used as a pest control agent in Asia, with a large global production. Almost all kinds of aromatic -OH can react with the gas easily in aprotic solvents, such as THF and acetonitrile.

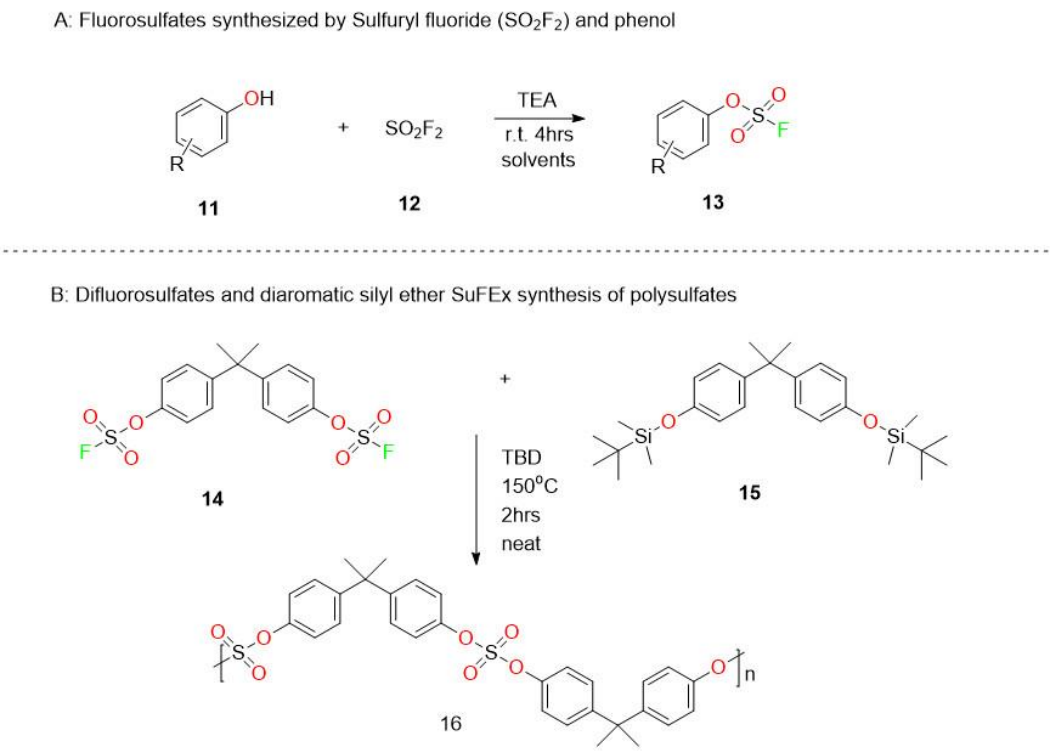

Scheme 1.03. (A) Fluorosulfates synthesized by Surlfuryl fluoride gas (B) Bisphenol A (BPA) derivative Polysulfates synthesis by SuFEx

Based on the high reactivity, the application of SuFEx is not limited to small molecules click conjugation. High molecular weight polysulfates can be achieved through polycondensation SuFEx. Bisphenol A (BPA) derivatives, bis (aryl fluorosulfates) (**14**), were melted together with bis (aryl silyl ethers) (**15**) in the presence of SuFEx catalysts at a high temperature to boil off the TBSF byproduct. Further purification is done by precipitating in methanol to yield white plastic textile polysulfates (**16**) (Scheme 1.03B). Comparing to BPA-polycarbonate, BPA-polysulfate has a more significant resistance to both heat and moisture.

1.03 Other SuFEx related researches

Considerable research efforts have been devoted to post-polymerization modification on polymer brushes through SuFEx reaction in our group,[7-9] Averick's group[10] and Chen's group.[11] Recently, SuFEx reaction has greatly impacted modern chemistry and is widely used in biological conjugation[12] of substrates with specific biomolecules.[13-14]

1.04 Si-electron withdrawing group SuFEx reactions

Although there are many chemists focused on the topic of SuFEx, most of the publications focus on discovering new pathways to synthesize different types of S-F bonds. However, people rarely do research on the other starting material, aromatic silyl ether. Theoretically, the driving force of SuFEx reaction should be ultra-stability of Si-F byproduct leaving as TMS-F or TBDMS-F, any other functional group connects with silyl group have a chance to undergo a similar process as SuFEx does. John E. Moses published an article[15] to discuss the reaction between sulfonyl fluorides and trimethylsilyl azide (TMS-N_3), which concluded that it works perfectly (high yields) with excess azide (1.5eq TMS-N_3) and 30%(mol) DBU as a catalyst in an aprotic solvent, such as acetonitrile and THF. This work motivated me to try different TMS derivatives to see whether there is any other Si-electron withdrawing group compound that could possibly undergo a SuFEx reaction (Scheme 1.04). The heteroatom bonded with Si is not limited to oxygen; some

silyl amides, like TMS-imidazole (**18**), have wonderful yields (>98%) with both base and $[FHF]^-$catalysts. TMS-N_3 (**19**) also works with both catalysts; in addition to an excess amount of azide needed in DBU catalyst, bifluoride anion catalyst can accelerate the reactants with stoichiometry.

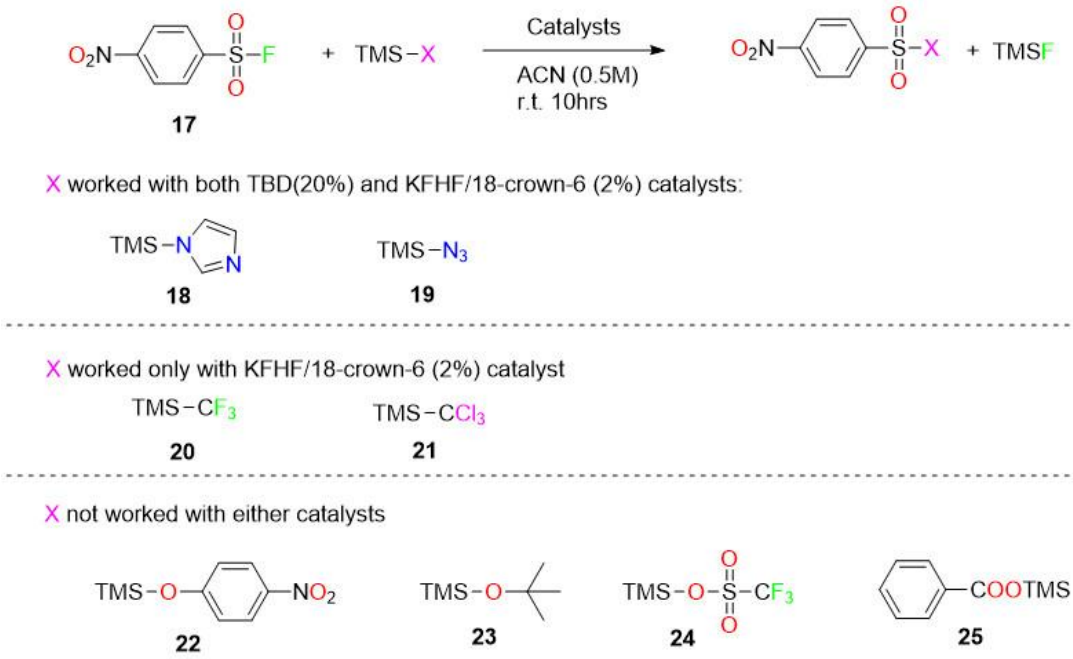

Scheme 1.04. Different Si-electron withdrawing group SuFEx reaction possibility under certain conditions (0.5M in acetonitrile, room temperature, 10hrs, 20 mol% TBD or 2 mol% KFHF/18-crown-6 as catalysts)

When it comes to a strong withdrawing group on the opposite position to aryl silyl ether, like nitro group (**22**), only the hydrolysis product, p-nitrophenol, crashed out as the final product. SuFEx S-O bond formation may be interrupted by the strong inductive and

resonance effect on the benzene ring. Unlike primary and secondary alkyl silyl ethers, tertiary silyl ether (**23**) will never react with sulfonyl fluorides or fluorosulfates, neither at a high temperature nor large catalysts feeding. TMS sulfate (24) and TMS benzoate (**25**) both failed at SuFEx tests, mostly because of the instability of the desired sulfate anhydride products.

The most exciting discovery in this attempt is both TMS-CF_3 (**20**), and TMS-CCl_3 (**21**) follow the SuFEx rule incredibly. Although several undefined byproducts show up in the reaction with TBD/DBU as the catalyst, bifluoride anion catalyst 2% (mol) gives a relatively high yield (>90%) for both at room temperature, stirring overnight in acetonitrile. The hypothesis is that strong electron-withdrawing groups may help to facilitate the SuFEx process.

Unfortunately, when we were preparing to wrap up my experiments and write a potential paper, Moses and co-workers[16] published a SuFEx trifluoromethylation of sulfonyl fluorides (**26**) and iminosulfur oxydifluorides (**28**) to get triflones (**27**) and bis(trifluoromethyl)sulfur oxyimines (**29**) (Scheme 1.05A and B). They chose another aprotic solvent, anhydrous DMSO, which lead to similar results and reactivity as compared to my findings.

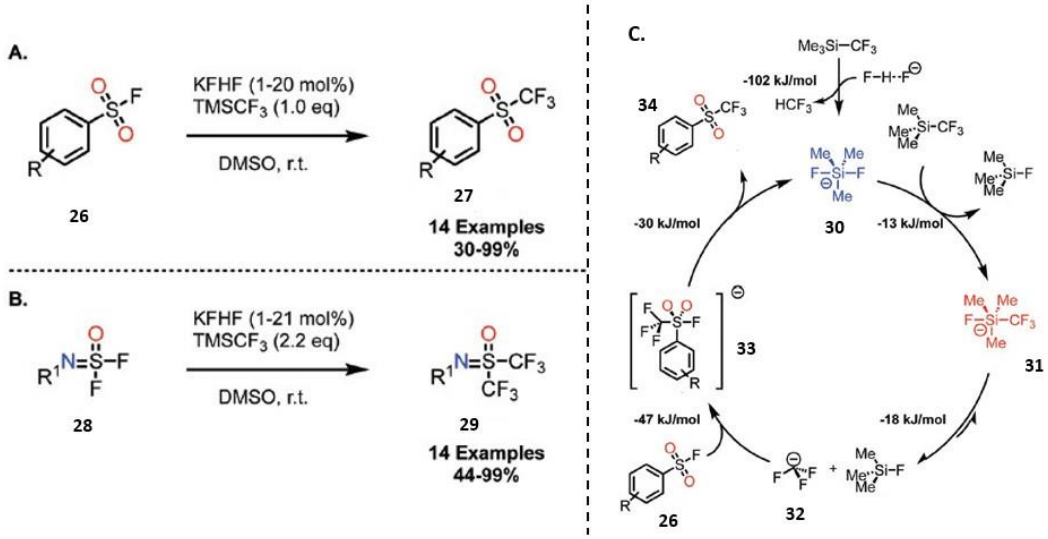

Scheme 1.05. Synthesis of (A) aryl triflones (**27**); (B) bis(trifluoromethyl)sulfur oxyimines (**28**); (C) Gibbs energy calculated mechanism for the conversion of sulfonyl fluorides (**26**) to triflone (**27**).

Moses and co-workers proposed a mechanism (Scheme 1.05C), which is supported by molecular modeling Gibbs energy calculation. The reaction initiates by mixing bifluoride anion with TMS-CF_3, forms a hypervalent silicon center anion (**30**). Following by converting to another intermediate (**31**), which can reversibly dissociate into the free $[CF_3]^-$ anion (**32**) and stable TMS-F, [10] releasing from the system because of the low boiling point. Free $[CF_3]^-$ anion (**32**) can nucleophilic attack the sulfur center of sulfonyl fluoride and get the final product triflone (**27**). The only piece which confused me a lot is the appearance of HCF_3 acid. There is no HCF_3 peak shows up in ^{19}F NMR spectrums based on my attempts.

1.05 SuFEx trichloromethylation

Herein, we followed the SuFEx procedure to efficiently synthesize trichlones (CCl_3SO_2-) and trichloromethyl sulfates (CCl_3SO_3-) from sulfonyl fluorides and fluorosulfates, which both have potential applications in pharmacy. The experiment involves S-F exchange with trichloromethyltrimethylsilane (TMS-CCl_3) catalysis by bifluoride anion $[FHF]^-$ in anhydrous aprotic solvents. Multiple substrates, including some polymer starting materials, are going to be processed.

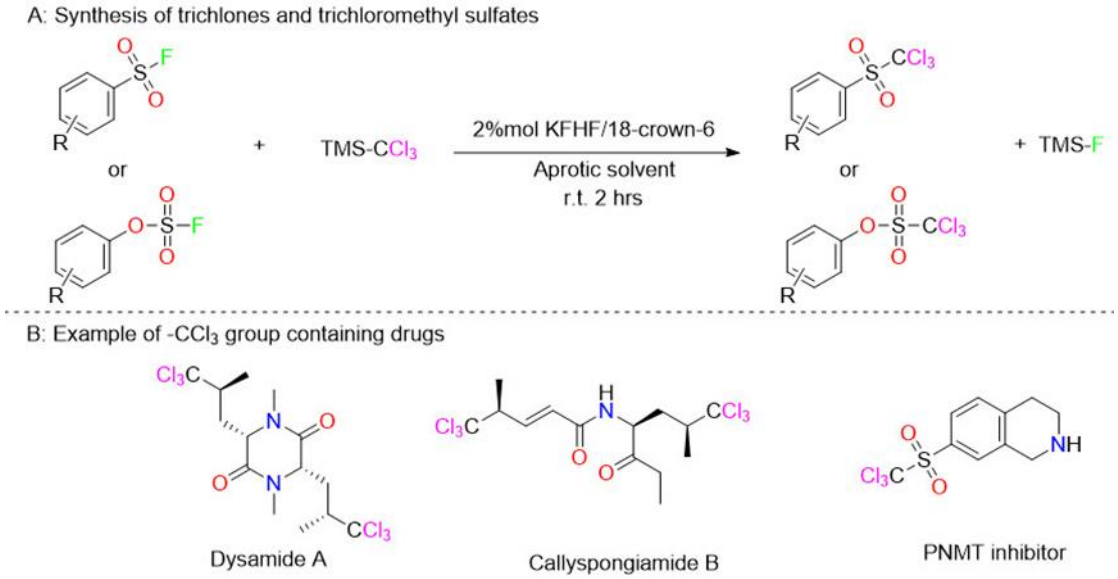

Scheme 1.06. (A) SuFEx trichloromethylation overview; (B) Drugs that contain the trichloromethyl group.

Although Moses and co-workers got the publication on TMS-CF_3, the puzzle of TMS-

CCl_3 is still waiting to be solved. Both are strong electron-withdrawing groups, but three chlorines have larger steric hindrance than three fluorines, which may cause different reaction rates or help elucidate the SuFEx mechanism.

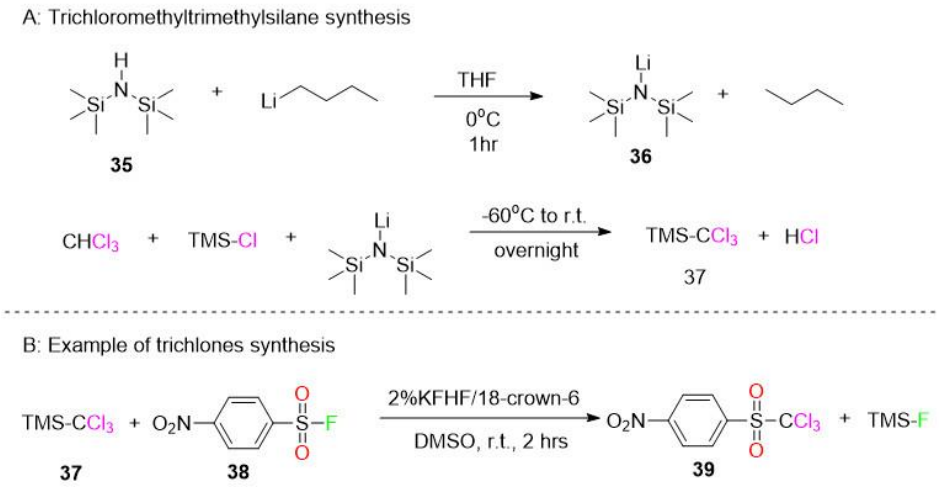

Scheme 1.07. (A) Synthesis of Trichloromethyltrimethylsilane (**27**); (B) One example of synthesized aryl trichlone condition.

Trichloromethyltrimethylsilane ($TMS-CCl_3$)[17] (Scheme 1.07A)

In a 100 mL 2-neck round bottom flask, under vacuum and refilled N_2 three times, HMDS (**35**) (0.02 mol, 4.2 mL) was dissolved in 4 mL of dried THF. An ice bath was used to cool the solution to0 ºC. *n*-BuLi (1.6 M in hexane, 0.02 mol, 13 mL) was injected into the flask, and the solution was stirred at 0 ºC for 1 hour. In a Schlenk flask, also under vacuum and refilled N_2 three times, chloroform (0.03 mol, 2.4 mL) was added to TMSCl (0.1 mol, 12.5 mL) at -78 ºC (Acetone/dry ice bath). The solution of LiHMDS (**36**) was

then added dropwise to the $CHCl_3$/TMSCl mixture via a cannula. The solution was warmed up slowly to room temperature overnight. The solution was poured into 100 g ice, HCl gas was released from the system spontaneously. After being extracted with hexane (2 times), the combined organic solution was dried with anhydrous $MgSO_4$, filtered, and concentrated by rotary evaporation. The crude product was purified by vacuum distillation, and a white crystalline solid was obtained (2.80 g, 72%) TMS-CCl_3 (**37**). ^{1}H NMR (400.1 MHz, $CDCl_3$) δ = 0.37 (s, 9 H), ^{13}C NMR (100.6 MHz, CDCl3) δ = -3.87, 95.41.

General procedure for trichlones and trichloromethyl sulfates synthesis

In a Schlenk flask, under vacuum and refilled N_2 three times, desired sulfonyl fluoride or fluorosulfate (0.1mol) and TMS-CCl_3 (0.1 mol) were dissolved in 2 mL anhydrous acetonitrile or DMSO at room temperature. KFHF (0.002 mol) and 18-crown-6 (0.002 mol) were added into the flask through a positive N_2 flow. The solution was allowed to stir at room temperature for 2 hours. After checked TLC to confirm total conversion, the product was simply dried in *vacuo*, or a flash chromatography was applied to remove impurities. Usually, white solids were achieved with a relatively high yield.

p-Nitrobenzene trichlone was listed here (Scheme 1.07B) as an example. It was a white solid, yield 90% after a flash column (EA/Hex=1:4, Rf=0.30). ^{1}H NMR (400 MHz, CDCl3) δ 8.49 (d, J = 8.7 Hz, 2H), 8.27 (d, J = 8.8 Hz, 2H); ^{13}C NMR (101 MHz, CDCl3) δ 136.96, 132.88, 124.27, 118.24, 79.57 (CCl_3); FTIR (KBr) ν_{max} 2970, 1530, 1340, 1080, 851, 793.

1.06 Computational simulation of Gibbs energy in SuFEx

On the other hand, we cooperated with Dr. Wheeler's group to get some calculation support. Comparing $TMSCCl_3$ to $TMSCF_3$, Gibbs energy of the conversions between hypervalent silicon center intermediates should be totally different. Even if the tendency of calculation is different, a new mechanism of SuFEx may be proposed by this study. Unfortunately, both the stability of intermediate and overall thermodynamics were not able to conclude a united rule for SuFEx reactions.

1.07 Reference

1. Thirumurugan, P.; Matosiuk, D.; Jozwiak, K., Click Chemistry for Drug Development and Diverse Chemical–Biology Applications. *Chemical Reviews* **2013,** *113* (7), 4905-4979.

2. Rostovtsev, V. V.; Green, L. G.; Fokin, V. V.; Sharpless, K. B., A Stepwise Huisgen Cycloaddition Process: Copper(I)-Catalyzed Regioselective "Ligation" of Azides and Terminal Alkynes. *Angewandte Chemie International Edition* **2002,** *41* (14), 2596-2599.

3. Dong, J.; Krasnova, L.; Finn, M. G.; Sharpless, K. B., Sulfur(VI) Fluoride Exchange (SuFEx): Another Good Reaction for Click Chemistry. *Angewandte Chemie International Edition* **2014,** *53* (36), 9430-9448.

4. Chen, Q.; Mayer, P.; Mayr, H., Ethenesulfonyl Fluoride: The Most Perfect Michael Acceptor Ever Found? *Angew Chem Int Ed Engl* **2016,** *55* (41), 12664-12667.

5. Smedley, C. J.; Giel, M.-C.; Molino, A.; Barrow, A. S.; Wilson, D. J. D.; Moses, J. E., 1-Bromoethene-1-sulfonyl fluoride (BESF) is another good connective hub for SuFEx click chemistry. *Chemical Communications* **2018,** *54* (47), 6020-6023.

6. Zhang, X.; Moku, B.; Leng, J.; Rakesh, K. P.; Qin, H.-L., 2-Azidoethane-1-sulfonylfluoride (ASF): A Versatile Bis-clickable Reagent for SuFEx and CuAAC Click Reactions. *European Journal of Organic Chemistry* **2019,** *2019* (8), 1763-1769.

7. Yatvin, J.; Brooks, K.; Locklin, J., SuFEx on the Surface: A Flexible Platform for Postpolymerization Modification of Polymer Brushes. *Angewandte Chemie International*

Edition **2015,** *54* (45), 13370-13373.

8. Yatvin, J.; Brooks, K.; Locklin, J., SuFEx Click: New Materials from SOxF and Silyl Ethers. *Chemistry – A European Journal* **2016,** *22* (46), 16348-16354.

9. Brooks, K.; Yatvin, J.; Kovaliov, M.; Crane, G. H.; Horn, J.; Averick, S.; Locklin, J., SuFEx Postpolymerization Modification Kinetics and Reactivity in Polymer Brushes. *Macromolecules* **2018,** *51* (2), 297-305.

10. Li, S.; Beringer, L. T.; Chen, S.; Averick, S., Combination of AGET ATRP and SuFEx for post-polymerization chain-end modifications. *Polymer* **2015,** *78*, 37-41.

11. Liu, W.; Dong, Y.; Zhang, S.; Wu, Z.; Chen, H., A rapid one-step surface functionalization of polyvinyl chloride by combining click sulfur(vi)-fluoride exchange with benzophenone photochemistry. *Chemical Communications* **2019,** *55* (6), 858-861.

12. Barrow, A. S.; Smedley, C. J.; Zheng, Q.; Li, S.; Dong, J.; Moses, J. E., The growing applications of SuFEx click chemistry. *Chemical Society Reviews* **2019,** *48* (17), 4731-4758.

13. Qinheng, Z.; Jordan L., W.; Seiya, K.; Diogo, S.-M.; Christopher J., S.; Gencheng, L.; Stefano, F.; John E., M.; Dennis W., W.; K. Barry, S., *"Sleeping Beauty" Phenomenon: SuFEx-Enabled Discovery of Selective Covalent Inhibitors of Human Neutrophil Elastase*. 2019.

14. Seiya, K.; Qinheng, Z.; Jordan L., W.; angelo, s.; Emily, C.; Nicholas, D.; Mitchell,

H.; Miyako, K.; Shinichi, K.; Victor, N.; K. Barry, S.; Dennis, W., *SuFEx-Enabled High-Throughput Medicinal Chemistry*. 2019.

15. Barrow, A. S.; Moses, J. E., Synthesis of Sulfonyl Azides via Lewis Base Activation of Sulfonyl Fluorides and Trimethylsilyl Azide. *Synlett* **2016,** *27* (12), 1840-1843.

16. Smedley, C. J.; Zheng, Q.; Gao, B.; Li, S.; Molino, A.; Duivenvoorden, H. M.; Parker, B. S.; Wilson, D. J. D.; Sharpless, K. B.; Moses, J. E., Bifluoride Ion Mediated SuFEx Trifluoromethylation of Sulfonyl Fluorides and Iminosulfur Oxydifluorides. *Angewandte Chemie International Edition* **2019,** *58* (14), 4552-4556.

17. Wahl, B.; Lee, D. S.; Woodward, S., 1,4-Addition of TMSCCl3 to (E)-Fumaric Esters and Thermal Rearrangement of the Adducts to 3,4-Dichloropent-2-enedioates. *European Journal of Organic Chemistry* **2015,** *2015* (27), 6033-6039.

CHAPTER 2

PHOSPHORUS-FLUORIDE AND BORON-FLUORIDE EXCHANGE REACTION

2.01 Phosphorus-Fluoride Exchange Reaction (PhoFEx)

Although the P-F bond energy (490 kJ/mol) is much higher than the S-F bond energy (284 kJ/mol), P-F has been proved extremely reactive. Diethylfluorophosphate was able to undergo an exchange reaction with trifluoromethyltrimethylsilane (TMS-CF_3) and yielded trifluoromethylphosphonate.[1]

General procedure for fluorophosphonates:

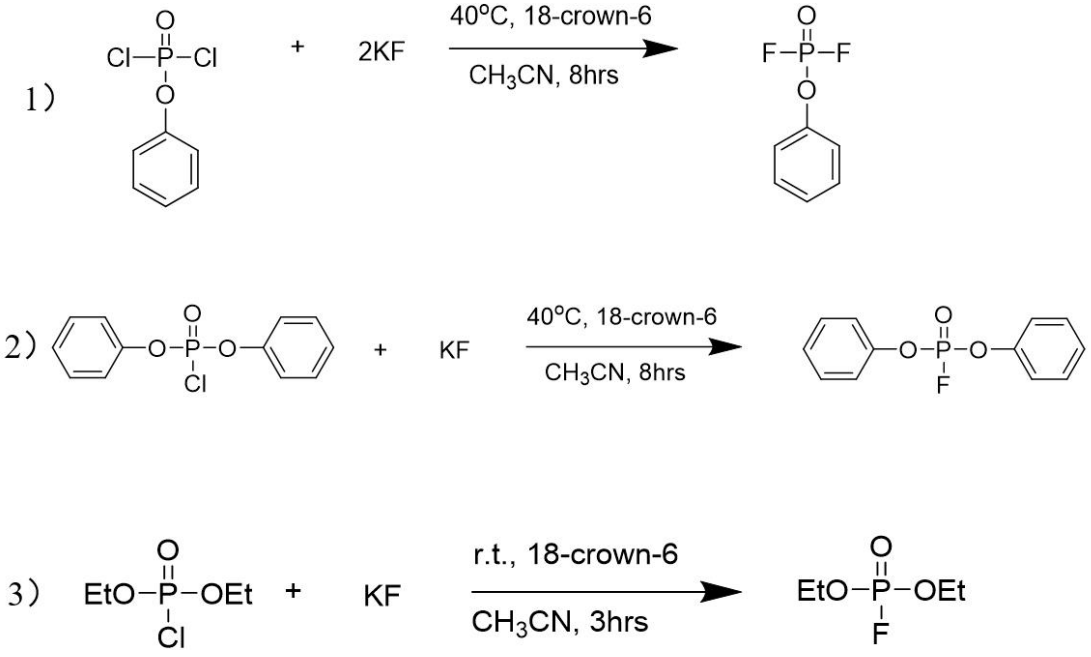

Scheme 2.01. Preparation of fluorophosphonates.

General procedure for PhoFEx:

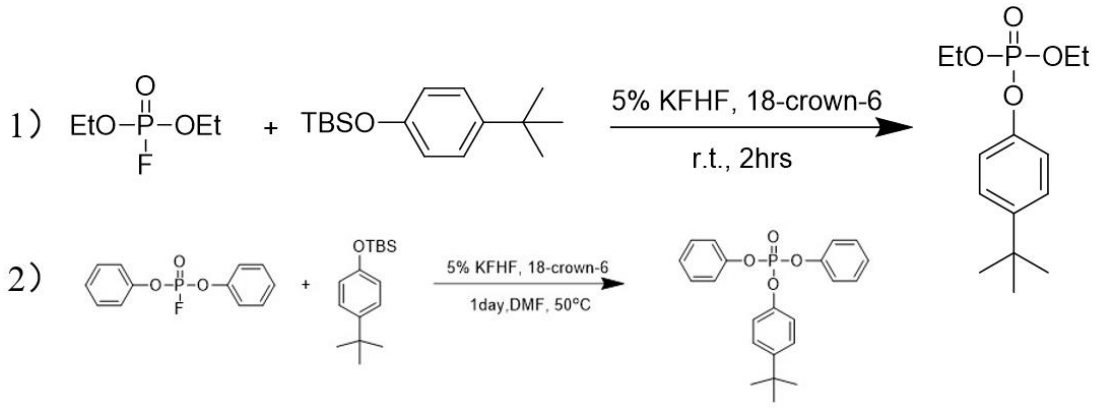

Scheme 2.02. Phosphorus- fluoride exchange reactions.

2.02 Transesterification reaction on organophosphates.

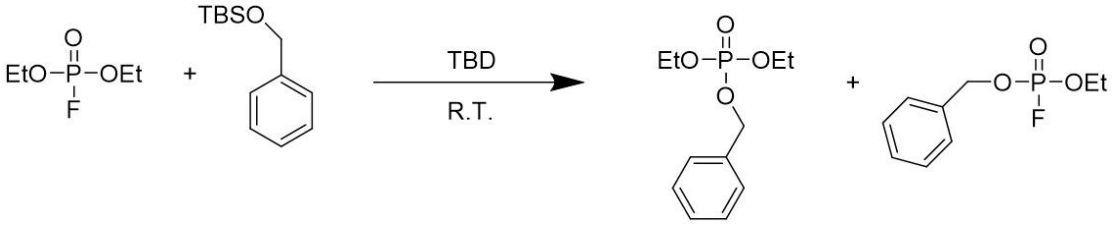

Scheme 2.03. Competing between PhoFEx and transesterification reaction.

Fluorophosphonates were obtained via the reaction between chlorophosphnates and potassium fluoride. Fluorophosphonates were much more hygroscopic comparing to fluorosulfates. Dry acetonitrile was required as the solvent (Scheme 2.01). Phosphorus-fluoride exchange reactions were less reactive than SuFEx, the best yield we could achieve was 80% (Scheme 2.02 A), and the formation of steric hindrance product was yielded as

low as 20% (Scheme 2.02 B). Unfortunately, the neurotoxicity of organic phosphonate halides is extremely formidable; this project was not fully explored in detail. The accidental discovery of the transesterification reaction on organophosphates was encouraging (Scheme 2.03).

2.03 Boron-Fluoride Exchange Reaction (BorFEx)

Since Si and F form the strongest single bond in nature under a non-protic environment,[2] the stability of Si-F can be the driving force for SuFEx reaction. Based on this point of view, we tried to find other similar examples. We sought to discover other hetero-atoms bonded with fluorine that could react with silyl ethers. Intriguingly, there were a few papers describing boron-fluorine bonds that can undergo reactions with silyl ethers. Both boron trifluoride diethyl etherate ($BF_3 \cdot OEt_2$) and trimethylsilyl trifluoromethanesulfonate (TMSOTf) are powerful and commonly used Lewis acids, and the mixture of them gives a stronger Lewis acid $BF_2OTf \cdot OEt_2$ and a side product trimethylsilyl fluoride (TMSF).[3] Organotrifluoroborate potassium salts are generally easy to handle and stable in ambient conditions. Vedejs invented the reaction between organoboronic acid, and potassium hydrogen difluoride (KFHF) aqueous solution[4] is a general and efficient way to prepare stable organotrifluoroborate potassium salt (Scheme 2.05A). Vedejs[4] also investigated that in the presence of 1 equivalent trimethylsilyl chloride (TMSCl) in aprotic solvents such as acetonitrile (ACN) and dimethyl sulfoxide (DMSO),

trifluoroborates (R-BF_3Ks) *via in situ* generated difluoroboranes (R-BF_2), TMSF, and potassium chloride side product precipitated out from the solution (Scheme 2.05B). Several papers took the benefit of the high reactivity of difluoroboranes, with the existence of fluorophile, such as excess equivalent of TMSCl with mild base,[5] silicon dioxide (SiO_2),[6] silicon tetrachloride ($SiCl_4$),[7] to synthesize boronic esters and boronic amides from the reaction between *in situ* difluoroboranes and alcohols/amines. Bode[8] successfully synthesized N-methyliminodiacetyl (MIDA) acylboronates from MIDA bis(trimethylsilyl) ester and trifluoroborates with $BF_3 \cdot OEt_2$ as the catalyst. Carreaux[9] found that pinacol boronic ester (Bpin) can be generated by the reaction between pinacol bis-(trimethylsilyl) ether and trifluoroborates with excess TMSCl as the catalyst. These examples mentioned above require a long reaction time and usually get a relatively low yield. To our knowledge, no one tried to use strong base (TBD, DBU etc.) as the catalyst between difluoroboranes and bis silyl ethers.

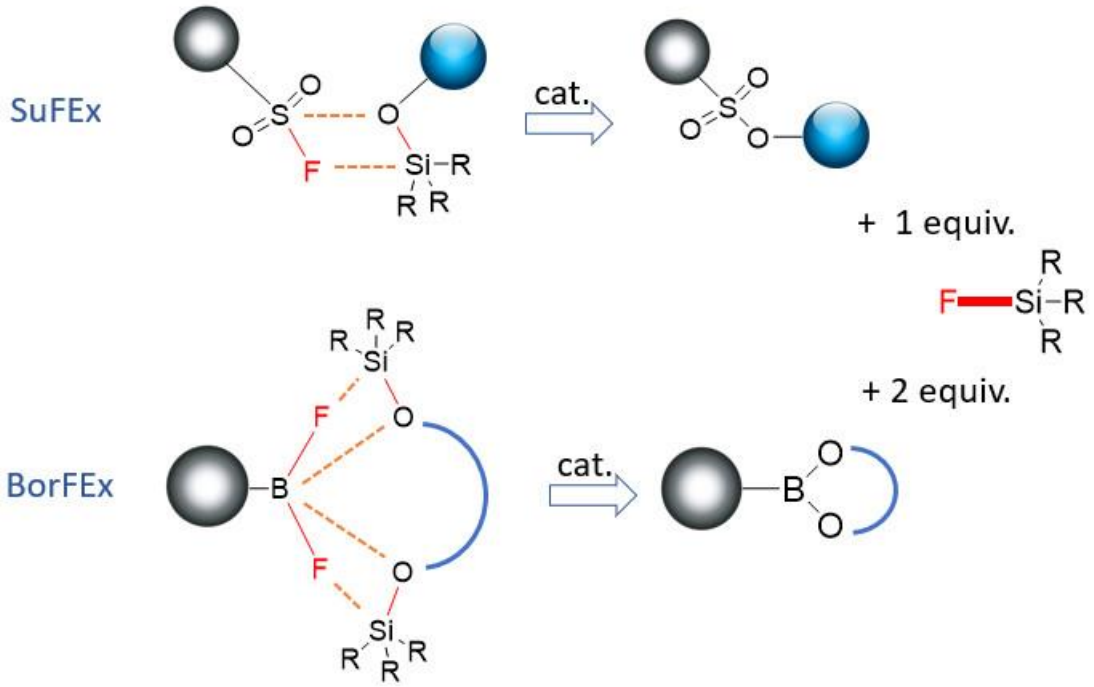

Scheme 2.04. Illustration of Sulfur (VI)-Fluoride Exchange (SuFEx) reaction and boron-fluoride exchange (BorFEx) reaction.

As shown in scheme 2.04, boron-fluoride exchange (BorFEx) reaction, which is very similar to SuFEx reaction, corresponded between *in situ* difluoroboranes and bis silyl ethers to form boronic esters. The side products for both are silyl fluoride, which contains the strongest single bond (Si-F) in nature. The orange dashed lines simply show the new forming bonds but do not indicate the mechanism behind them, as the total mechanism of SuFEx is still a mystery. Moses[10] proposed a mechanism for the bifluoride-catalyzed transformation of sulfonyl fluorides into triflones, but no one really proposed a detailed mechanism for strong base catalysts (TBD, DBU).

2.04 Preparation of boronic esters by BorFEx

General procedure for BorFEx (Scheme 2.05 B and C): Aryl trifluoroborate potassium salts (5 mmol) were added to a flame-dried Schlenk flask and then filled with nitrogen atmosphere. DMSO (2 mL) was injected into the flask and dissolved the salt by vigorous stirring. TMSCl (1 eq to -BF_3K group) was injected into the solution to form aryl difluoroboranes *via in situ*, and side product KCl was immediately precipitate out as white solids. The solution was transferred by a long needle and a syringe, then passed a 0.25 um Teflon filter and injected into another Schlenk flask with silyl ether (2 eq -TMS group to 1 eq -BF_2 group) in DCM (5 mL). TBD catalyst (0.1eq to -BF_2 group) was dissolved in DCM (1 mL) and injected into the mixture immediately. By tracing the formation of the boronic ester by TLC, usually less than 20mins, the mixture was brought up directly to a flash column for purification and yield the boronic ester product. (**Caution:** difluoroboranes are ultra-reactive, be very careful when handling them. Even 1 mL of this gas will cause vigorous bubbling when injected into the solution).

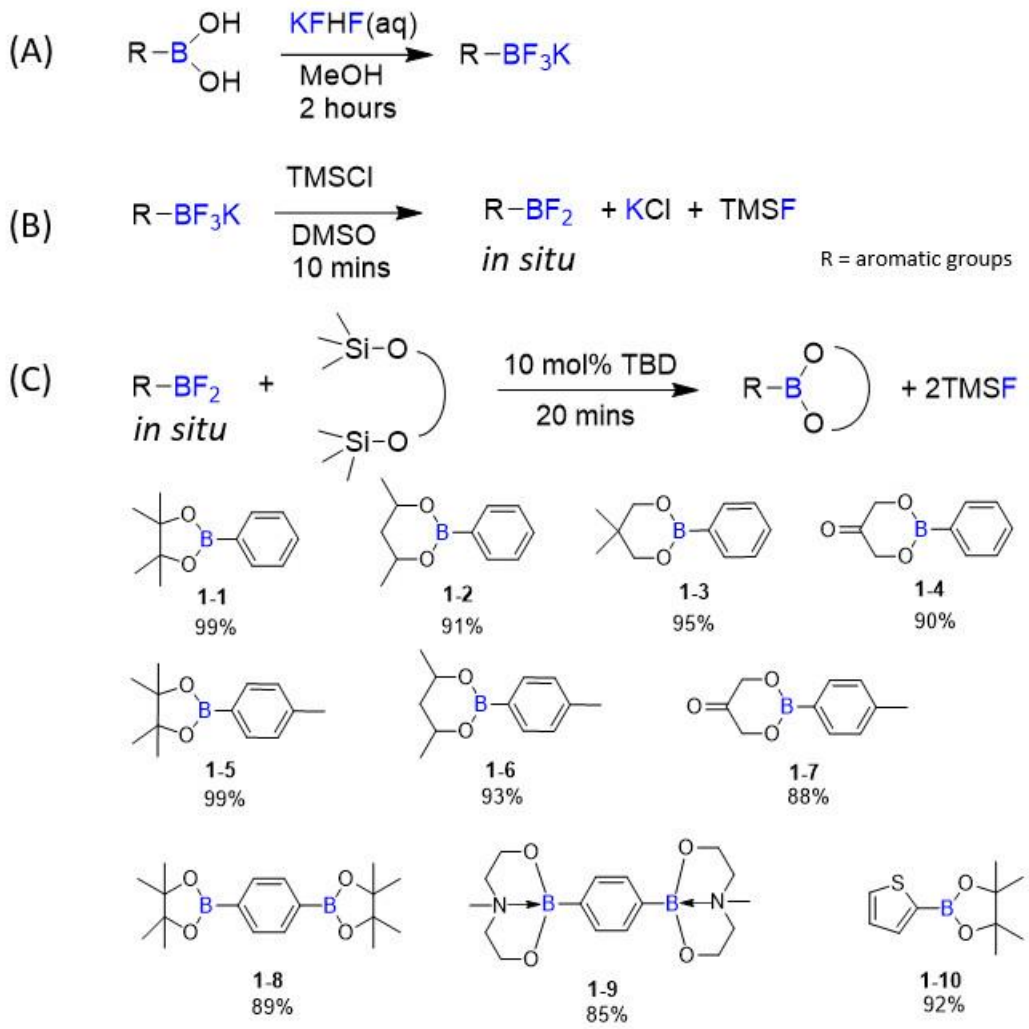

Scheme 2.05. Synthesis of (A) Organotrifluoroborate potassium salts (B) Difluoroboranes *via in situ* (C) Boronic esters through BorFEx with 10 mol% TBD as the catalyst.

Several examples of high reactivity BorFEx reactions are shown in Scheme 2.05. The original starting material, aromatic boronic acid were either commercially available or easily generated from bromide substitutes by Grignard reaction with trimethyl borate.[11] KFHF saturated aqueous solution was mixed with boronic acid methanol solution, and trifluoroborate potassium salts (R-BF_3K) precipitated out as white powders. By dissolving

dry R-BF_3K in anhydrous DMSO, a concentrated solution can *in situ* generate difluoroborane (R-BF_2) in 10 mins after the injection of TMSCl. Difluoroborane is extremely reactive and needed to be handled carefully. R-BF_2 solution was passed a 0.25 nm Teflon filter to remove KCl salts and directly mixed with bis silyl ether. With the existence of 10 mol% TBD as the catalyst, the BorFEx reaction is super-fast. Strikingly, within 20 mins, most silyl ethers were reacted tracing by thin-layer chromatography (TLC). The resulting solution was directly worked up by a flash column and had a high yield of corresponding boronic ester (Scheme 2.05C). These listed boronic esters all have a cyclic structure with 5 or 6-member rings, which are the most commonly used as boron protecting groups due to their stability towards hydrolysis. Apparently, introducing bifunctional R-$(BF_3K)_2$ as the starting material, diboronic esters can be achieved by BorFEx as well (1-8,9). It should be noted that 1-9 has a chelation structure which further increases the stability to hydrolysis. Not only can benzene derivatives undergo this procedure, but other hetero aromatic substitutes like thiophene (1-10) also worked perfectly.

Besides bis alkyl silyl ethers which could form boron ester protecting groups, mono silyl ethers and aromatic silyl ethers have also been tried with BorFEx conditions but paradoxically could not get desired product. As shown in Scheme 2.06, two equivalent of alkyl silyl ethers could not form boron dialkyl ester through BorFEx, even if the reaction time were prolonged to overnight, only hydrolysis products, boronic acid, and alkyl alcohol were found in the solution. Similarly, in SuFEx reaction, only aromatic silyl ethers can form stable sulfuric ester products; because alkyl sulfuric esters are not stable, the α-carbon

is easy to get nucleophilic attack and break the sulfuric ester S-O bond. On the contrary, boron esters generated from BorFEx (Scheme 2.05C) have a 5 or 6-member ring stable structure, which resists this kind of α-position nucleophilic attack. Pinacol-protected boron esters B(pin) (1-1) even has two tertiary carbons on α-position, which has the best stability and the highest yield. As can be seen from Scheme 2.06 B and C, surprisingly, catechol bis silyl ether and phenol silyl ether was not able to form desired product through BorFEx, only hydrolysis product shown up. This suggests BorFEx should have a totally different mechanism to SuFEx, or the stability of aromatic boronic esters are worse than 5 or 6-member ring alkyl boronic esters. When it comes to pentaerythritol tetra silyl ether (Scheme 2.06D), bis pentaerythritol protected boronic esters was shown on the TLC plates and NMR spectrum of the mixture but get hydrolysis through the flash column and not able to be separated. The center sp^3 configuration leads to restriction because two aromatic planes are not favorable to be mutually perpendicular with each other. Therefore, the stability of boronic ester products is the key to the success of the BorFEx reaction.

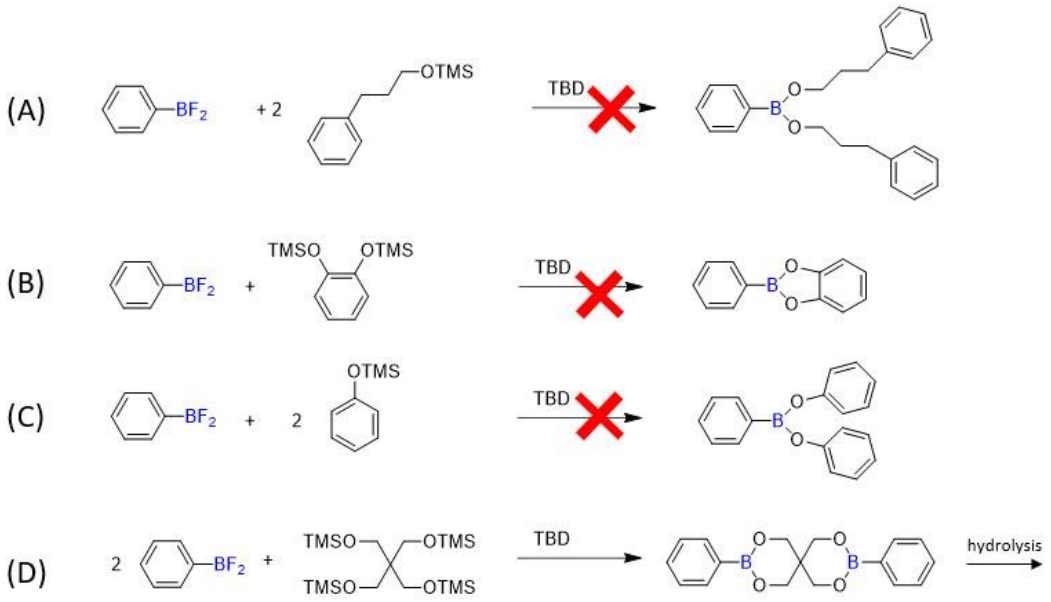

Scheme 2.06. Examples for unstable boronic esters, which failed to achieve from BorFEx

2.05 Other available ways to obtain boronic esters

Miyaura borylation reaction[12] is one of the common methods to synthesize aromatic boron esters. For instance, aryl B(pin) can be generated by palladium catalyst cross-coupling of bis(pinacolato)diboron (B_2pin_2) with aryl halides. There is another general condensation way[13] to prepare boronic esters from the reaction between boronic acid and diol. Usually, a Dean-Stark apparatus and long heat-up time are essential, or a water remover like magnesium oxide (MgO)[14] must be included. BorFEx reaction is faster compared to both Miyaura borylation and condensation. BorFEx only needs room temperature for several minutes, and no toxic metal catalyst, which is an advantage of using BorFEx to synthesize boronic esters.

2.06 Reference.

1. Herath, M. B.; Creager, S. E.; Kitaygorodskiy, A.; DesMarteau, D. D., Perfluoroalkyl Phosphonic and Phosphinic Acids as Proton Conductors for Anhydrous Proton-Exchange Membranes. *ChemPhysChem* **2010,** *11* (13), 2871-2878.

2. Dong, J.; Krasnova, L.; Finn, M. G.; Sharpless, K. B., Sulfur(VI) Fluoride Exchange (SuFEx): Another Good Reaction for Click Chemistry. *Angewandte Chemie International Edition* **2014,** *53* (36), 9430-9448.

3. Myers, E. L.; Butts, C. P.; Aggarwal, V. K., BF3·OEt2 and TMSOTf: A synergistic combination of Lewis acids. *Chemical Communications* **2006,** (42), 4434-4436.

4. Vedejs, E.; Chapman, R. W.; Fields, S. C.; Lin, S.; Schrimpf, M. R., Conversion of Arylboronic Acids into Potassium Aryltrifluoroborates: Convenient Precursors of Arylboron Difluoride Lewis Acids. *The Journal of Organic Chemistry* **1995,** *60* (10), 3020-3027.

5. Churches, Q. I.; Hooper, J. F.; Hutton, C. A., A General Method for Interconversion of Boronic Acid Protecting Groups: Trifluoroborates as Common Intermediates. *The Journal of Organic Chemistry* **2015,** *80* (11), 5428-5435.

6. Davies, G. H. M.; Mukhtar, A.; Saeednia, B.; Sherafat, F.; Kelly, C. B.; Molander, G. A., Azaborininones: Synthesis and Structural Analysis of a Carbonyl-Containing Class of Azaborines. *The Journal of Organic Chemistry* **2017,** *82* (10), 5380-5390.

7. An, Z.; Wu, M.; Kang, J.; Ni, J.; Qi, Z.; Yuan, B.; Yan, R., Synthesis of Fused B-Containing Heterocyclic Compounds and Their Relevant Optical Properties. *European Journal of Organic Chemistry* **2018,** *2018* (34), 4812-4817.

8. Noda, H.; Bode, J. W., Synthesis and chemoselective ligations of MIDA acylboronates with O-Me hydroxylamines. *Chemical Science* **2014,** *5* (11), 4328-4332.

9. Touchet, S.; Carreaux, F.; Molander, G. A.; Carboni, B.; Bouillon, A., Iridium-Catalyzed Allylic Amination Route to α-Aminoboronates: Illustration of the Decisive Role of Boron Substituents. *Adv Synth Catal* **2011,** *353* (18), 3391-3396.

10. Smedley, C. J.; Zheng, Q.; Gao, B.; Li, S.; Molino, A.; Duivenvoorden, H. M.; Parker, B. S.; Wilson, D. J. D.; Sharpless, K. B.; Moses, J. E., Bifluoride Ion Mediated SuFEx Trifluoromethylation of Sulfonyl Fluorides and Iminosulfur Oxydifluorides. *Angewandte Chemie International Edition* **2019,** *58* (14), 4552-4556.

11. Leermann, T.; Leroux, F. R.; Colobert, F., Highly Efficient One-Pot Access to Functionalized Arylboronic Acids via Noncryogenic Bromine/Magnesium Exchanges. *Organic Letters* **2011,** *13* (17), 4479-4481.

12. Takagi, J.; Takahashi, K.; Ishiyama, T.; Miyaura, N., Palladium-Catalyzed Cross-Coupling Reaction of Bis(pinacolato)diboron with 1-Alkenyl Halides or Triflates: Convenient Synthesis of Unsymmetrical 1,3-Dienes via the Borylation-Coupling Sequence. *Journal of the American Chemical Society* **2002,** *124* (27), 8001-8006.

13. Gillis, E. P.; Burke, M. D., A Simple and Modular Strategy for Small Molecule Synthesis: Iterative Suzuki−Miyaura Coupling of B-Protected Haloboronic Acid Building Blocks. *Journal of the American Chemical Society* **2007,** *129* (21), 6716-6717.

14. Dumbre, D. K.; Yadav, P. N.; Bhargava, S. K.; Choudhary, V. R., Suzuki–Miyaura cross-coupling reaction between aryl halides and phenylboronic acids over gold nano-particles supported on MgO (or CaO) and other metal oxides. *Journal of Catalysis* **2013,** *301*, 134-140.

CHAPTER 3

DIOXABOROLANE METATHESIS VITRIMER BY CROSS-LINKED BY BORFEX

3.01 Introduction of vitrimer

Obviously, boronic esters synthesized by BorFEx could have an application to be the reagent of Suzuki-Miyaura cross-coupling,[1] the original starting material trifluoroborate potassium salts (R-BF_3K) itself is already a good Suzuki coupling reagent. Nevertheless, in the polymer research field, boronic esters also play an important role and have some interesting applications. Vitrimers are a new class of cross-linked polymer networks, first defined by Leibler,[2] with exchangeable dynamic covalent bonds incorporated into the system.[3] Association and dissociation of the covalent cross-links gives the material good mechanical properties, solvent resistance, and recyclability. Recently, dramatic research efforts have been devoted to finding new dynamic exchange reactions and vitrimer designs. To name a few of them, transesterification, [2, 4-7] disulfide linkages,[8-9] siloxane exchange,[10] urethane exchange,[11-12] imine exchange, [13] olefin metathesis,[14] Diels–Alder reaction,[15] and dioxaborolane metathesis,[16] which is the exchange reactions between boronic esters. Dioxaborolane metathesis was demonstrated in a number of studies recently[17-18], by bonding boronic esters on polymer side chains. We found that BorFEx reaction can also be

used to synthesize vitrimers with dynamic boronic esters incorporated in.

3.02 Preparation of EVOBE vitrimer.

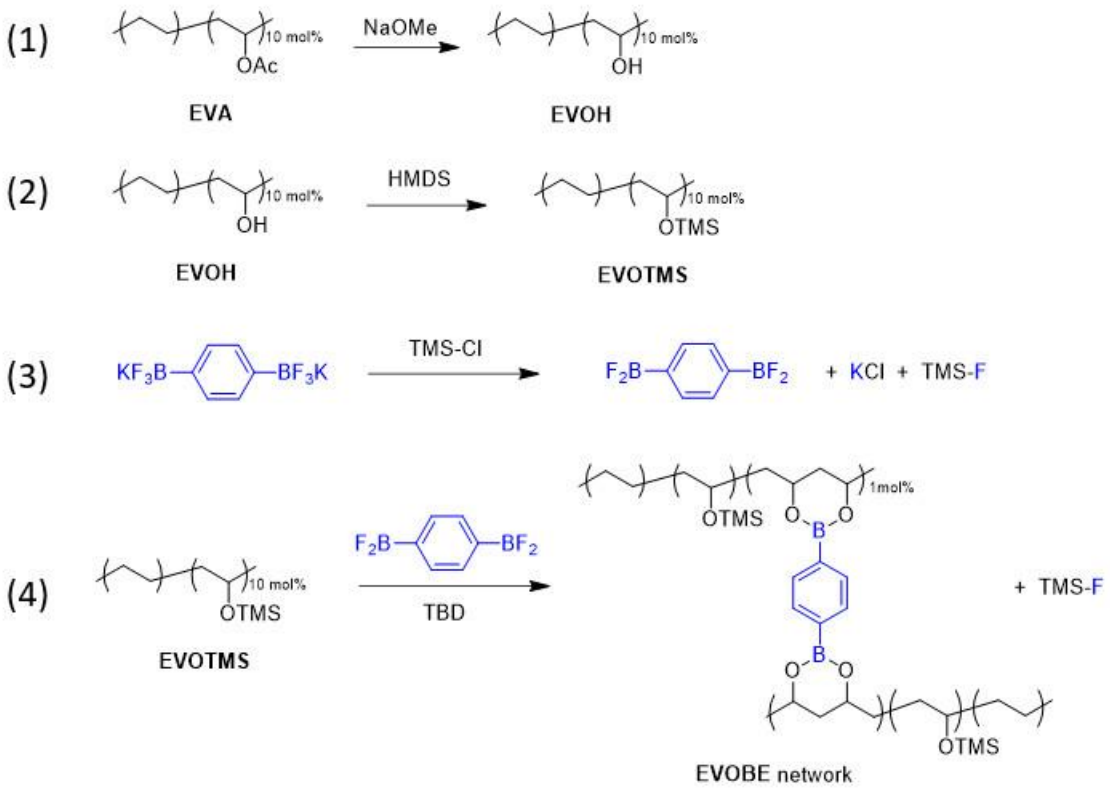

Scheme 3.01. Synthesis of EVOTMS Polymer and EVOBE Vitrimer

Hydrolysis of EVA (Scheme 3.01-1): Poly(ethylene-co-vinyl acetate) (EVA) (20 g, purchased from Sigma aldrich, 10 mol% VA) was dissolved in 400 mL toluene at 75 °C in a 1000 mL round flask. With vigorous stirring, 25 wt.% sodium methoxide in methanol (1.5 eq, 13.8 g) was added to the polymer solution and stirred overnight. The resultant suspension was maintained at 75 °C and quenched by HCl (3M, 1 eq, 21 mL). When the

mixture was stirred for 20mins, it was directly precipitated into cold MeOH. The filtered crude polymer was re-dissolved in toluene (400 mL) at 75 °C and precipitated into cold MeOH again. The polymer was filtered and dried in *vacuo* overnight at 85 °C to yield poly(ethylene-co-vinyl alcohol) (EVOH).

Silylation of EVOH (Scheme 3.01-2): EVOH (10 g) was dissolved in 200 mL toluene at 75 °C in a 500 mL round flask. With vigorous stirring, bis(trimethylsilyl)amine (HMDS, 3 eq, 59.0 mL) was added through an additional funnel. The mixture was allowed to stir overnight at 75 °C. The solvents and excess HMDS were removed in vacuo overnight at 75 °C to yield yellow EVOTMS.

Synthesis of EVOBE vitrimer (Scheme 3.01-3,4): First, EVOTMS (14 g, 100eq, 0.318 mol -OTMS group) was dissolved in 200 mL toluene at 75 °C in a 500 mL round flask. Following the general procedure for BorFEx, dipotassium phenylene-1,4-bis(trifluoroborate) ($Ph(BF_3K)_2$) (0.92 g, 1 eq, 3.18 mmol) was added to a flame-dried Schlenk flask and then filled with nitrogen atmosphere. DMSO (2 mL) was injected into the flask and dissolved the salt by vigorous stirring. TMSCl (0.809 mL, 1 eq to $-BF_3K$ group, 6.36 mmol) was injected into the solution to form phenylene-1,4-difluoroboranes *via in situ*. The solution was transferred by a long needle, and a syringe then passed a 0.25 um Teflon filter and injected into the EVOTMS polymer solution. TBD catalyst (0.099 g, 0.1eq to $-BF_2$ group, 0.64 mmol) was dissolved in DCM (1 mL) and injected into the mixture immediately. The gelation was observed at once, and the stirring bar stopped

within one minute. The gelation was dried in *vacuo* overnight at 85 °C to yield a yellow EVOBE vitrimer.

By introducing boron-fluoride exchange reaction into a polymer system, interestingly, we designed a dynamic cross-linked network with boronic esters embedded in polymer backbones, which can undergo dioxaborolane metathesis to show vitrimer behaviors. As shown in Scheme 3.01, a low vinyl acetate containing (10 mol%) poly(ethylene-co-vinyl acetate) (EVA) was hydrolyzed with sodium methoxide to form poly(ethylene-co-vinyl alcohol) (EVOH) with quantitively 10 mol% hydroxy groups. These hydroxy groups are fully converted into silyl ethers through bis(trimethylsilyl)amine silylation reaction. The cross-linker phenylene-1,4-bis(difluoroborane) was generated *in situ* by the reaction between dipotassium phenylene-1,4-bis(trifluoroborate) and trimethylsilyl chloride (TMS-Cl) in dry DMSO. All the details for polymers and small molecules syntheses and characterizations are listed in the Supporting Information.

EVOTMS was dissolved in dry toluene at 60 °C by vigorous stirring. With the addition of catalyst triazabicyclodecene (TBD) and the injection of cross-linker, boron fluorine exchange reaction will take place at two silyl ether repeat units adjacent to each other. The concentration of cross-linker is 1 mol% to -OTMS groups in the polymer backbone. On the other hand, catalyst TBD is 10 mol% to -BF_2 groups in the cross-linker. After mixing, gelation took place within one minute as the magnetic stirring bar was

stopped. The gelled polymer network was dried at 85°C under vacuum overnight to remove solvents.

By incubating the EVOBE vitrimer material in dry toluene at 80 °C overnight, an insoluble gel fraction of around 83% was determined. The thermal stability of the vitrimer was demonstrated by thermogravimetric analysis (TGA). The differential scanning calorimetry (DSC) curve shows a broad melting peak at ~98°C for EVOBE vitrimer because most of the polymer backbone is semi-crystalline polyethylene.

3.03 Dioxaborolane metathesis in EVOBE network.

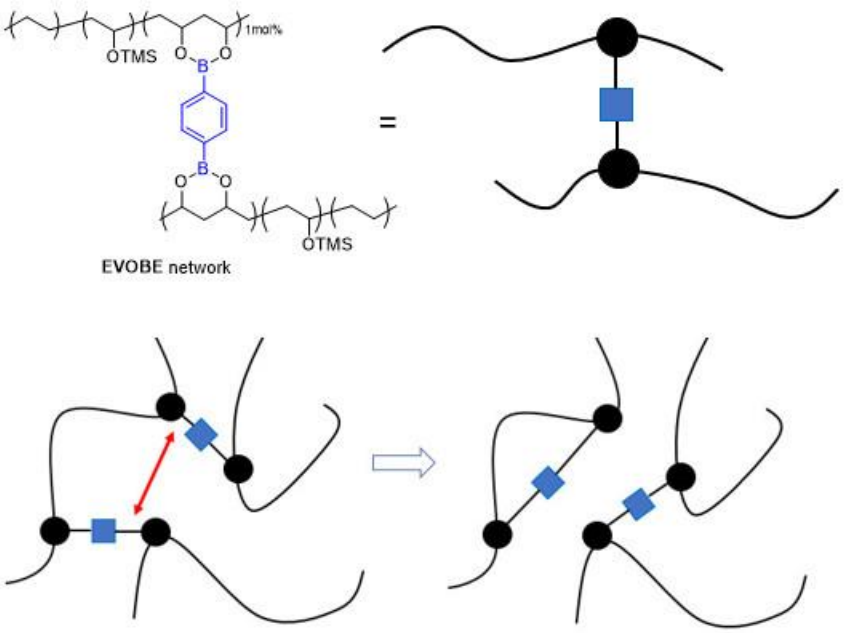

Figure 3.01. Illustration of the potential dioxaborolane metathesis in EVOBE network.

(Black lines: EVOTMS polymer backbone; Black beads: 5 or 6-member ring boronic ester embedded in polymer backbone; Blue square: phenyl linkage).

In Figure 3.01, we can see the potential dioxaborolane metathesis dynamic exchange in the EVOBE network. Compared to other vitrimer materials[16-18] using dioxaborolane metathesis as the exchange reaction, alkyl boronic esters consists of the partial polymer backbone in the EVOBE network, not the side chains. On the other hand, the boronic esters exchange reaction can only happen between two crosslinking points, as the red double arrow shown in Figure 3.01, and forming two new cross-linking points.

3.04 Stress relaxation of EVOBE network.

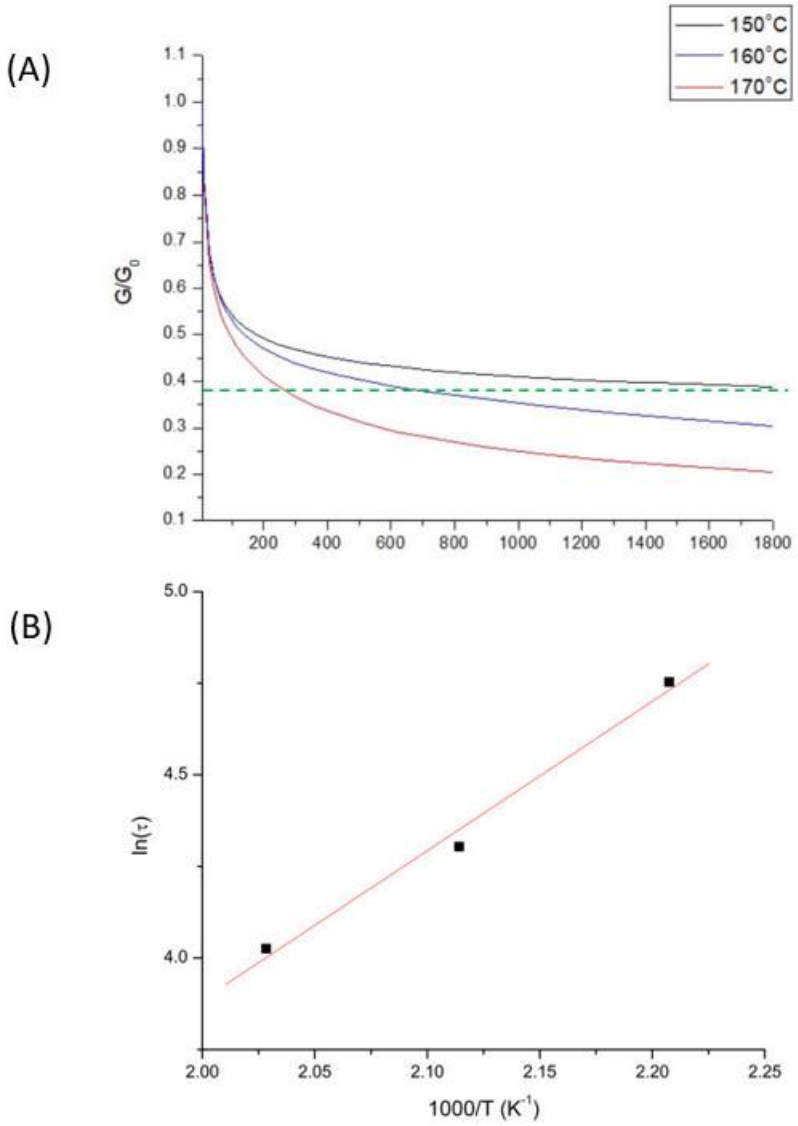

Figure 3.02. (A) Stress relaxation test of EVOBE vitrimer using 10% strain on dynamic mechanical analysis (DMA) (B) An Arrhenius linear fit of stress relaxation plots.

As shown in Figure (3.02 A), the stress relaxation study of EVOBE vitrimer was tested on dynamic mechanical analysis (DMA) by tracing the stress/modulus change at a

constant 10% strain. Individually, samples are tested at various temperatures from 150 to 170 °C. Sample at higher temperature has a faster relaxation than lower temperature, which reach the totally relaxed green dash line, 1/e=36.8%.[2] The relaxation time at this point is defined as τ^*. Based on the Arrhenius equation, $\tau^* = \tau^0 \exp(Ea/RT)$, we can accordingly plot $\ln(\tau^*)$ to 1000/T (Figure 3.02 B) and calculate the activation energy of the dioxaborolane metathesis exchange reaction in EVOBE vitrimer system is 33.9 kJ/mol. According to recent developments of vitrimer study on dioxaborolane metathesis, this number is low comparing to other boronic ester vitrimer systems.[16-17] It can be explained by low cross-link density (<1%) increase the possibility of chain movement. From this point of view, there is no evidence shows boronic ester formed on polymer backbone has any difference from those formed on side chains. All testing temperatures were higher than the melting point of the polyethylene, somehow excluded the potential problem caused by the crystallinity of the polyethylene backbone.

3.05 Tensile test of EVOBE network.

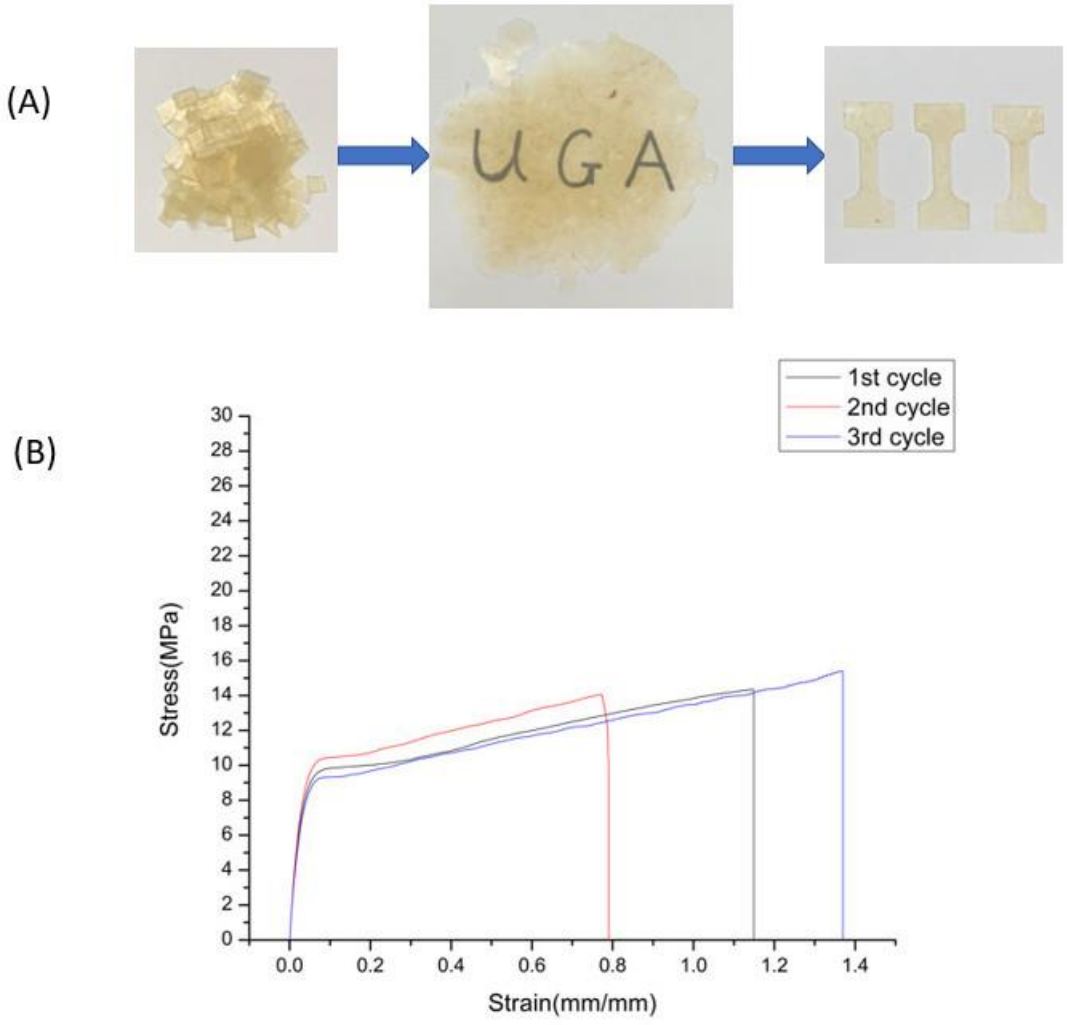

Figure 3.03. (A) Sample preparation by shredding into pieces, hot pressing, and cutting into dog bone for tensile test. (B) Instron tensile test for 3 times recycled EVOBE vitrimers.

As can be seen from Figure 3.03A, EVOBE vitrimer dried by vacuum can be cut into small pieces by scissor, and set between two pre-heated Teflon plates for hot pressing at 150°C, ~1000 psi, holding for 20mins and cooling for 1 hour to get a film with thickness

around 0.5mm. An ASTM standard dog bone cutter is used to get samples ready for Instron tensile test. Used dog bones were cut into small pieces by scissors for the next cycle. Figure 3.03 B not only shows the recyclability of EVOBE vitrimer but also tells us Young's modulus of this material is around 300MPa, which increased dramatically comparing to EVA (20MPa), EVOH (18MPa), and EVOTMS (25MPa). On the other hand, the elongation ability of the EVOBE vitrimer is fair compared to other cross-linked polymer structures. The mechanical properties almost remain the same for the three cycles.

3.06 Conclusion.

In a nutshell, we report a new boron-fluoride exchange reaction (BorFEx) and one of its applications for vitrimer design. The discovery was inspired by the driving force of the second generation click chemistry SuFEx, the strongest covalent bond (Si-F) in nature. Organodifluoroboranes are able to consist of a variety of bis silyl ethers and generate stable 5 o 6-member ring cyclic boronic esters in 20 mins with the attendance of 10 mol% TBD as the catalyst. One of the biggest advantages is that the starting material of BorFEx: organotrifluoroborate potassium salts (R-BF_3K), are very easy to achieve and are able to stay stable at ambient conditions for a long time resisting hydrolysis. Although it may not be the most convenient way to synthesize boronic esters, the super-high reactivity of BorFEx can cross-link EVOTMS polymer chains in minutes and achieve an EVOBE network by using a bis difluoroborane cross-linker. Indeed, the EVOBE network can

undergo an associative exchange mechanism via dioxaborolane metathesis, which can be called a vitrimer. Comparing to other boronic ester vitrimers[16-17], BorFEx is able to directly build boronic esters in the polymer backbone, which is more efficient to skip the step to extend the side groups on each repeat unit or the synthesis of newly designed monomers. On the other hand, there is no evidence that shows boronic esters bonded on polymer backbone have a slower relaxation or higher activation energy. Both great mechanical properties of thermosets and reprocessablility of thermoplastics have been achieved. With the high reactivity, BorFEx is able to be widely applied in different areas as SuFEx does, from small molecule connection to post-polymerization modification and biological conjugation.

3.07 Reference.

1. Miyaura, N.; Yamada, K.; Suzuki, A., A new stereospecific cross-coupling by the palladium-catalyzed reaction of 1-alkenylboranes with 1-alkenyl or 1-alkynyl halides. *Tetrahedron Letters* **1979,** *20* (36), 3437-3440.

2. Montarnal, D.; Capelot, M.; Tournilhac, F.; Leibler, L., Silica-Like Malleable Materials from Permanent Organic Networks. *Science* **2011,** *334* (6058), 965.

3. Kloxin, C. J.; Scott, T. F.; Adzima, B. J.; Bowman, C. N., Covalent Adaptable Networks (CANs): A Unique Paradigm in Crosslinked Polymers. *Macromolecules* **2010,** *43* (6), 2643-2653.

4. Capelot, M.; Montarnal, D.; Tournilhac, F.; Leibler, L., Metal-Catalyzed Transesterification for Healing and Assembling of Thermosets. *Journal of the American Chemical Society* **2012,** *134* (18), 7664-7667.

5. Capelot, M.; Unterlass, M. M.; Tournilhac, F.; Leibler, L., Catalytic Control of the Vitrimer Glass Transition. *ACS Macro Letters* **2012,** *1* (7), 789-792.

6. Chabert, E.; Vial, J.; Cauchois, J.-P.; Mihaluta, M.; Tournilhac, F., Multiple welding of long fiber epoxy vitrimer composites. *Soft Matter* **2016,** *12* (21), 4838-4845.

7. Yang, Y.; Pei, Z.; Li, Z.; Wei, Y.; Ji, Y., Making and Remaking Dynamic 3D Structures by Shining Light on Flat Liquid Crystalline Vitrimer Films without a Mold. *Journal of the American Chemical Society* **2016,** *138* (7), 2118-2121.

8. Takahashi, A.; Goseki, R.; Ito, K.; Otsuka, H., Thermally Healable and Reprocessable Bis(hindered amino)disulfide-Cross-Linked Polymethacrylate Networks. *ACS Macro Letters* **2017,** *6* (11), 1280-1284.

9. Ma, Z.; Wang, Y.; Zhu, J.; Yu, J.; Hu, Z., Bio-based epoxy vitrimers: Reprocessibility, controllable shape memory, and degradability. *Journal of Polymer Science Part A: Polymer Chemistry* **2017,** *55* (10), 1790-1799.

10. Schmolke, W.; Perner, N.; Seiffert, S., Dynamically Cross-Linked Polydimethylsiloxane Networks with Ambient-Temperature Self-Healing. *Macromolecules* **2015,** *48* (24), 8781-8788.

11. Yan, P.; Zhao, W.; Fu, X.; Liu, Z.; Kong, W.; Zhou, C.; Lei, J., Multifunctional polyurethane-vitrimers completely based on transcarbamoylation of carbamates: thermally-induced dual-shape memory effect and self-welding. *RSC Advances* **2017,** *7* (43), 26858-26866.

12. Zheng, N.; Fang, Z.; Zou, W.; Zhao, Q.; Xie, T., Thermoset Shape-Memory Polyurethane with Intrinsic Plasticity Enabled by Transcarbamoylation. *Angewandte Chemie International Edition* **2016,** *55* (38), 11421-11425.

13. Li, H.; Bai, J.; Shi, Z.; Yin, J., Environmental friendly polymers based on schiff-base reaction with self-healing, remolding and degradable ability. *Polymer* **2016,** *85*, 106-113.

14. Lu, Y.-X.; Guan, Z., Olefin Metathesis for Effective Polymer Healing via Dynamic

Exchange of Strong Carbon–Carbon Double Bonds. *Journal of the American Chemical Society* **2012,** *134* (34), 14226-14231.

15. Polgar, L. M.; van Duin, M.; Broekhuis, A. A.; Picchioni, F., Use of Diels–Alder Chemistry for Thermoreversible Cross-Linking of Rubbers: The Next Step toward Recycling of Rubber Products? *Macromolecules* **2015,** *48* (19), 7096-7105.

16. Röttger, M.; Domenech, T.; van der Weegen, R.; Breuillac, A.; NicolaÿR.; Leibler, L., High-performance vitrimers from commodity thermoplastics through dioxaborolane metathesis. *Science* **2017,** *356* (6333), 62-65.

17. Wang, Z.; Gu, Y.; Ma, M.; Chen, M., Strong, Reconfigurable, and Recyclable Thermosets Cross-Linked by Polymer–Polymer Dynamic Interaction Based on Commodity Thermoplastics. *Macromolecules* **2020,** *53* (3), 956-964.

18. Breuillac, A.; Kassalias, A.; NicolaÿR., Polybutadiene Vitrimers Based on Dioxaborolane Chemistry and Dual Networks with Static and Dynamic Cross-links. *Macromolecules* **2019,** *52* (18), 7102-7113.

CHAPTER 4

DIALKYL PHOSPHITE TRANSESTERIFICATION VITRIMER

4.01 Introduction

Transesterification of phosphate esters has been developed for decades in different applications. The most well-known phosphate ester linkages are between neighbor blocks of DNAs and RNAs, which chose by nature to build stable nucleotide polymer chains and store everlasting genetic information. Especially in RNAs [1-2], the existence of the 2'-hydroxy group has the potential ability to undergo the transesterification reaction with 3', 5'-phosphodiester bonds and leads to the cleavage of mono-nucleotide building block (Scheme 4.01A). In polymeric materials, polyphosphates established through polycondensation between phosphates and diols have rarely been reported,[3] comparing to polyesters build through polycondensation, only low molecular weight polyphosphate oligomers were obtained. On the contrary, highly controlled cationic catalyzed ring-opening polymerization (ROP) of cyclic phosphates and phosphonates has been well-developed.[4] These polymeric organophosphate materials provide outstanding properties, such as flame retardancy,[5-6] antifouling,[7], and hyper-branching materials.[8] Recently, with the development of dynamic cross-linked networks, vitrimers formed by transesterification of phosphate diesters[9] and triesters[10] as the dynamic exchange reaction have been reported.

Both of the materials have significant reprocessability, maintaining their mechanical properties after several cycles. However, to the best of our knowledge, transesterification of dialkyl phosphite (also named dialkyl *H*-phosphonates) as the bond exchange reaction has not been implemented in dynamic cross-linked networks.

In this work, we introduce dialkyl phosphite as a dynamic cross-linker in the polymeric network, which performs an exchange reaction with hydroxyl groups on poly(ethylene-co-vinyl alcohol) (EVOH) backbone through nucleophilic substitution transesterification. (Scheme 4.01B)

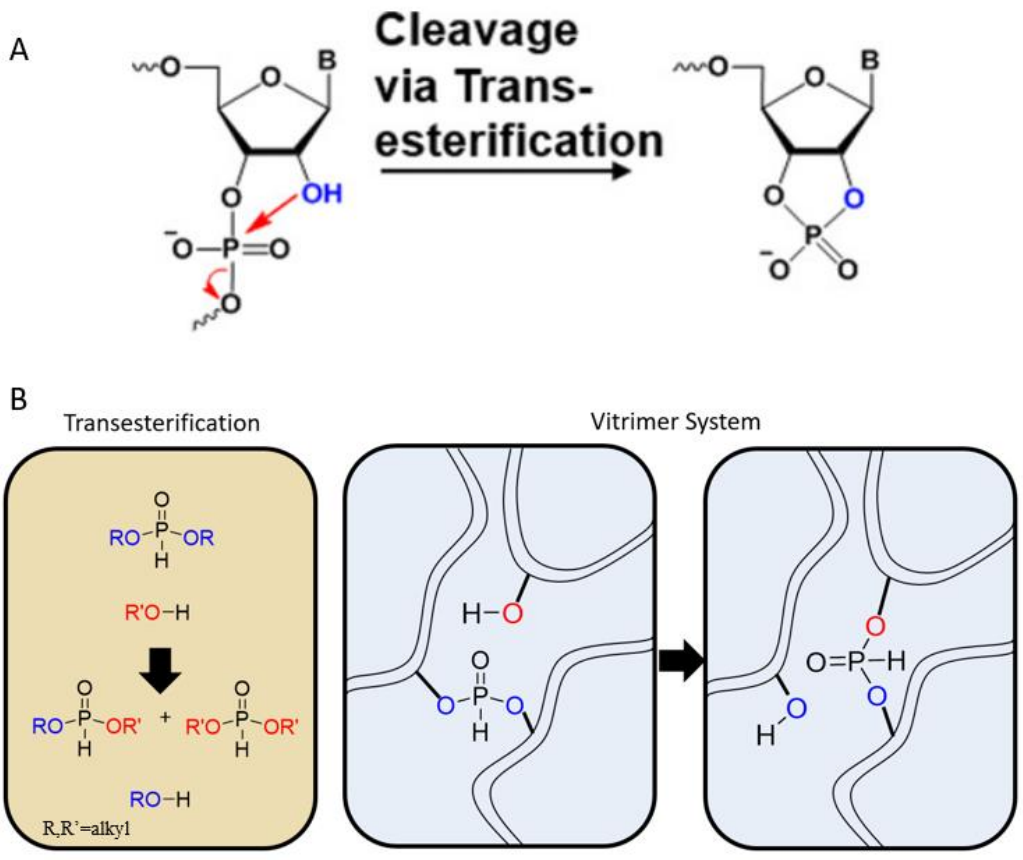

Scheme 4.01. (A) Cleavage of 3', 5'-phosphodiester bonds in RNAs via transesterification. (B) Transesterification exchange reaction in dialkyl phosphite and the dynamic cross-

linked vitrimer system in EVOH.

4.02 Catalysts screening for transesterification reaction of dialkyl phosphites

Similar to phosphate triesters, without external catalysts, transesterification on dialkyl phosphate at relatively high temperatures has been reported early in 1953,[11], and a continuous flow transesterification study of dialkyl phosphites in the absence of a catalyst was elaborated using a microwave reactor. [12] Dialkyl phosphites are generally able to undergo transesterification above 100°C, but the reaction under catalytic conditions and lower temperatures has not been concluded in detail. As mentioned above in Chapter 2, we accidentally found that organic bases, such as Triazabicyclodecene (TBD), have the potential to accelerate the rate of the transesterification reaction on phosphate esters even at ambient temperature. Herein, the catalysts screening for transesterification reaction between diethyl phosphite (DEP) and 3-Phenyl-1-propanol (PhPol) has been reported with different organic bases. Both mono- and di-substituted products are able to be separated through column chromatography and HPLC-UV to quantify the conversion ratio of starting materials.

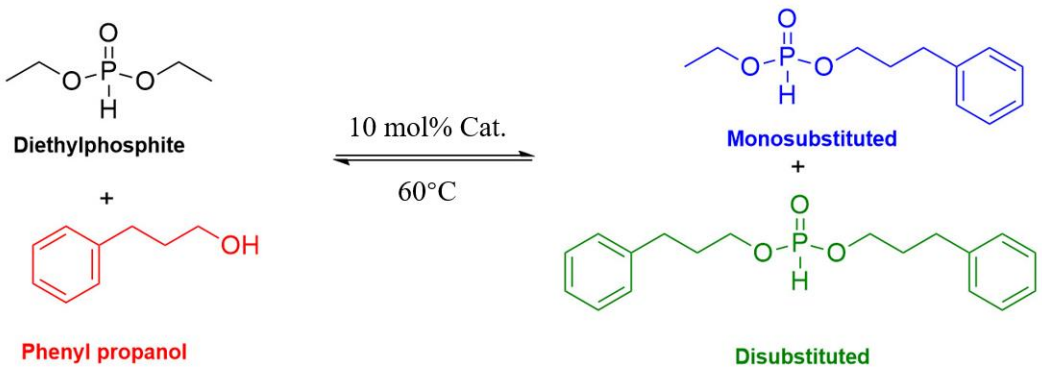

Scheme 4.02. Transesterification reaction between diethyl phosphite (DEP) and 3-Phenyl-1-propanol (PhPol).

General procedure for catalyst screening: Diethyl phosphite (0.276 g, 2.0 mmol, 1 *equiv.*) and 3-Phenyl-1-propanol (0.545 g, 4.0 mmol, 2 *equiv.*) were dissolved in dry acetonitrile (4.0 mL). The result mixture was heated up to 60°C. Organic base catalyst (0.4 mmol, 0.2 *equiv.*) was added and kept stirring at 60°C for 18 hours. After checked by TLC to confirm the existence of product, the reaction mixture was directly separated by column chromatography (Ethyl Acetate/Hexanes = 1.5/1, v/v) to obtain mono-substituted ethyl phenyl propyl phosphite (EPhPP), R_f = 0.38. ^{1}H-NMR (400 MHz, $CDCl_3$): δ 7.69 and 5.96p.p.m. (d, 1H), 7.32-7.19 (m, 5H), 4.19-4.06 (m, 4H), 2.76-2.72 (t, 2H), 2.04-2.01 (m, 2H), 1.38-1.35 (t, 3H); ^{13}C NMR (101 MHz, $CDCl_3$) δ 140.78, 128.44, 126.14, 125.77, 64.81, 61.93, 32.01, 31.65, 16.37; ^{31}P NMR (162 MHz, $CDCl_3$) δ 7.63 (s); EI-MS (m/z): 229 $[M+H]^+$. Di-substituted diphenyl propyl phosphite (DPhPP), R_f = 0.52. ^{1}H NMR (400 MHz, $CDCl_3$) δ 7.73 and 5.99 (d, 1H), 7.32 (m, 4H), 7.23 (m, 6H), 4.17-4.07 (m, 4H), 2.80-2.72 (m, 4H), 2.06 (m, 4H); ^{13}C NMR (101 MHz, $CDCl_3$) δ 140.77, 128.52, 126.19, 64.96,

32.01, 31.68; ^{31}P NMR (162 MHz, $CDCl_3$) δ 7.93 (s); EI-MS (m/z): 341 $[M+Na]^+$.

After the separation of EPhPP and DPhPP, the unique retention times of starting material PhPol and products EPhPP/DPhPP in a certain eluent combination (Acetonitrile/Water = 65/35, v/v) were obtained by using high-performance liquid chromatography (HPLC) and ultraviolet (UV) detector (Figure. 4.01 A). The UV absorbance spectrum of them was almost the same because of the similarity in structure of phenyl propyl functional groups. The united maximum of absorbance was at wavelength λ = 260 nm. On the other hand, DEP has no UV absorbance at λ = 260 nm, which never shows a peak in the following HPLC curves. By Beer-Lambert law, a series of standard solutions with concentrations of 0.010, 0.025, 0.050, 0.075, 0.100M were tested by HPLC-UV for PhPol, EPhPP, and DPhPP to obtain the calibration curve between concentration and peak area. The further calculation for different catalyst conversions and kinetics measurements were determined by the calibration curves.

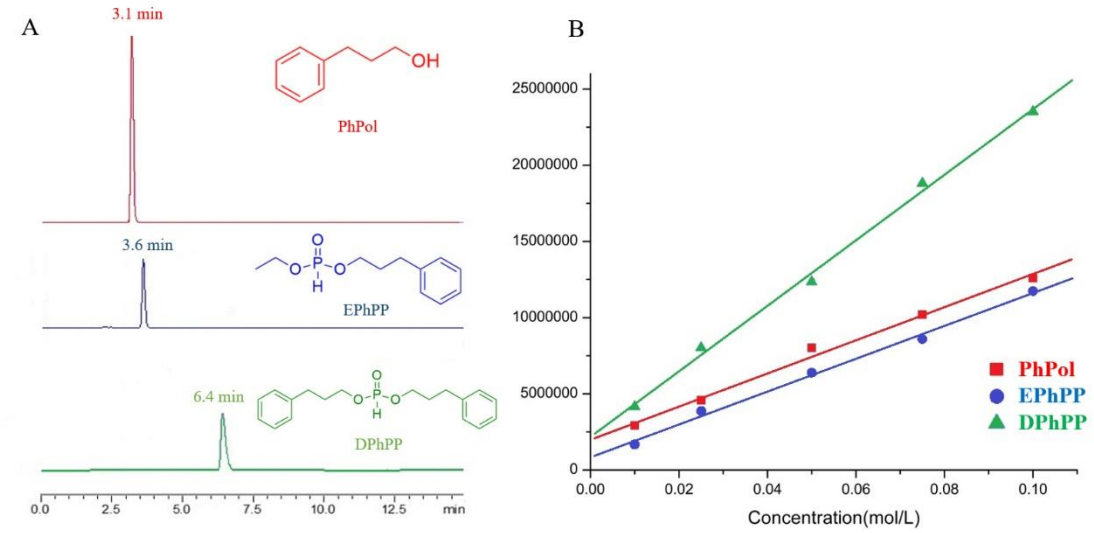

Figure 4.01. (A) Retention time of starting material PhPol and products EPhPP/DPhPP by using HPLC-UV (Acetonitrile/Water = 65/35 v/v) at the wavelength λ = 260 nm. (B) Calibration curve of PhPol, EPhPP, and DPhPP for HPLC-UV characterization and kinetics measurements.

As shown in Figure 4.02, comparing A, B, C, D, E to F, after 18 hours reaction time, almost all the organic bases have the ability to increase the ratio of conversion at 60°C to equilibriums, despite the basicity. Tetramethyl-1,6-hexane diamine (TMHDA) has the best ratio of conversion at equilibrium, though the pKa of its conjugate acid is almost the same as triethylamine (TEA) and tetramethylethylenediamine. The six CH_2 alkyl spacer between amines has a potential catalytically pathway for bi-molecule reaction, which may be different from simple nucleophilic substitution.

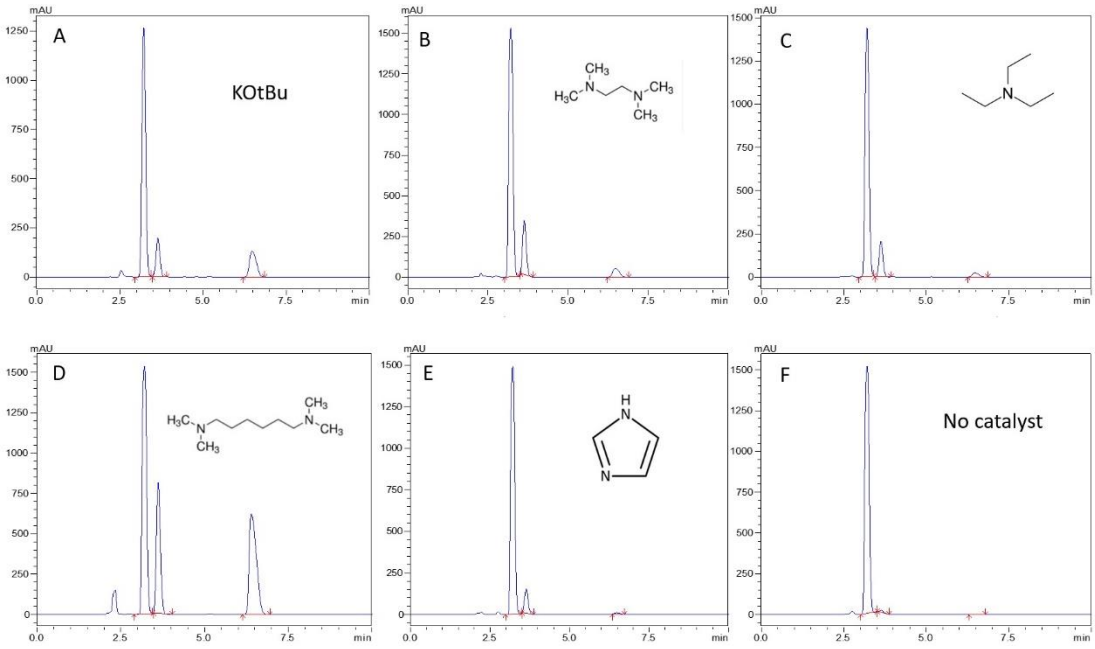

Figure 4.02. HPLC spectrums for different organic bases as catalysts (10 mol %) for DEP and PhPol transesterification reaction at 60°C for 18 hours. Organic catalyst list: (A) Potassium *tert*-butoxide. (B) *N,N,N′,N′*-Tetramethylethylenediamine. (C) Triethylamine. (D) *N,N,N′,N′*-Tetramethyl-1,6-hexane diamine. (E) Imidazole. (F) No catalyst/ blank control.

Among all the attempts, triazabicyclodecene (TBD), as a super-strong organic base, was able to catalyze the model transesterification reaction even at ambient temperature (Figure. 4.03), as well as the rate of reaction was surprisingly fast, which formed equilibrium within one hour. Unfortunately, TBD is not stable in the atmosphere at evaluated temperature for the following vitrimer system. The highest conversion catalyst, TMHDA, was chosen for the kinetics studies and used to establish dynamic cross-linked polymeric material.

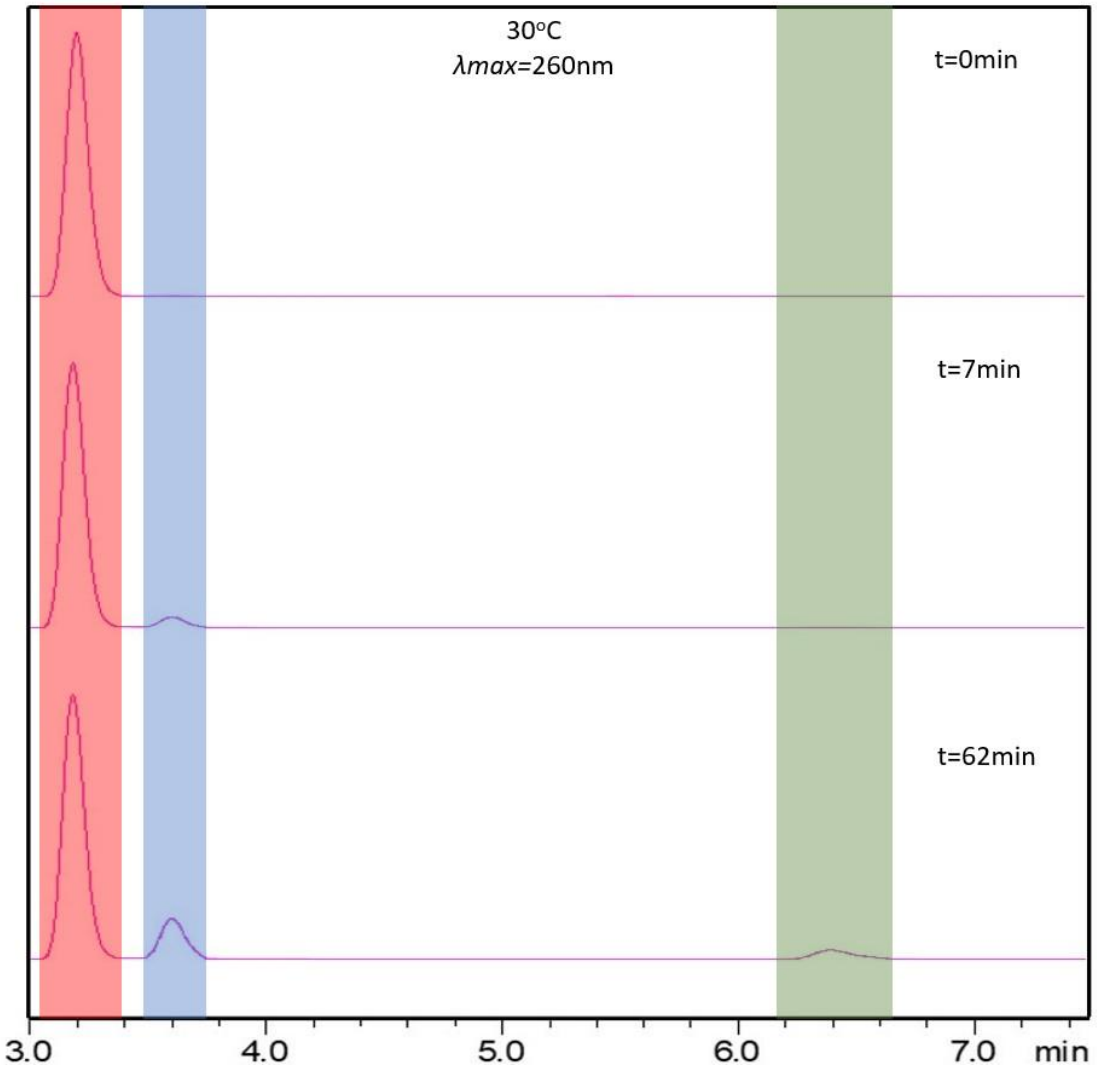

Figure 4.03. Time-dependent (within one hour) HPLC curves for DEP and PhPol model reaction with TBD as a catalyst at 30°C.

4.03 Kinetics study for transesterification reaction of dialkyl phosphites

General procedure for kinetics studies: Diethyl phosphite (0.055 g, 0.4 mmol, 1 *equiv.*) and 3-Phenyl-1-propanol (0.545 g, 4.0 mmol, 10 *equiv.*) were dissolved in dry acetonitrile

(1.0 mL) in a sealed vial. The resultant mixture was heated up to certain temperatures. Tetramethyl-1, 6-hexane diamine (TMHDA) (0.069 g, 0.4 mmol, 1 *equiv.*) was added at once. Every 10 minutes, 10 μL of the mixture was transferred into a vial by a syringe and diluted with acetonitrile (1.0 mL). The solution was prepared for HPLC measurement.

By adding 10 *equiv.* of PhPol, which was dramatically excess of DEP (1 *equiv.*), the reaction progress was analyzed using high-performance liquid chromatography- ultraviolet (HPLC-UV). TMHDA was identified as the highest conversion organic base catalyst that provided rapid transesterification between DEP and PhPol at various temperatures from 50 to 110 °C. All expected substitutions were observed, and no side products exist.

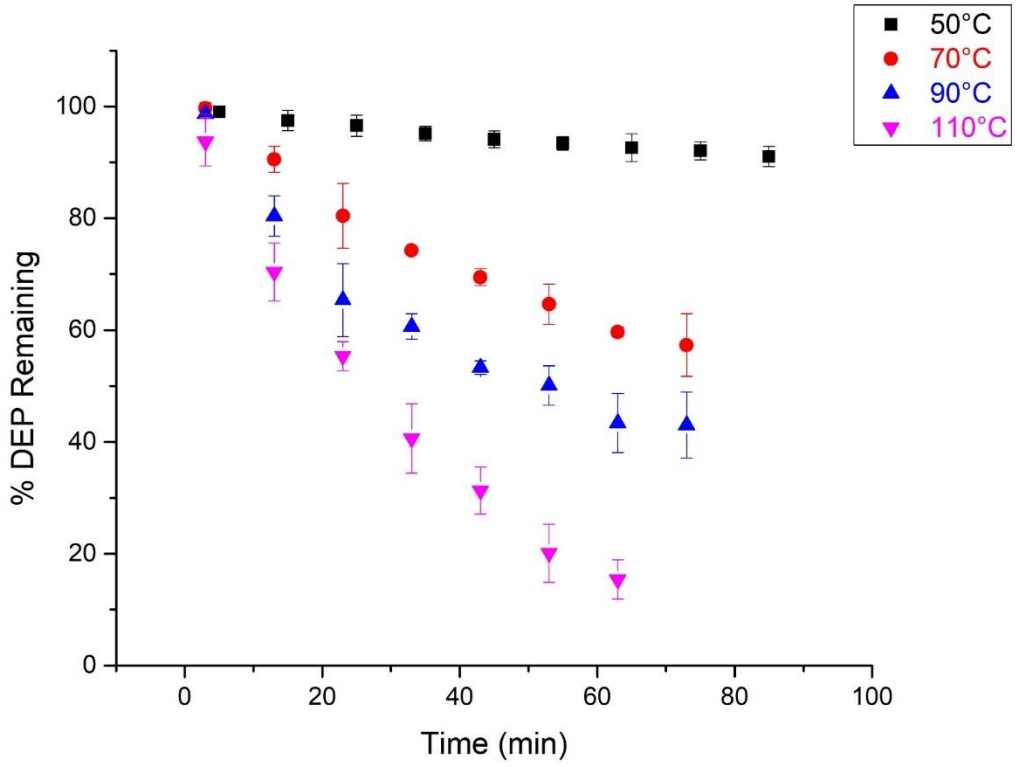

Figure 4.04. Kinetic data of diethyl phosphite (DEP) concentration versus time for the pseudo-first-order transesterification model reaction of DEP and PhPol in the presence of 10 mol% tetramethyl-1, 6-hexane diamine (TMHDA).

The rate of disappearance of DEP was calculated by the assumption of products and monitored as a function of temperature, which followed pseudo-first-order kinetics (Figure 4.04). The reference rate was used to determine an Arrhenius activation energy (E_a) of 54.9±2.5 kJ/mol for transesterification reaction of dialkyl phosphites (Figure 4.05).

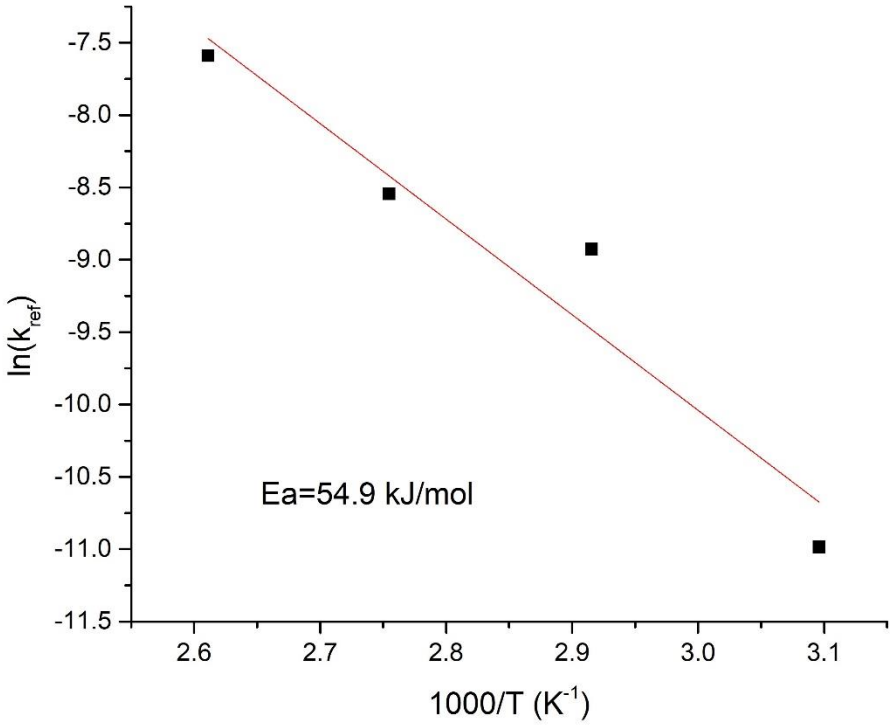

Figure 4.05. Temperature-dependent kinetics afford an Arrhenius activation energy (E_a) of 54.9±2.5 kJ/mol for transesterification reaction between DEP and PhPol.

4.04. Preparation of dynamic cross-linked EVOH.

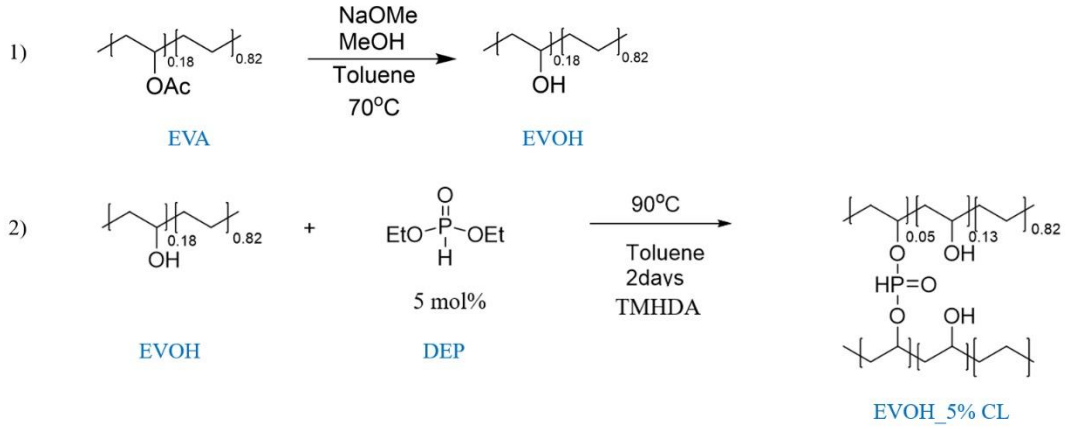

Scheme 4.03. (1) Hydrolysis of poly(ethylene-vinyl acetate) (EVA); (2) EVOH cross-linked by DEP via transesterification to form EVOH_5% CL vitrimer.

Hydrolysis of poly(ethylene-vinyl acetate) (EVA): Poly(ethylene-vinyl acetate) (EVA) (40g, Celanese 1807EG, 18 mol% VA) was dissolved in 300 mL toluene and heated up to 70°C while stirring. After one hour for fully dissolving, 25 wt% sodium methoxide in methanol (1.1 *equiv.* 42.5 mL) was added. The solution turned cloudy and stirred overnight. HCl solution (2M, 1.1 *equiv.* 20.0 mL) was added while a gentle stirring for 10 mins. The aqueous layer was removed by a long glass pipet. The organic layer was precipitated into cold MeOH (2L) while vigorously stirring. The crude product (pale yellow) was filtered and re-dissolved in 300 mL toluene, then precipitated into cold MeOH (2L) until the color was totally white. The product was dried under vacuum overnight at 80°C to yield poly(ethylene-vinyl alcohol) (EVOH).

General procedure for EVOH vitrimer preparation: Poly(ethylene-vinyl alcohol) (EVOH) (10g, 18 mol% VOH) was dissolved in 100 mL toluene and heated up to 90°C while stirring. Diethyl phosphite (DEP) (2 or 5 mol% to VOH) and catalyst tetramethyl-1, 6-hexane diamine (TMHDA) (10 mol% to DEP) were added slowly. The solution was stirred for 2 days until a gel formed. The gel was dried under vacuum overnight at 80°C to yield EVOH vitrimer (EVOH_2% CL and EVOH_5% CL). The cross-linked EVOH was then cut into small pieces (approximately 1 mm^3) with scissors and hot-pressed into a thin film by Carver Press at 170°C and pressurized to 5 tons (~1000 psi) for 20 minutes followed by a 120-minute cool down to ambient temperature with pressure. For reprocessing, the samples were re-cut into small pieces and re-pressed.

The samples of EVOH, EVOH_2% CL, and EVOH_5% CL were characterized by Fourier-transform infrared spectroscopy (FT-IR). Peaks at 1250 cm^{-1} and 950 cm-1 represented the existence of P=O double bond stretching and P-O-C bending, respectively, which confirmed the phosphite cross-linkage in EVOH_2% CL and EVOH_5% CL vitrimers.

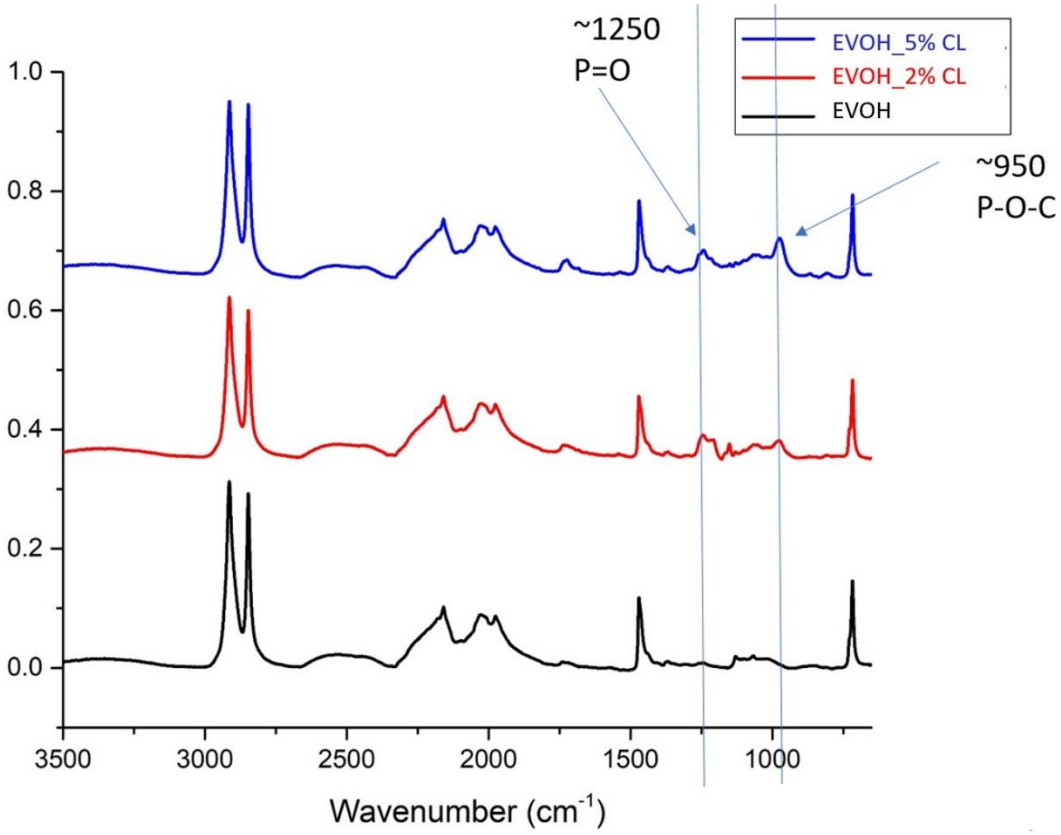

Figure 4.06. IR spectrums for EVOH, EVOH_2% CL and EVOH_5% CL.

4.05 Gel fraction testing for reprocessed vitrimer samples.

Thin-film vitrimer samples were cut into 1 cm x 1cm square and suspended in excess toluene (20 mL) in a small vial. The vial was heated up to 90°C for overnight. The samples were swollen in toluene, and uncross-linked EVOH chains were dissolved in toluene and left the vitrimer system. The swollen samples were removed from the vial and dried under vacuum overnight at 80°C. The weight before and after testing was listed in Table 4.01, and gel fraction was calculated. Further calculation of molecular weight between crosslinks (M_c) was provided in the appendix.

Table 4.01. Gel fraction data for reprocessed EVOH_2% CL and EVOH_5% CL.

Sample	2%CL 1st cycle	2%CL 2nd cycle	2%CL 3rd cycle	5%CL 1st cycle	5%CL 2nd cycle	5%CL 3rd cycle
Before (mg)	80.5	78.0	70.9	99.8	95.6	96.0
After (mg)	73.2	71.3	65.6	90.8	87.8	89.9
Fraction (%)	90.9	91.4	92.5	91.0	91.8	93.6

4.06 Thermal stability of vitrimer samples.

The thermal properties of the vitrimer samples were carefully tested. The differential scanning calorimetry (DSC) curve for EVOH_5% CL (Figure 4.07 B) showed a broader peak around 96°C, comparing to EVOH at 109°C, indicated only a small portion of EVOH chains in EVOH_5% CL network, which has a low molecular weight, was not cross-linked and melted during the scan.

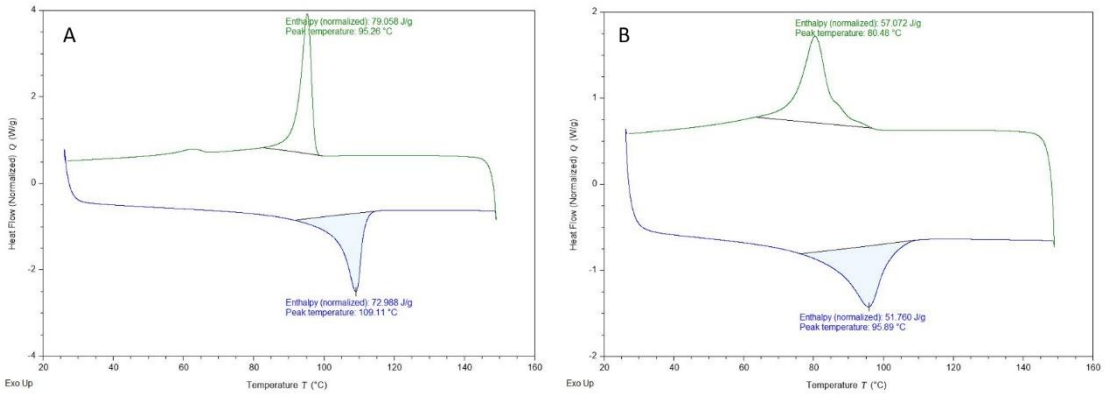

Figure 4.07. DSC curves of (A) EVOH; (B) EVOH_5% CL from 30°C to 150°C with 10°C/min ramp rate.

Thermogravimetric analysis (TGA) presented all EVOH and the vitrimers having outstanding thermal stability under nitrogen gas protection (Figure 4.08). Surprisingly, 5% weight loss of EVOH is as high as 445°C, and the weight losses in vitrimers before 400°C are mostly catalyst TMHDA, which has a boiling point at 200°C. The free hydroxyl groups on EVOH have no effect on thermal performance.

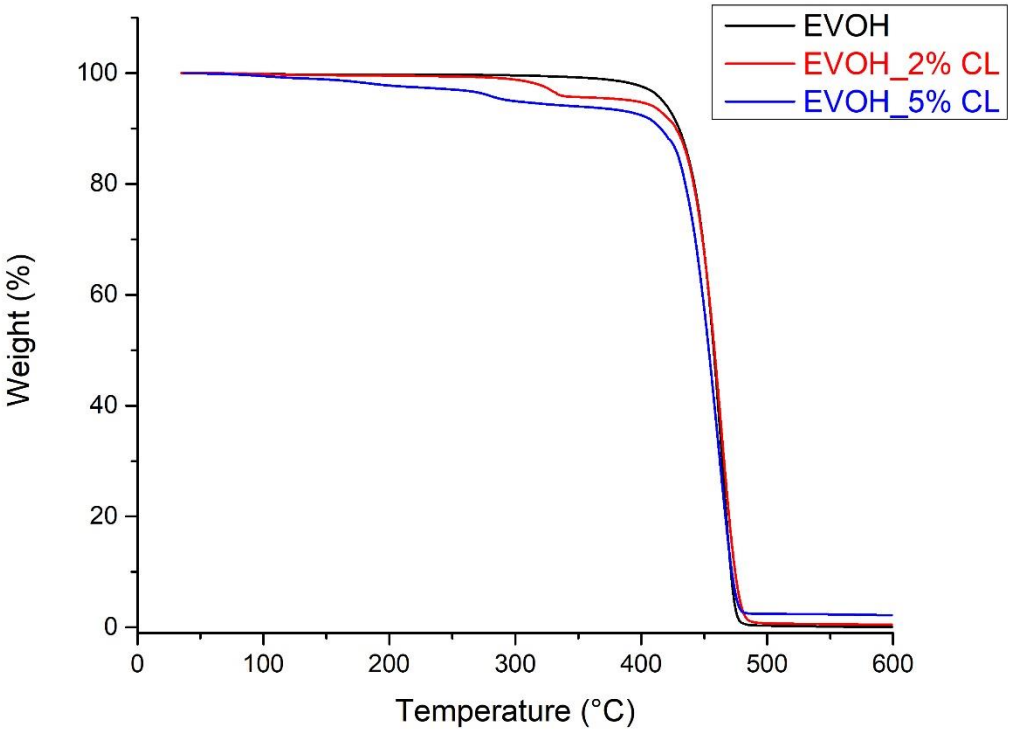

Figure 4.08. TGA curves of EVOH, EVOH_2% CL and EVOH_5% CL from 35°C to 600°C with 10°C/min ramp rate under nitrogen gas protection.

4.07 Mechanical property of vitrimer samples.

Dynamic mechanical analysis (DMA) frequency sweep curves clearly indicated rubber plateau after the melting transition. Both EVOH_2% CL and EVOH_5% CL showed an improved melt strength and stability at high temperatures. The storage modulus at the rubber plateau of EVOH_5% CL is larger than EVOH_2% CL, which demonstrated a higher cross-link density, and the plateau onset temperature of the EVOH_5% CL also meet the melting transition on the DSC curve.

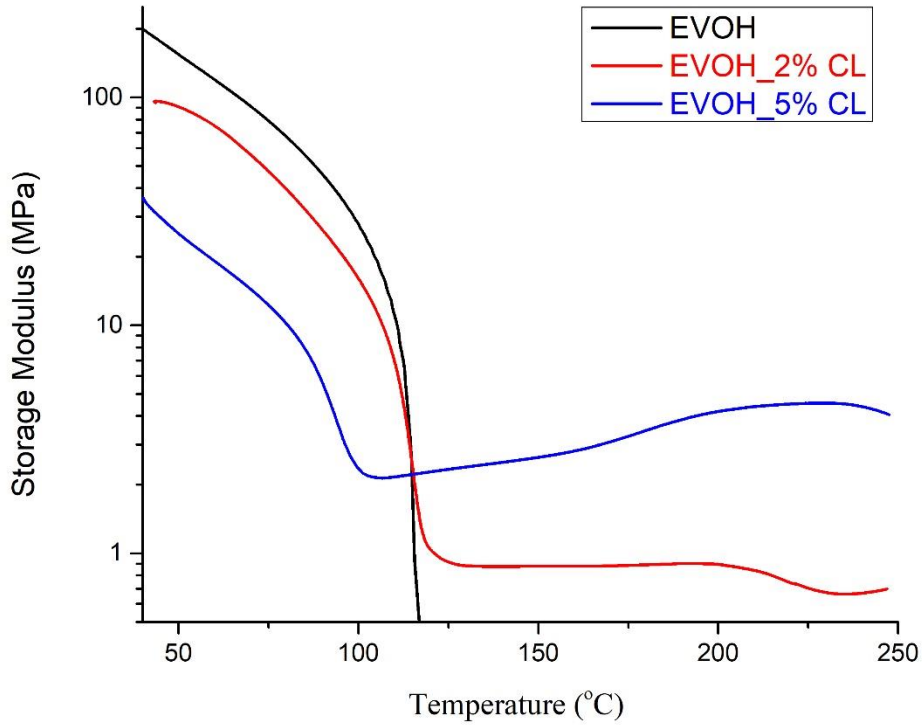

Figure 4.09. DMA frequency sweep curves of EVOH, EVOH_2% CL and EVOH_5% CL from 40°C to 250°C with 3°C/min ramp rate, 1% strain and 1Hz frequency.

4.08 Creep of vitrimer samples.

Furthermore, the creep resistance was improved by the dynamic cross-linked network (Figure 4.10). EVOH_5% CL exhibited scarcely creep at 80 °C. However, when the temperature increased higher than the melting point of EVOH, the vitrimer showed rapid elastic response at the beginning, then a creep region. Temperature-dependent transesterification reaction leads to a faster creep for the vitrimer at a higher temperature. All the samples showed permanent deformation after recovery, which demonstrated the

exchange reaction between covalent bonds occurred and changed the shape of the material.

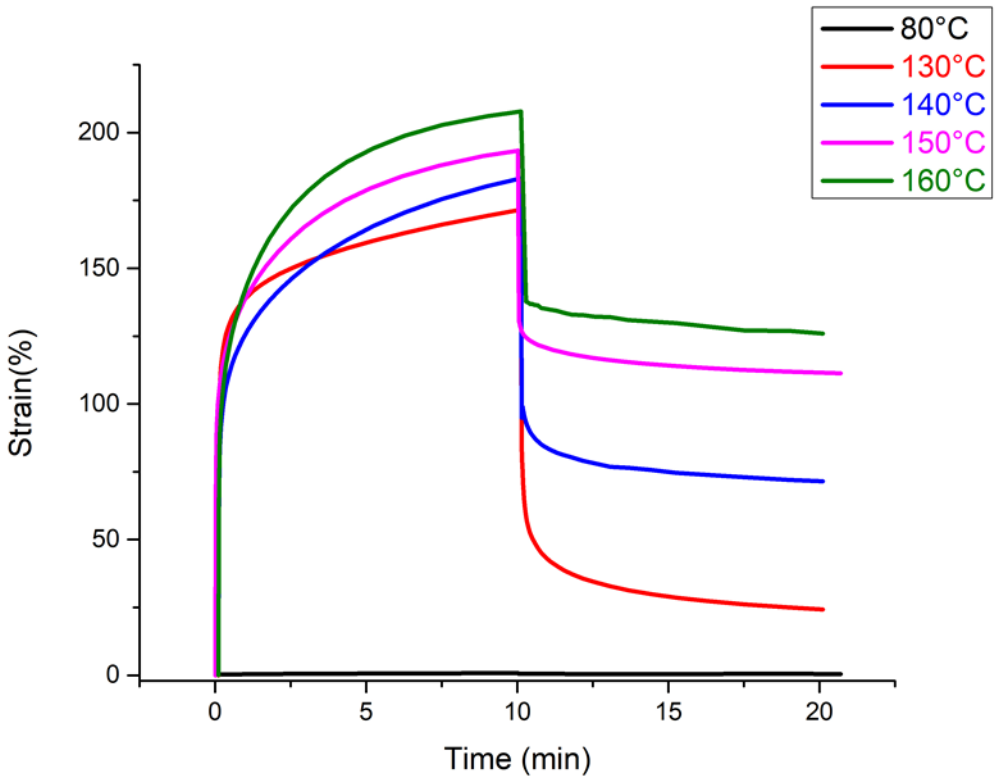

Figure 4.10. Creep tests of EVOH_5% CL vitrimer at different temperatures under 0.1 MPa stress. Both creep time and recovery time are 10 minutes.

4.09 Stress relaxation of vitrimer samples.

As shown in Figure 4.11, stress relaxation studies of EVOH_2% CL (A) and EVOH_5% CL (C) vitrimers were tested on DMA by tracing the stress/modulus change at a constant 10% strain. Individually, samples are tested at various temperatures from 150 to 190 °C. Sample at higher temperature has a faster relaxation than lower temperature, which reach the totally relaxed line, 1/e=36.8%.[13] The relaxation time at this point is defined as τ*.

Based on the Arrhenius equation, $\tau^* = \tau^0 \exp(E_a/RT)$, we accordingly plotted $\ln(\tau^*)$ to 1000/T and calculated the activation energies of bulk transesterification exchange reaction for flow in EVOH_2% CL (B) and EVOH_5% CL (D) vitrimers were 144.5±3.6 kJ/mol and 121.1±0.5 kJ/mol, respectively. Comparing to the activation energy from small-molecule model reaction (Figure 4.05), the numbers here are doubled. The hydroxyl groups on EVOH are all secondary groups, which have a decrease in reaction rate comparing to the primary alcohol groups in PhPol. On the other hand, the hydrogen bonds between EVOH polymer chains could also increase the interaction force, which drives up the activation energies for flow in the vitrimer system. Fewer cross-link points for transesterification reaction could bring about the fact that EVOH_2% CL has slightly higher activation energy. Another important parameter of vitrimers is the topology freezing transition temperature (T_v), which is calculated in the appendix.

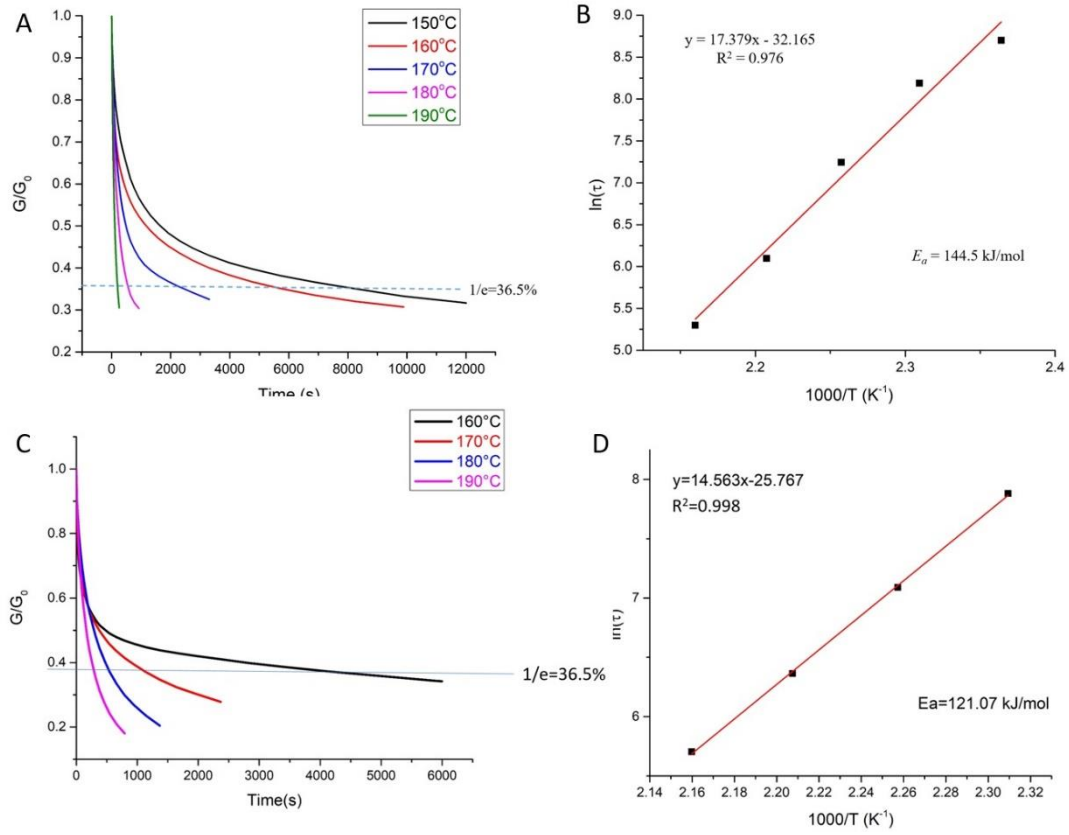

Figure 4.11. Stress relaxation studies of (A) EVOH_2% CL and (C) EVOH_5% CL with a 10% constant strain. Arrhenius activation energies (E_a) of (B) EVOH_2% CL and (D) EVOH_5% CL.

4.10 Tensile tests of vitrimer samples.

Dog bone-shaped samples were cut by ASTM D-412 tensile sample cutting die from the vitrimer thin films. The dog bones were mixed with the remaining films and cut into small pieces for reprocessing by hot press (Figure 4.12).

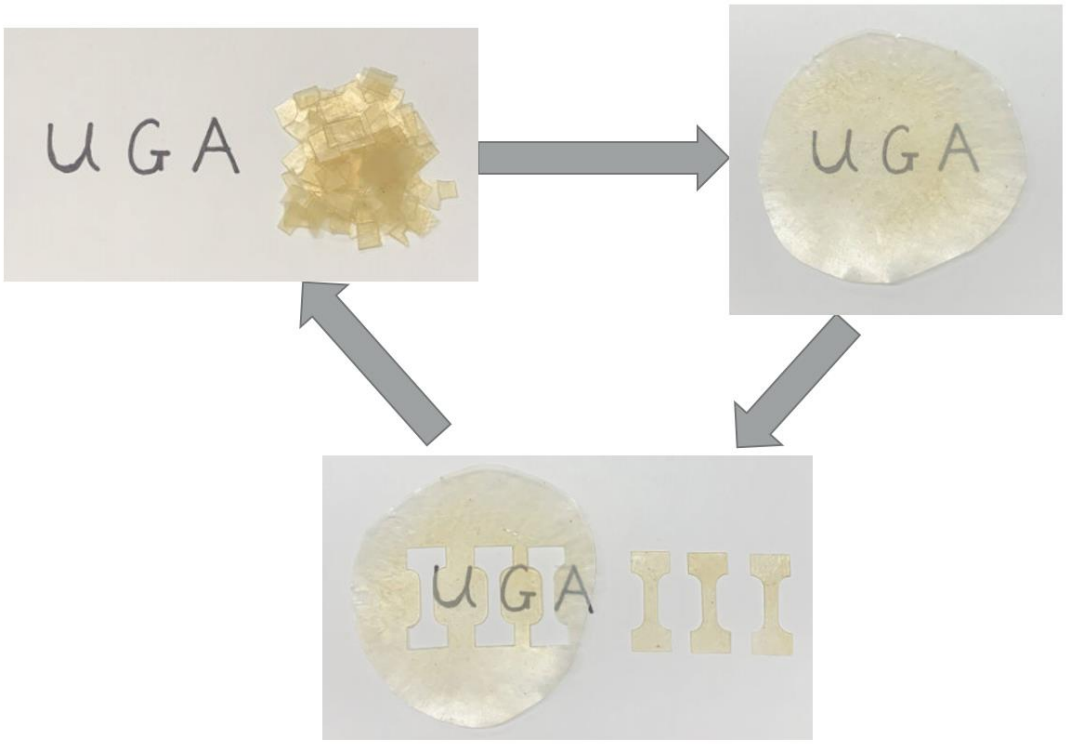

Figure 4.12. The vitrimers were cut into pieces and hot-pressed into film, tensile tested, and reprocessed three times.

Young's modulus, tensile strength, and elongation at break remain almost constant for the three cycles. Detailed data could be found in the table in the appendix.

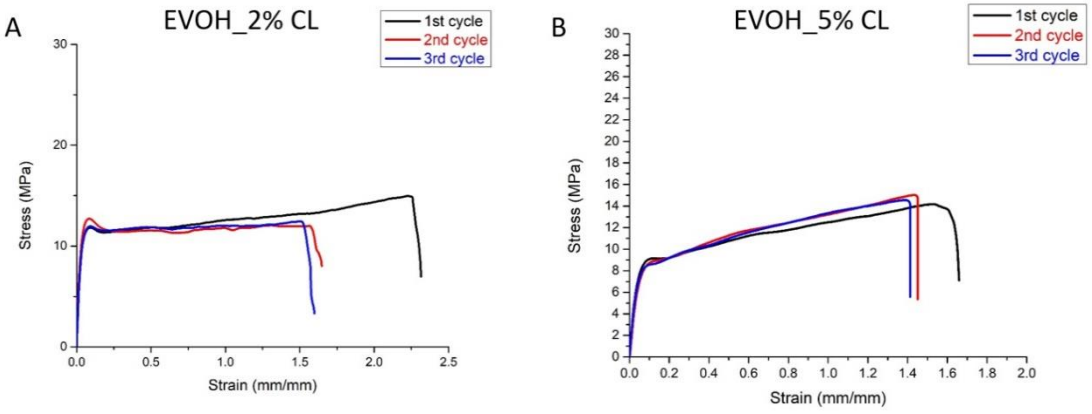

Figure 4.13. Three cycles tensile tests of (A) EVOH_2% CL and (B) EVOH_5% CL.

4.11 Vitrimers in extrusion.

After obtained single-step dynamic cross-linked EVOH material, a large amount of polymeric material was produced, on the other hand, like all other vitrimer materials, searching for a pathway to expand the material to industry level turned into the focal point. Nevertheless, hot pressing fits well for academic research. Continuous processing through extrusion is always a better way to handle a large quantity of material.

Unfortunately, dynamic cross-linked networks are barely impossible to put into extruder directly. As shown in Figure 4.14, EVOH_5% CL vitrimer was not flowing in the extruder and flushed out samples with rough surface morphology compared to EVOH on the left, and it was easy to break into powder.

Figure 4.14. Picture of EVOH and EVOH_5% CL flushed out of extruder at 200°C.

By opening the extruder to see what exactly happened when EVOH_5% CL was extruded (Figure 4.15), higher pressure regions (~200 bar), such as the backchannel for cycling and blending and the front tip of the drills, vitrimer films were formed perfectly. On the other hand, the vitrimer exploded into powder immediately when the material

passed low-pressure regions, like the exit of the backchannel and the extruder. This phenomenon demonstrated the exchange reaction in the vitrimer system is not only controlled by temperature but also influenced by pressure.

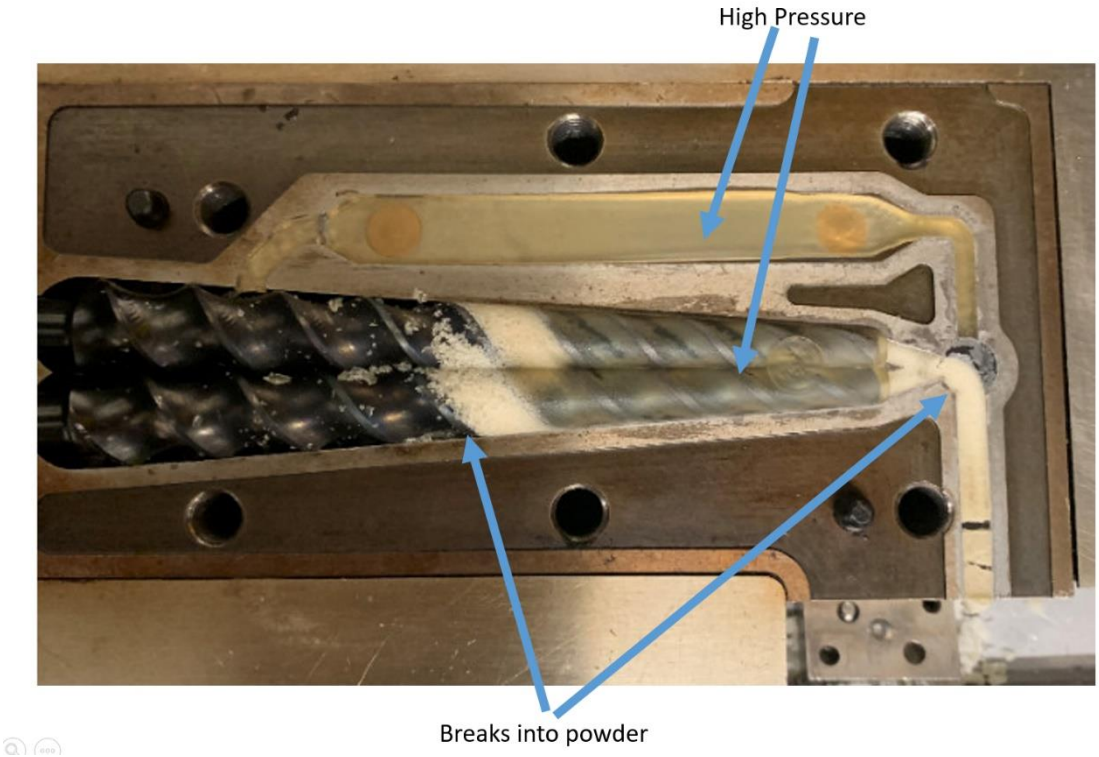

Figure 4.15. Picture of the opened extruder after flush out EVOH_5% CL.

Recently discovered, dimaleimide bis(dioaborolane) enables commercial polyethylene (PE) to be converted into a vitrimer via one-step reactive extrusion.[14] The mechanical dynamic cross-linked PE was easily reprocessed by extrusion or compression molding. Remarkably, the gel content was approximately 40%, which indicated the material was not fully cross-linked, PE chains were implanted as a lubricant for flow. Coincidentally, by adding Zn(II) catalysts combined with a slight excess of diols into polyurethane (PU)

vitrimer during extrusion, mixed PU samples were successfully melt-processed in an extruder on a large scale.[15] The diols not only diluted the polymeric network but also reversed crosslinking via the urethane linkages. We were inspired by these fantastic ideas and tried to blend our EVOH vitrimer with different polymers with hydroxyl groups on the backbone to reduce the cross-link density and decrease the viscosity during extrusion.

By mixing EVOH and EVOH_5% CL vitrimer powders together in the extruder for 6 minutes at 150°C, polymer resin with smooth surface could be generated (Figure 4.16). The weight ratio of vitrimer was brought to 30% as the highest, otherwise the samples were not be diluted enough to form a smooth surface. The resins were directly injection molded at 70°C for 10 seconds, and opened at once. The perfect dog bone shaped samples were left on bench for 24 hours before studied the mechanical properties. Even the ratio of vitrimer was up to 30%, no significant change in either the Young's modulus, or the elongation at break of the blending. In a nutshell, certain blends of EVOH and vitrimer successfully melt-processed in an extruder on a large scale.

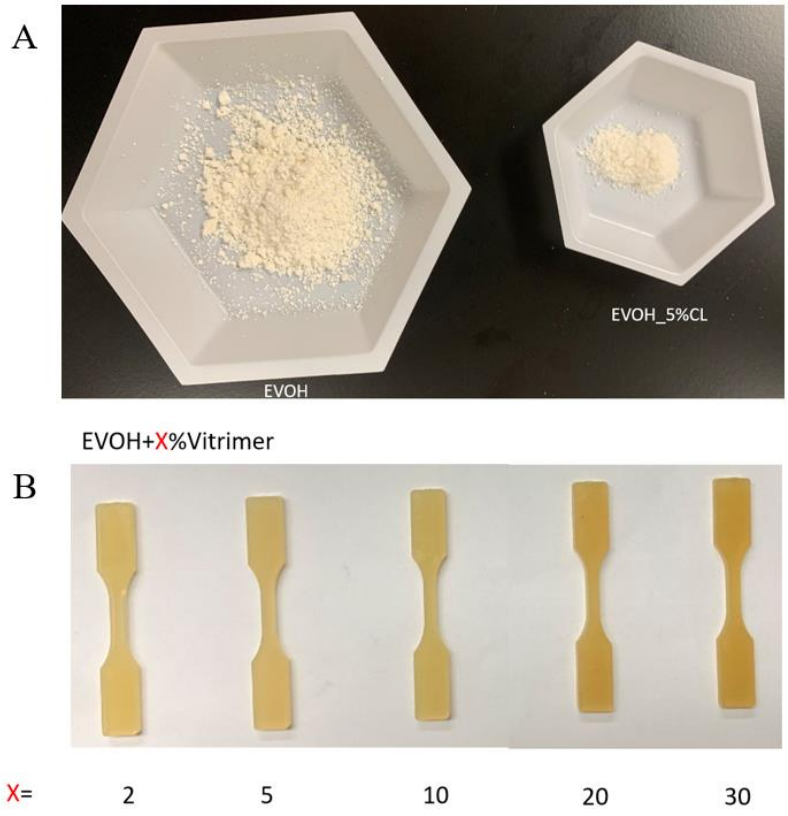

Figure 4.16. (A) EVOH and EVOH_5% CL vitrimer powders grinded by the cryogenic grinder. (B) Injection molded dog bones with different mixture ratios between EVOH and EVOH_5% CL.

4.12 Reference

1. Ren, M.; Cheng, Y.; Duan, Q.; Zhou, C., Transesterification Reaction and the Repair of Embedded Ribonucleotides in DNA Are Suppressed upon the Assembly of DNA into Nucleosome Core Particles. *Chemical Research in Toxicology* **2019,** *32* (5), 926-934.

2. Lönnberg, H., Cleavage of RNA phosphodiester bonds by small molecular entities: a mechanistic insight. *Organic & Biomolecular Chemistry* **2011,** *9* (6), 1687-1703.

3. Branham, K. E.; Mays, J. W.; Gray, G. M.; Bharara, P. C.; Byrd, H.; Bittinger, R.; Farmer, B., Polycondensations of dimethyl phosphonate with diols: SEC and 1P and 13C NMR spectroscopic studies. *Polymer* **2000,** *41* (9), 3371-3379.

4. Nifant'ev, I. E.; Shlyakhtin, A. V.; Bagrov, V. V.; Komarov, P. D.; Kosarev, M. A.; Tavtorkin, A. N.; Minyaev, M. E.; Roznyatovsky, V. A.; Ivchenko, P. V., Controlled ring-opening polymerisation of cyclic phosphates, phosphonates and phosphoramidates catalysed by heteroleptic BHT-alkoxy magnesium complexes. *Polymer Chemistry* **2017,** *8* (44), 6806-6816.

5. Annakutty, K. S.; Kishore, K., Flame retardant polyphosphate esters: 1. Condensation polymers of bisphenols with aryl phosphorodichloridates: synthesis, characterization and thermal studies. *Polymer* **1988,** *29* (4), 756-761.

6. Yang, A.-H.; Deng, C.; Chen, H.; Wei, Y.-X.; Wang, Y.-Z., A novel Schiff-base polyphosphate ester: Highly-efficient flame retardant for polyurethane elastomer. *Polymer Degradation and Stability* **2017,** *144*, 70-82.

7. Müller, W. E. G.; Wang, X.; Guo, Y.-W.; Schröder, H. C., Potentiation of the cytotoxic activity of copper by polyphosphate on biofilm-producing bacteria: a bioinspired approach. *Mar Drugs* **2012,** *10* (11), 2369-2387.

8. Liu, J.; Huang, W.; Zhou, Y.; Yan, D., Synthesis of Hyperbranched Polyphosphates by Self-Condensing Ring-Opening Polymerization of HEEP without Catalyst. *Macromolecules* **2009,** *42* (13), 4394-4399.

9. Feng, X.; Li, G., Versatile Phosphate Diester-Based Flame Retardant Vitrimers via Catalyst-Free Mixed Transesterification. *ACS Applied Materials & Interfaces* **2020,** *12* (51), 57486-57496.

10. Majumdar, S.; Zhang, H.; Soleimani, M.; van Benthem, R. A. T. M.; Heuts, J. P. A.; Sijbesma, R. P., Phosphate Triester Dynamic Covalent Networks. *ACS Macro Letters* **2020,** *9* (12), 1753-1758.

11. Malowan, J. E.; Traise, T. P.; Toy, A. D. F., Dioctyl Phosphite. In *Inorganic Syntheses*, 1953; pp 61-62.

12. Bálint, E.; Tajti, Á.; Tóth, N.; Keglevich, G., Continuous Flow Alcoholysis of Dialkyl H-Phosphonates with Aliphatic Alcohols. *Molecules* **2018,** *23* (7), 1618.

13. Montarnal, D.; Capelot, M.; Tournilhac, F.; Leibler, L., Silica-Like Malleable Materials from Permanent Organic Networks. *Science* **2011,** *334* (6058), 965-968.

14. Maaz, M.; Riba-Bremerch, A.; Guibert, C.; Van Zee, N. J.; NicolaÿR., Synthesis of

Polyethylene Vitrimers in a Single Step: Consequences of Graft Structure, Reactive Extrusion Conditions, and Processing Aids. *Macromolecules* **2021,** *54* (5), 2213-2225.

15. Khan, A.; Naveed, M.; Rabnawaz, M., Melt-reprocessing of mixed polyurethane thermosets. *Green Chemistry* **2021,** *23* (13), 4771-4779.

Appendix 1. Calculation of T_v

The topology freezing temperature, T_v, is defined as the temperature when viscosity reaches 10^{12} Pa, the material transformed from a viscoelastic solid into a liquid. The viscosity can be calculated from the rubbery plateau storage modulus by the Maxwell equation.

$$\eta = G \cdot \tau^* = \frac{E}{2(1+\nu)} \cdot \tau^*$$

Where:

G = shear modulus

τ^* = relaxation time

E = storage modulus

v = Poisson's ratio

As the EVOH_5% CL vitrimer is generated from EVOH with 18% vinyl alcohol, we could approximately put the Poisson's ratio for LDPE (0.43) into the equation. The storage modulus (E) at the rubber plateau was obtained from Figure 4.09, and the viscosity η was defined as 10^{12} Pa. The extrapolated relaxation time τ^* calculated here was put back into the Arrhenius equation in Figure 4.10 to find T_v of EVOH_5% CL equals 82°C, respectively.

Appendix 2. Calculation of M_c

The molecular weight between cross-link points, M_c, is calculated by the following equation.

$$Mc = 2(1 + \nu)\frac{\rho RT}{E}$$

Where:

E = storage modulus of the rubber plateau

v = Poisson's ratio

ρ = density of the material

T = temperature of the rubber plateau

By putting the values at rubber plateau in Figure 4.09 and Poisson's ratio for LDPE (0.43) into the equation, the M_c value for EVOH_5% CL vitrimer was calculated to be 5.4 kDa, respectively.

Appendix 3. NMR, Mass and FT-IR spectra.

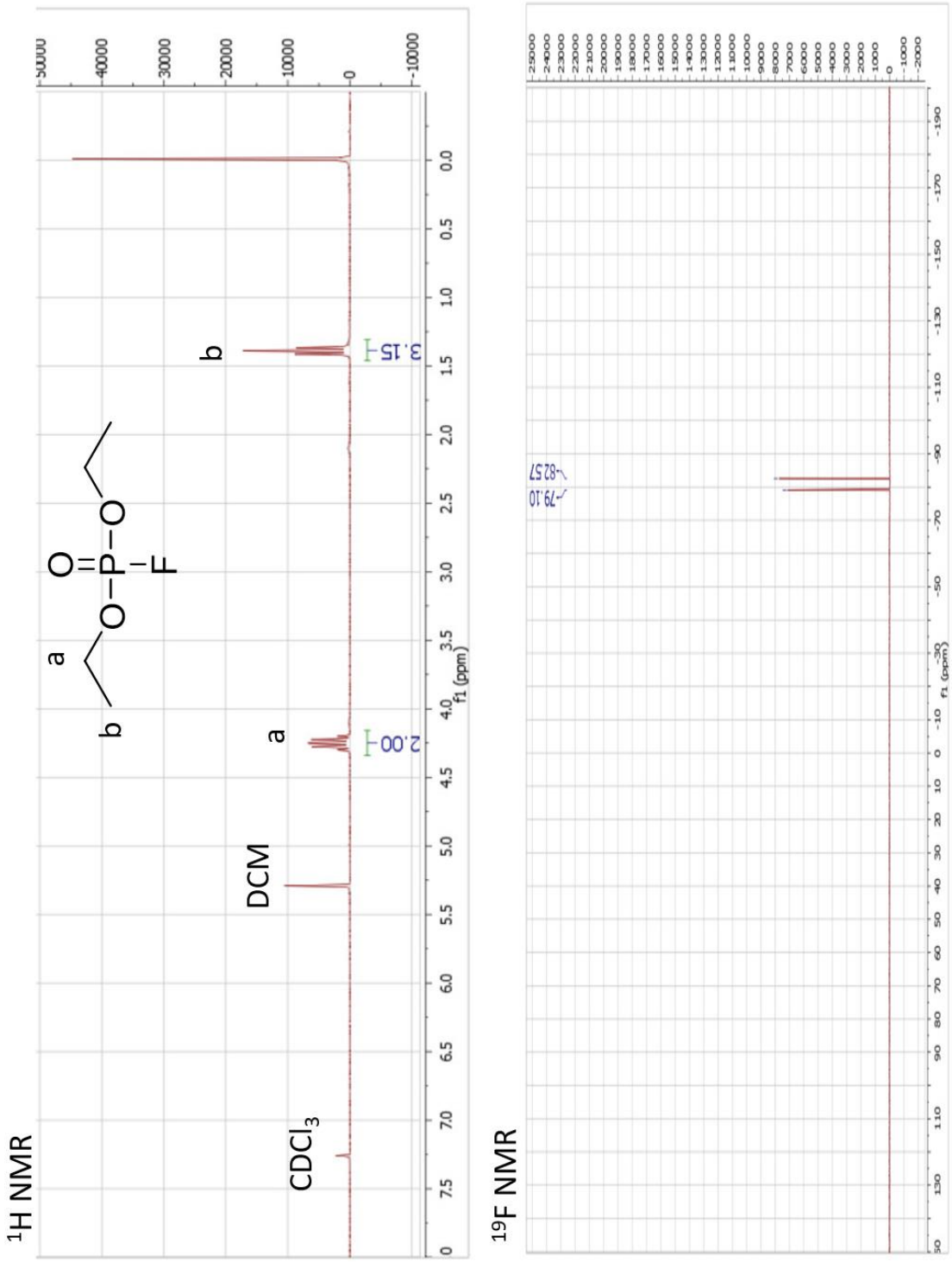

^{1}H NMR

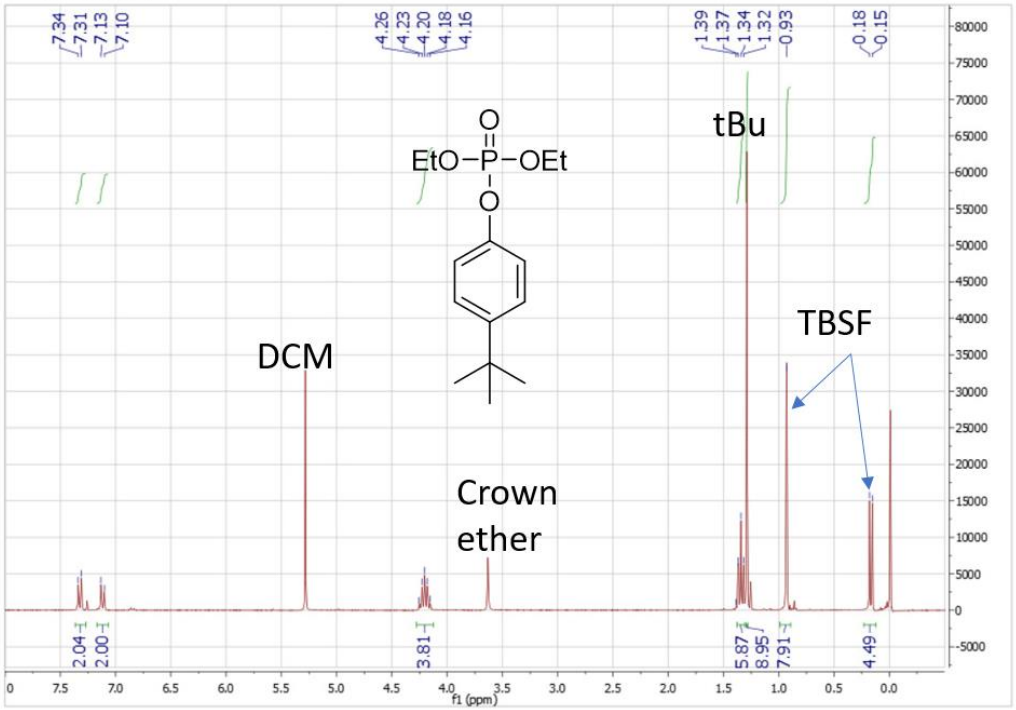

^{31}P NMR

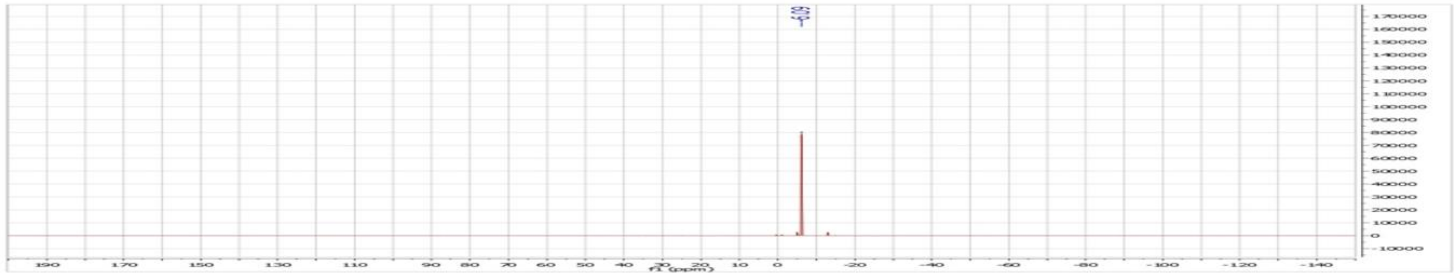

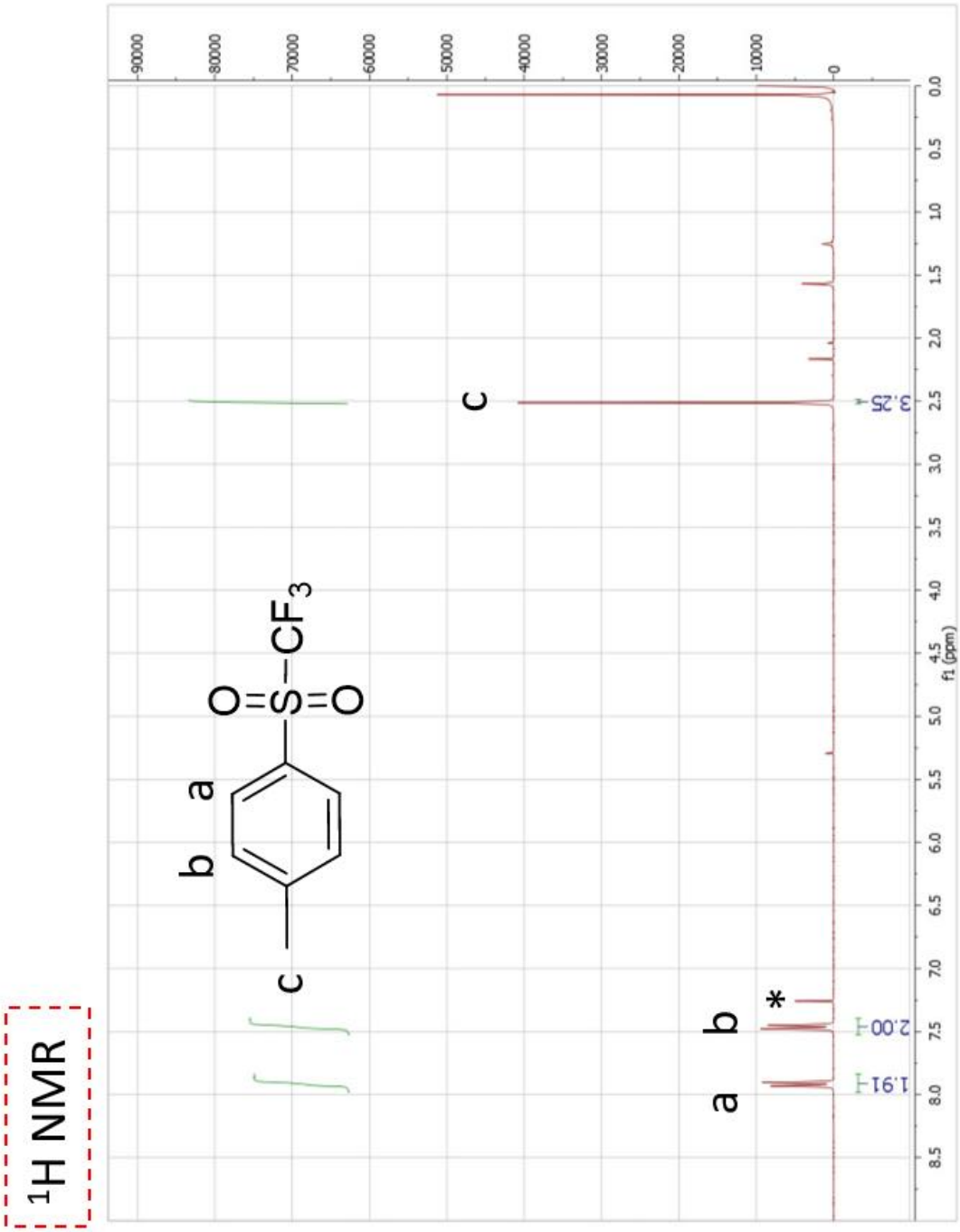
^{1}H NMR
b a
O
S
CF3
O
c
a b
*
c
3.25
2.00
1.91
f1 (ppm)

^{19}F NMR

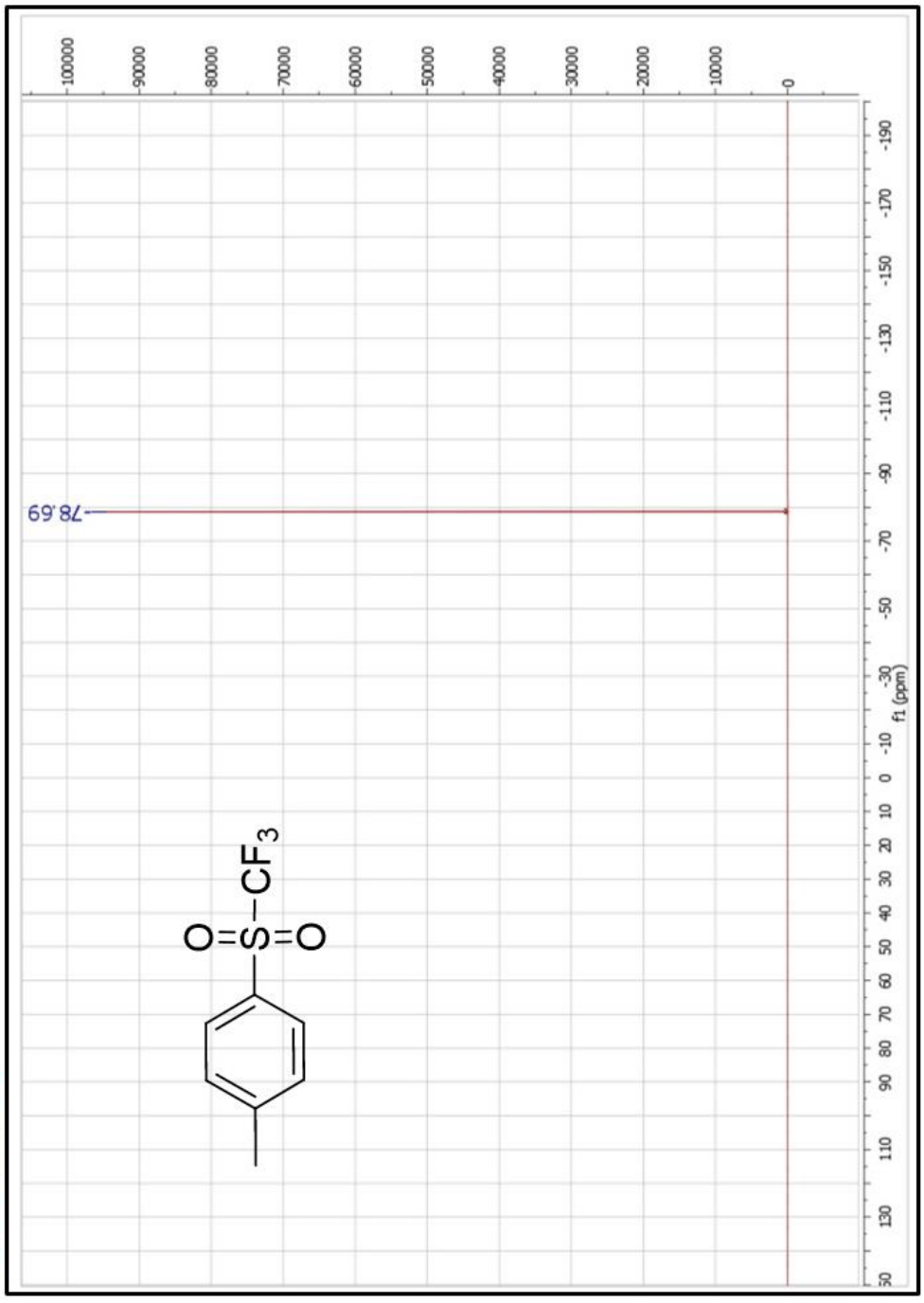

^{1}H NMR

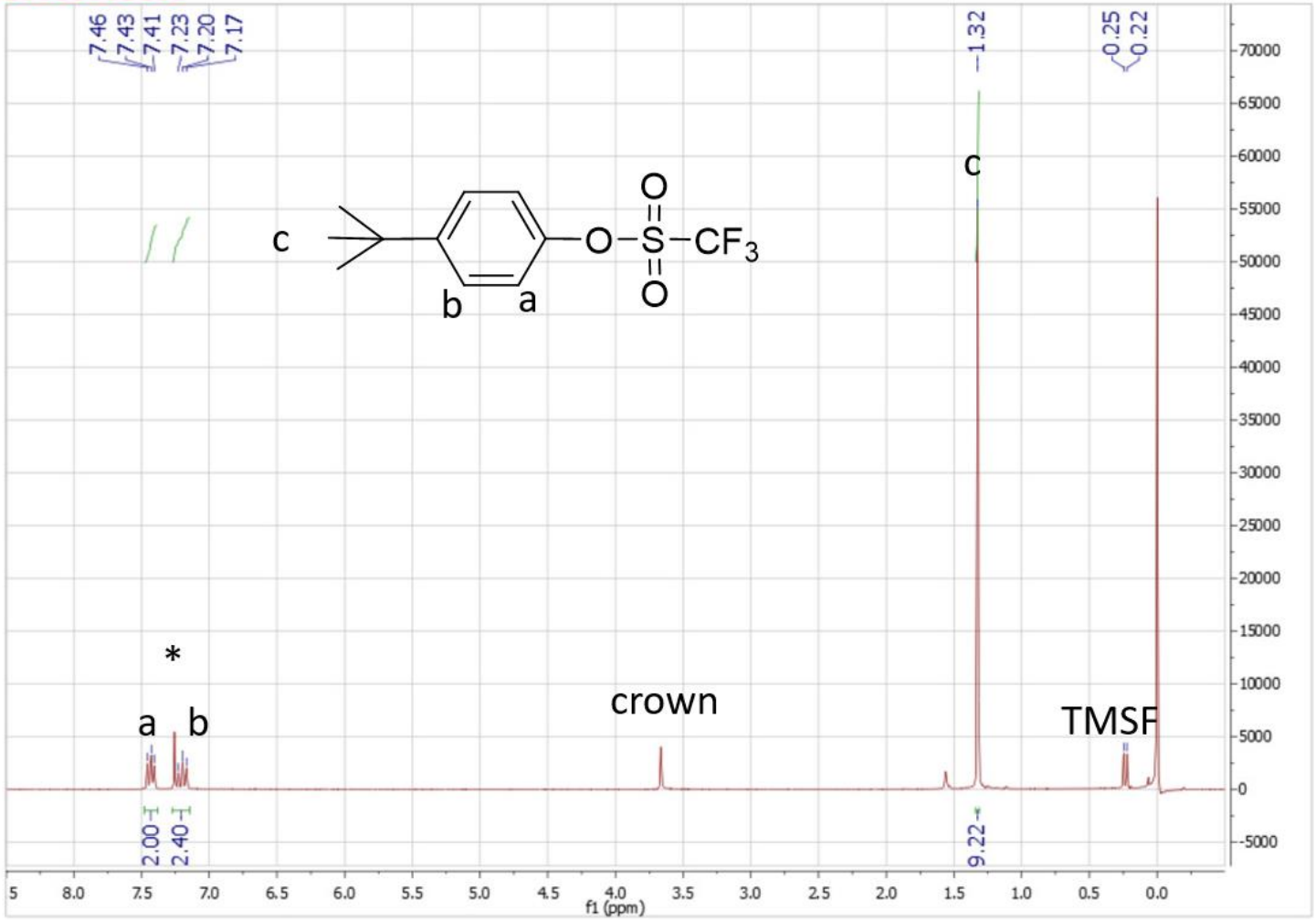
7.46
7.43
7.41
7.23
7.20
7.17
1.32
0.25
0.22
c
O
S
CF3
b
a
*
a
b
crown
TMSF
2.00
2.40
9.22
f1 (ppm)

^{1}H NMR

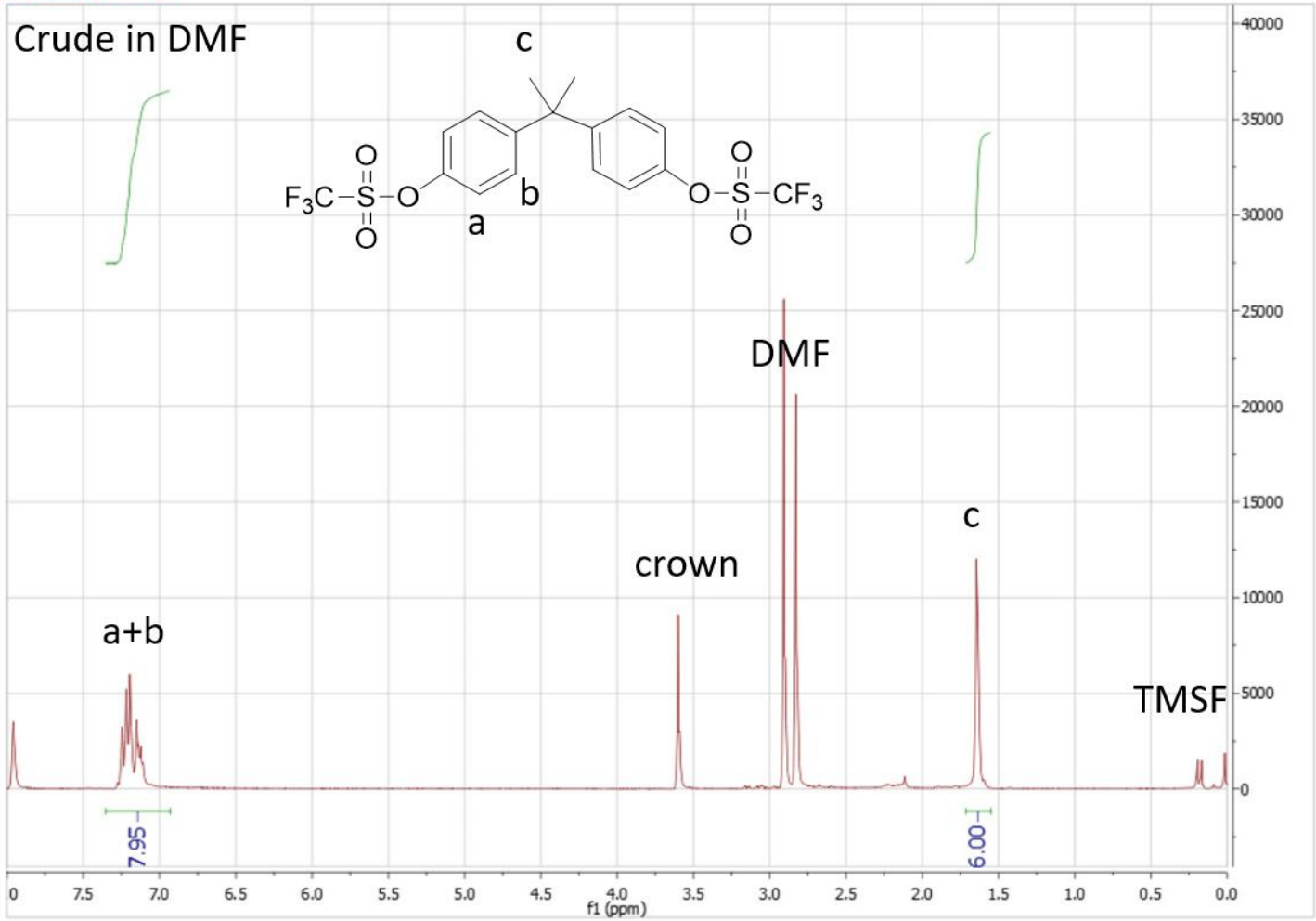

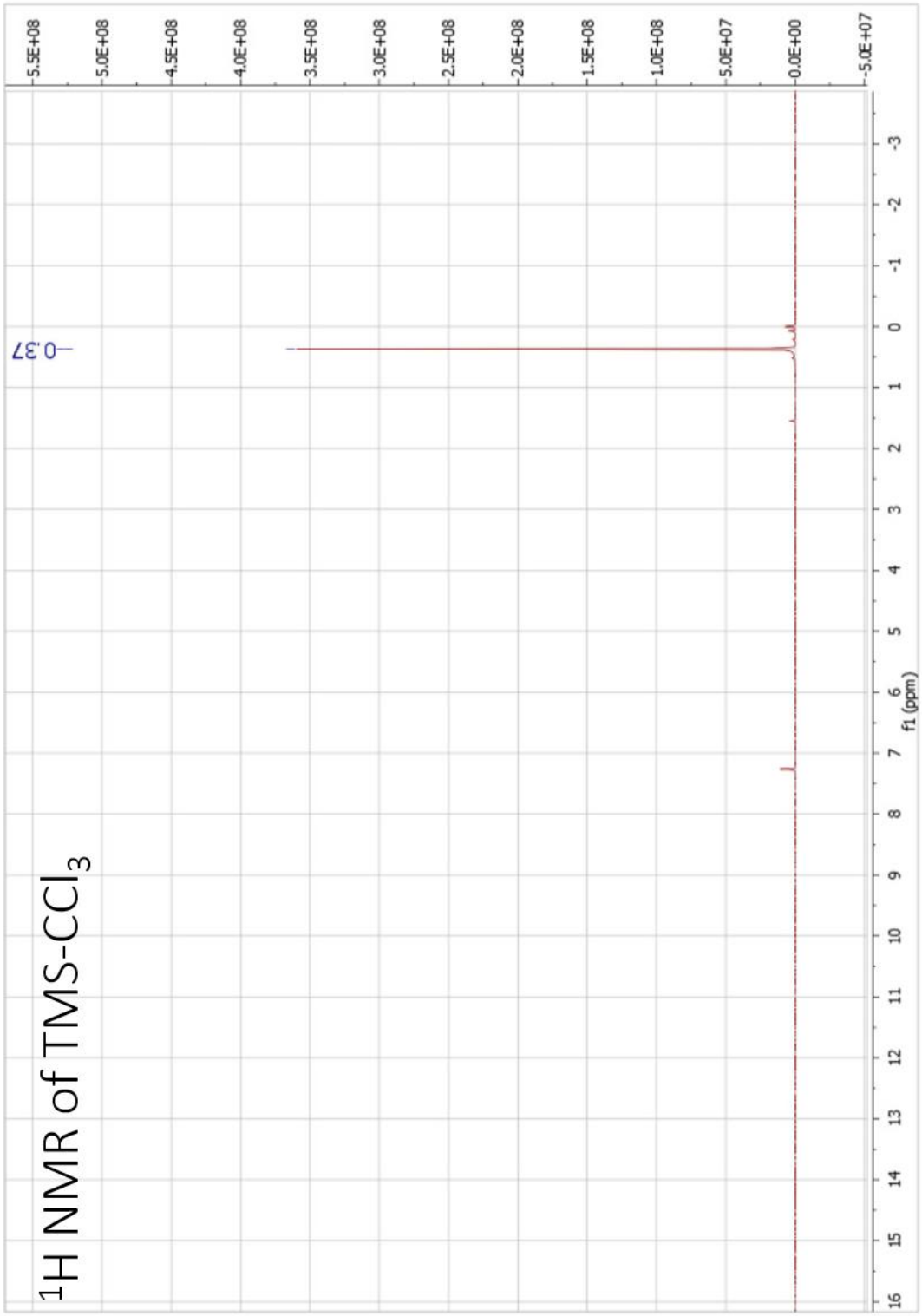
1H NMR of TMS-CCl3
0.37
f1 (ppm)

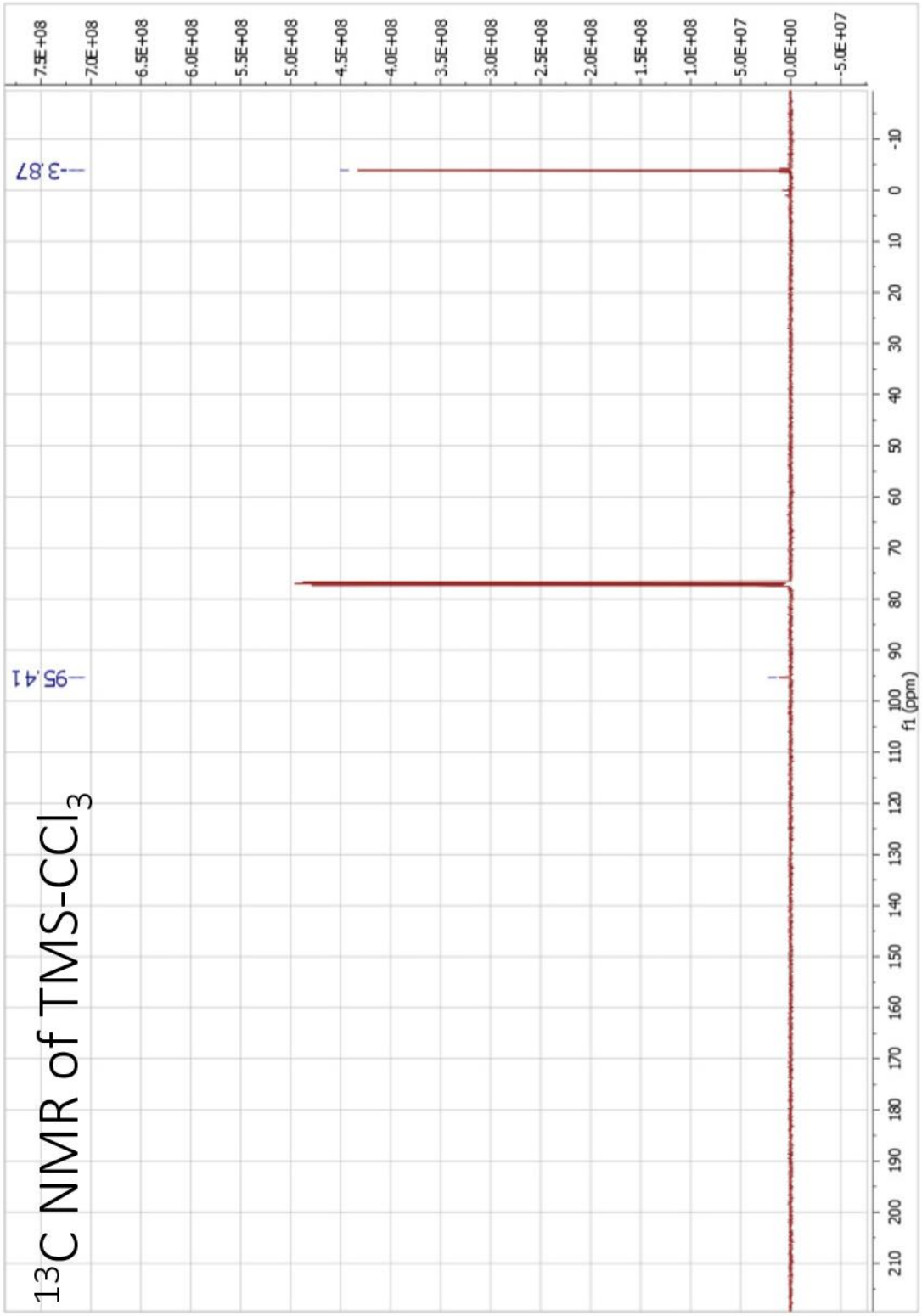
^{13}C NMR of TMS-CCl$_3$
95.41
-3.87
f1 (ppm)

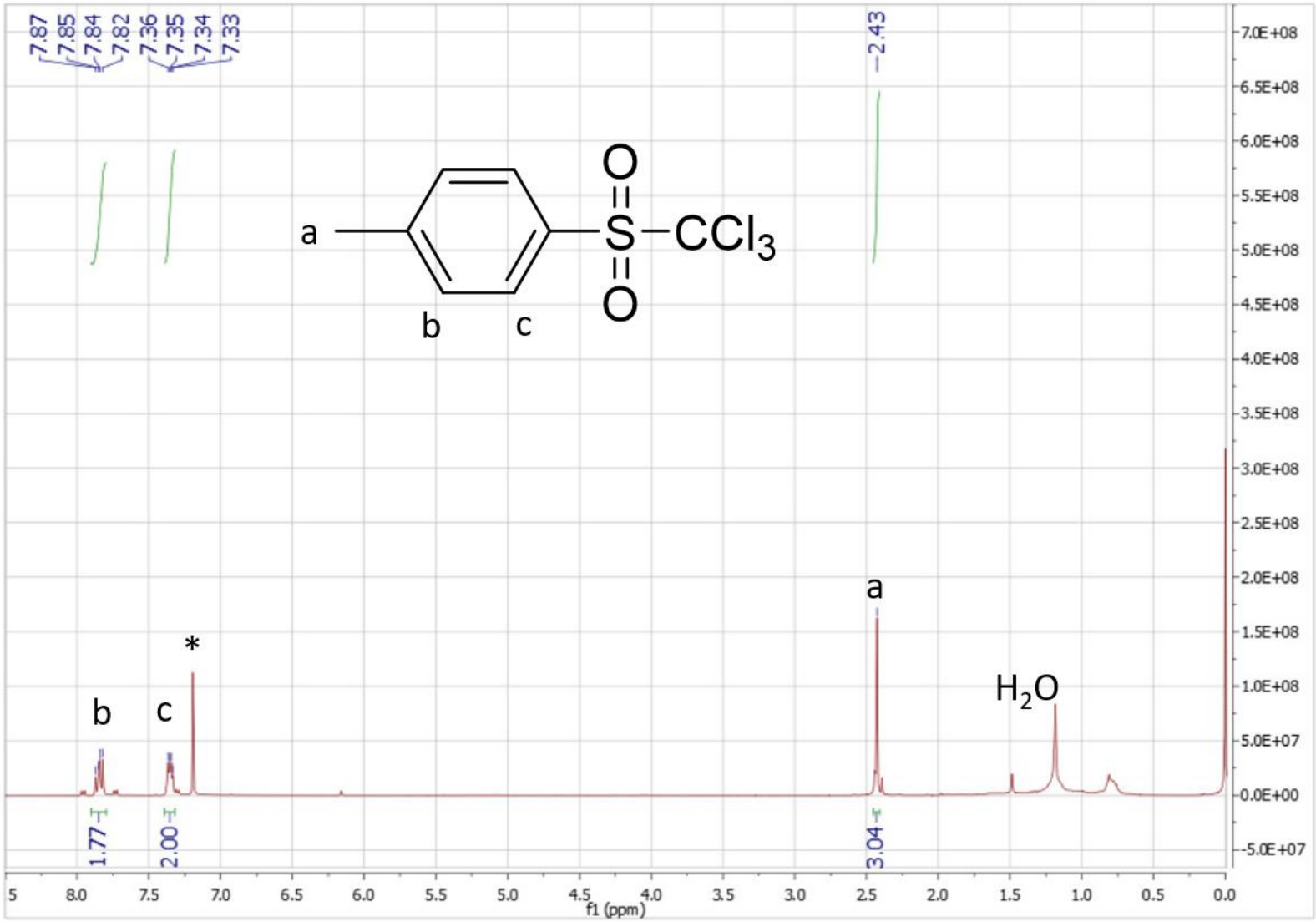
7.87
7.85
7.84
7.82
7.36
7.35
7.34
7.33
2.43
a
O
S
O
CCl3
b
c
*
b
c
a
H2O
1.77
2.00
3.04
f1 (ppm)

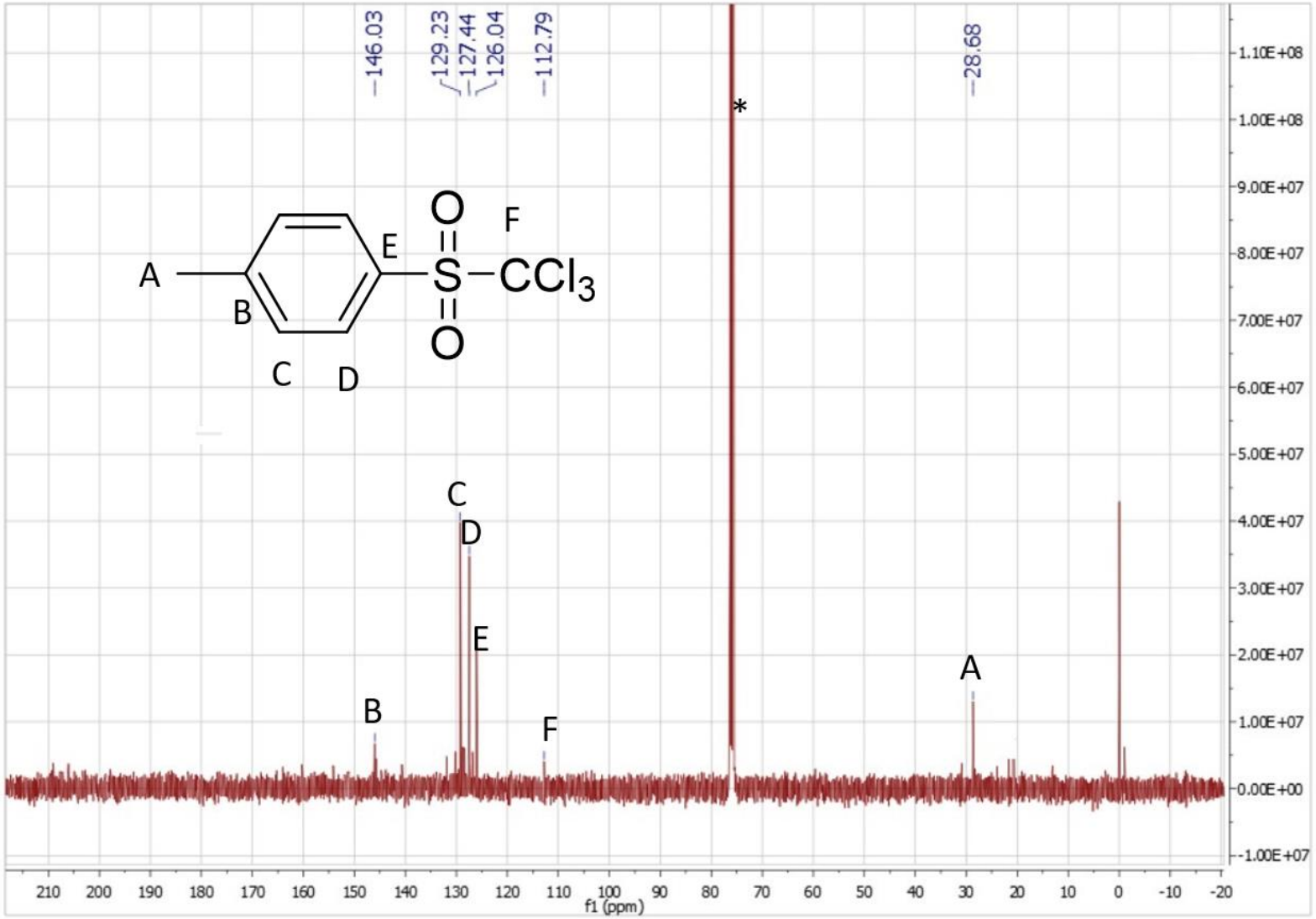
146.03
129.23
127.44
126.04
112.79
28.68
*
A
B
C
D
E
F
O
S
CCl3
f1 (ppm)

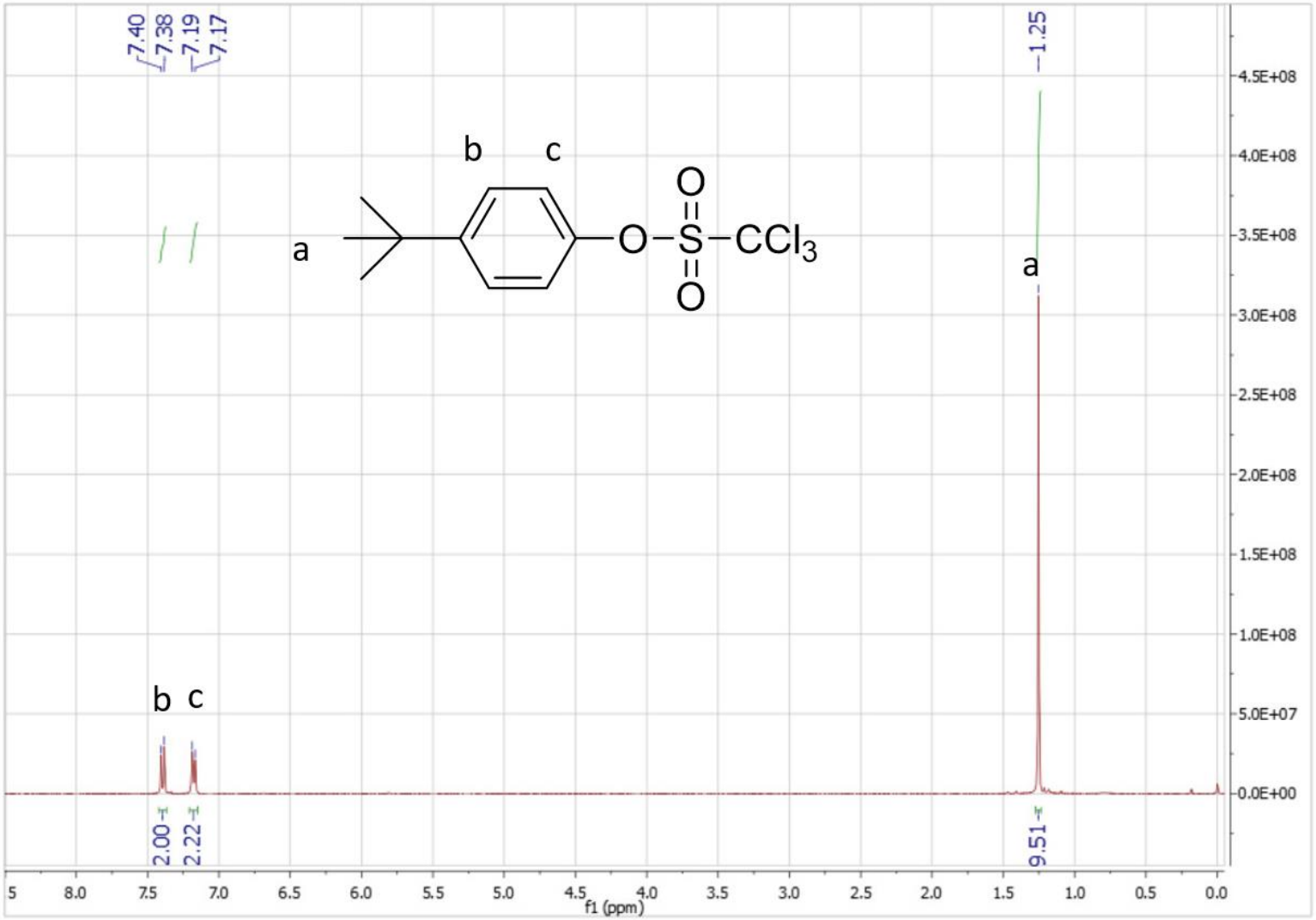
7.40
7.38
7.19
7.17
1.25
a
b
c
O
S
CCl3
b c
a
2.00
2.22
9.51
4.5E+08
4.0E+08
3.5E+08
3.0E+08
2.5E+08
2.0E+08
1.5E+08
1.0E+08
5.0E+07
0.0E+00
f1 (ppm)

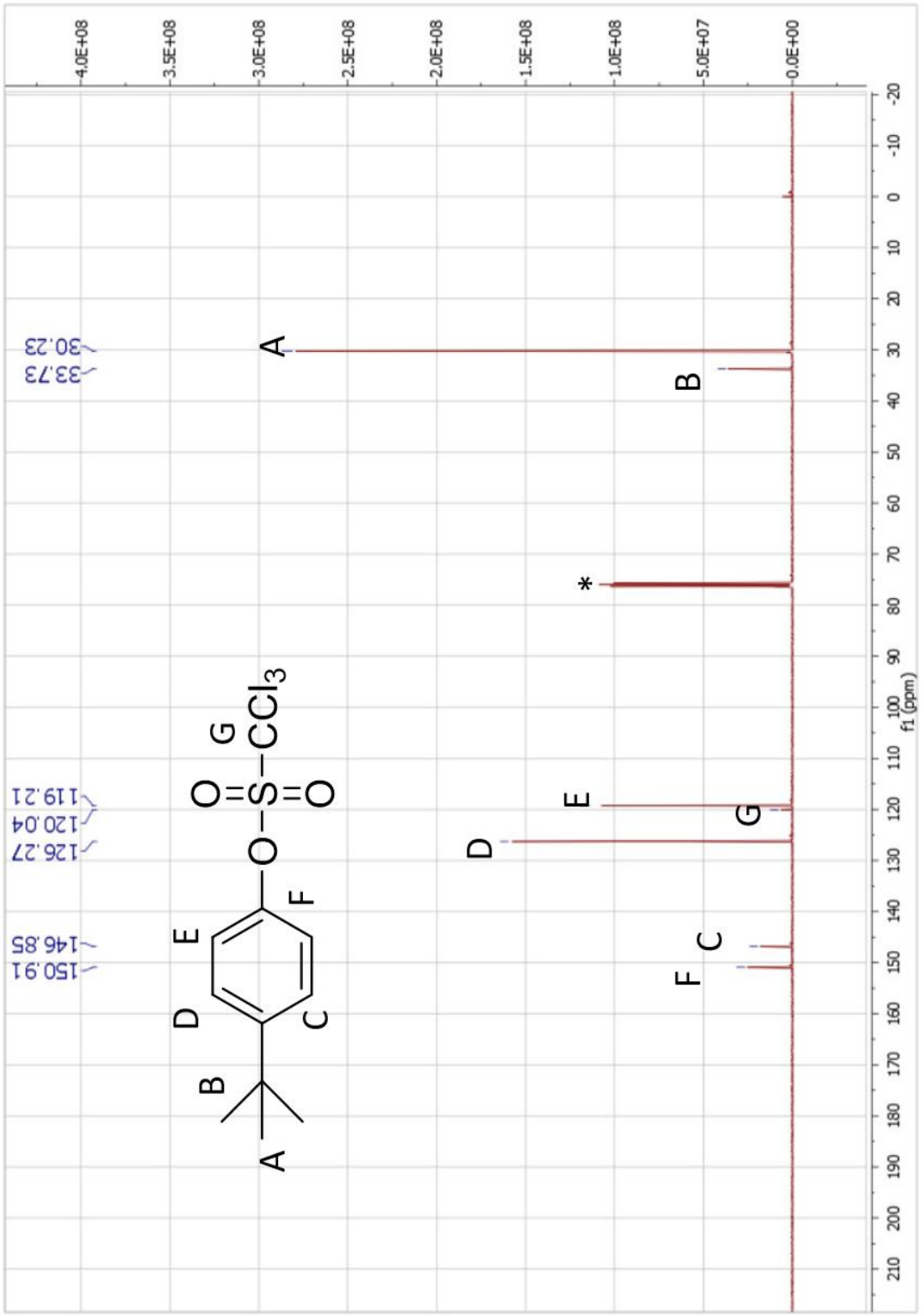
4.0E+08
3.5E+08
3.0E+08
2.5E+08
2.0E+08
1.5E+08
1.0E+08
5.0E+07
0.0E+00
-20
-10
0
10
20
30
40
50
60
70
80
90
100
110
120
130
140
150
160
170
180
190
200
210
f1 (ppm)
A
B
*
E
D
G
F
C
30.23
33.73
119.21
120.04
126.27
146.85
150.91
O
S
O
CCl3
A
B
C
D
E
F
G

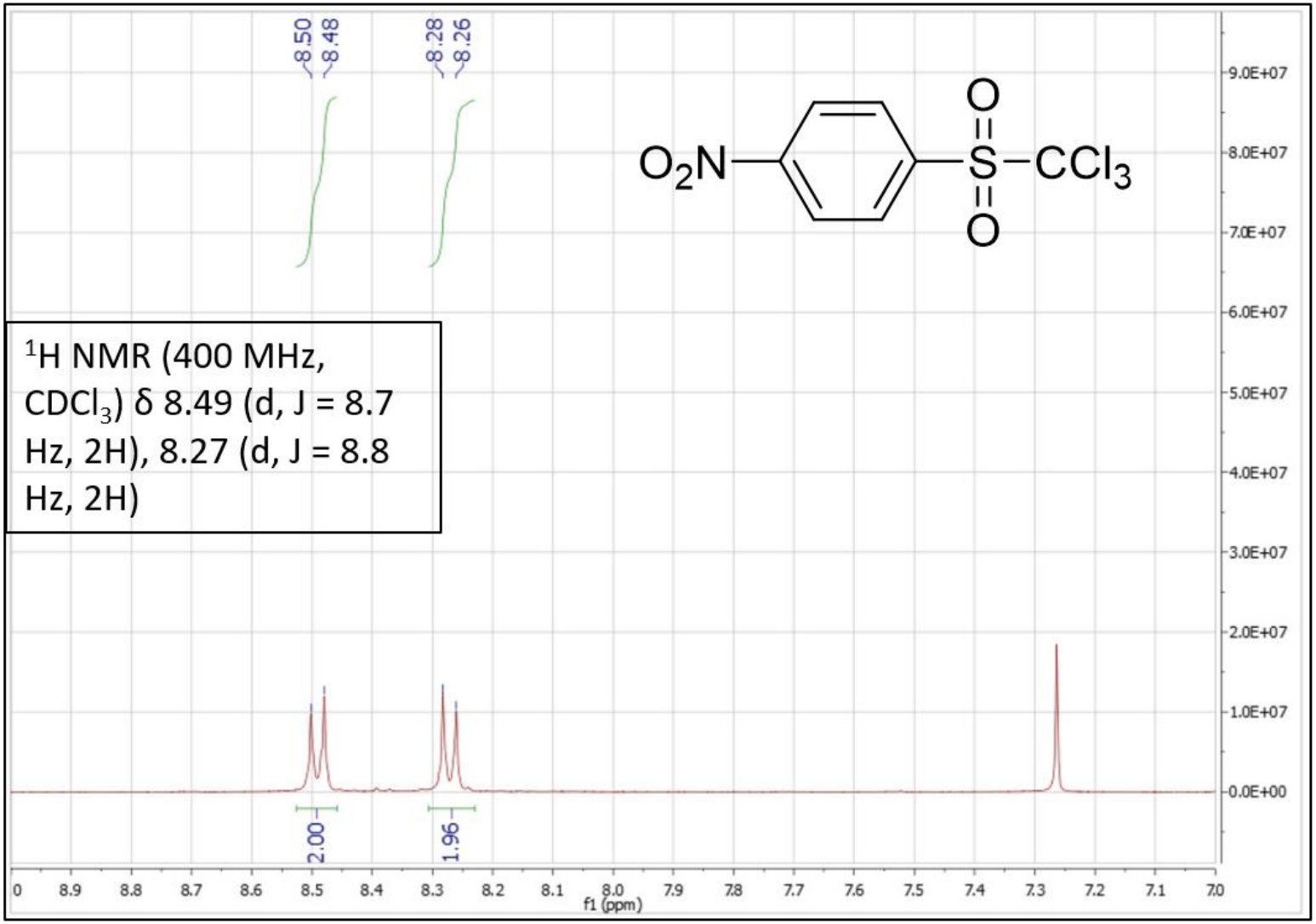
8.50
8.48
8.28
8.26
O_2N
O
S
CCl_3
O
^{1}H NMR (400 MHz, $CDCl_3$) δ 8.49 (d, J = 8.7 Hz, 2H), 8.27 (d, J = 8.8 Hz, 2H)
9.0E+07
8.0E+07
7.0E+07
6.0E+07
5.0E+07
4.0E+07
3.0E+07
2.0E+07
1.0E+07
0.0E+00
2.00
1.96
f1 (ppm)

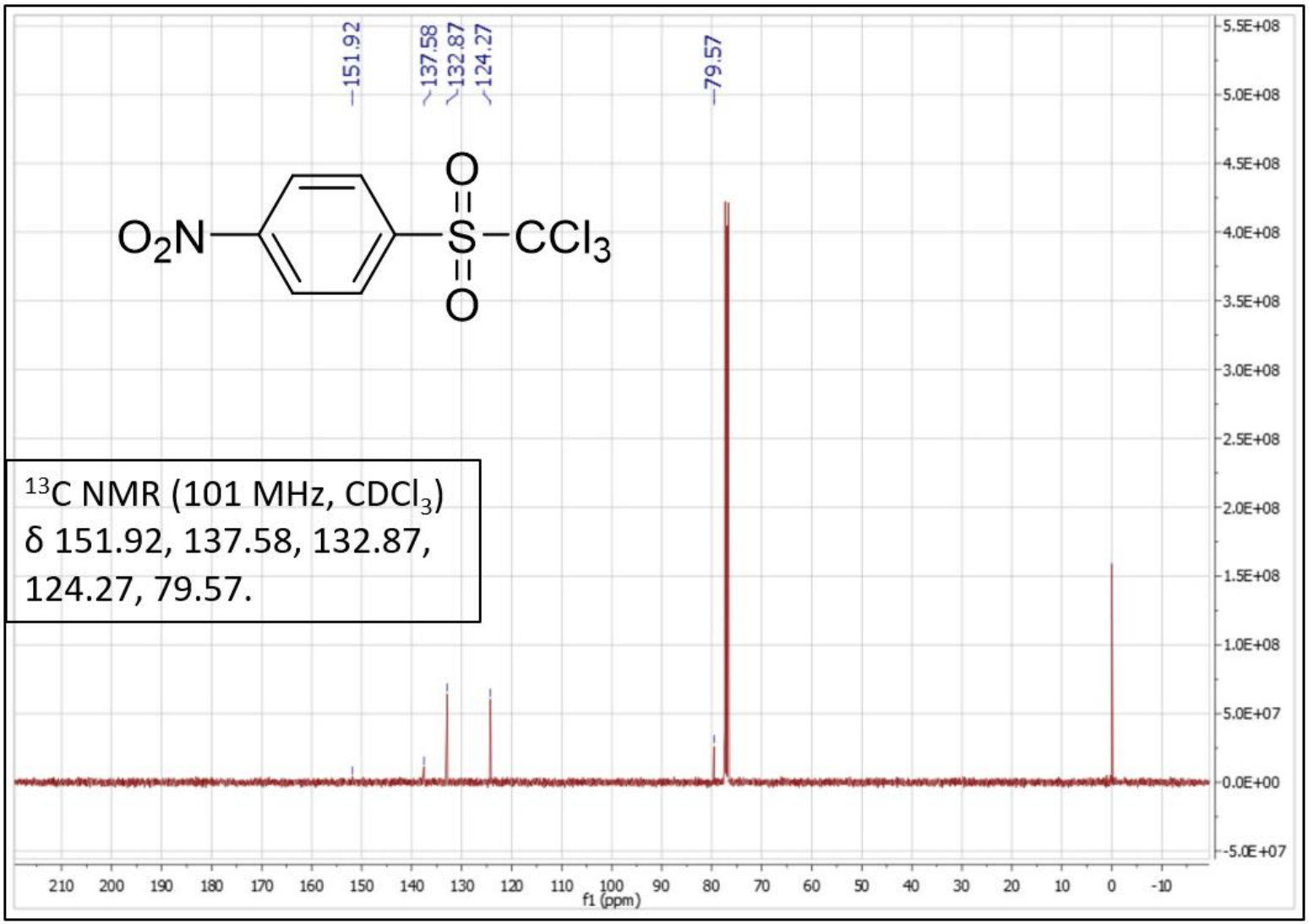

^{13}C NMR (101 MHz, $CDCl_3$)
δ 151.92, 137.58, 132.87, 124.27, 79.57.

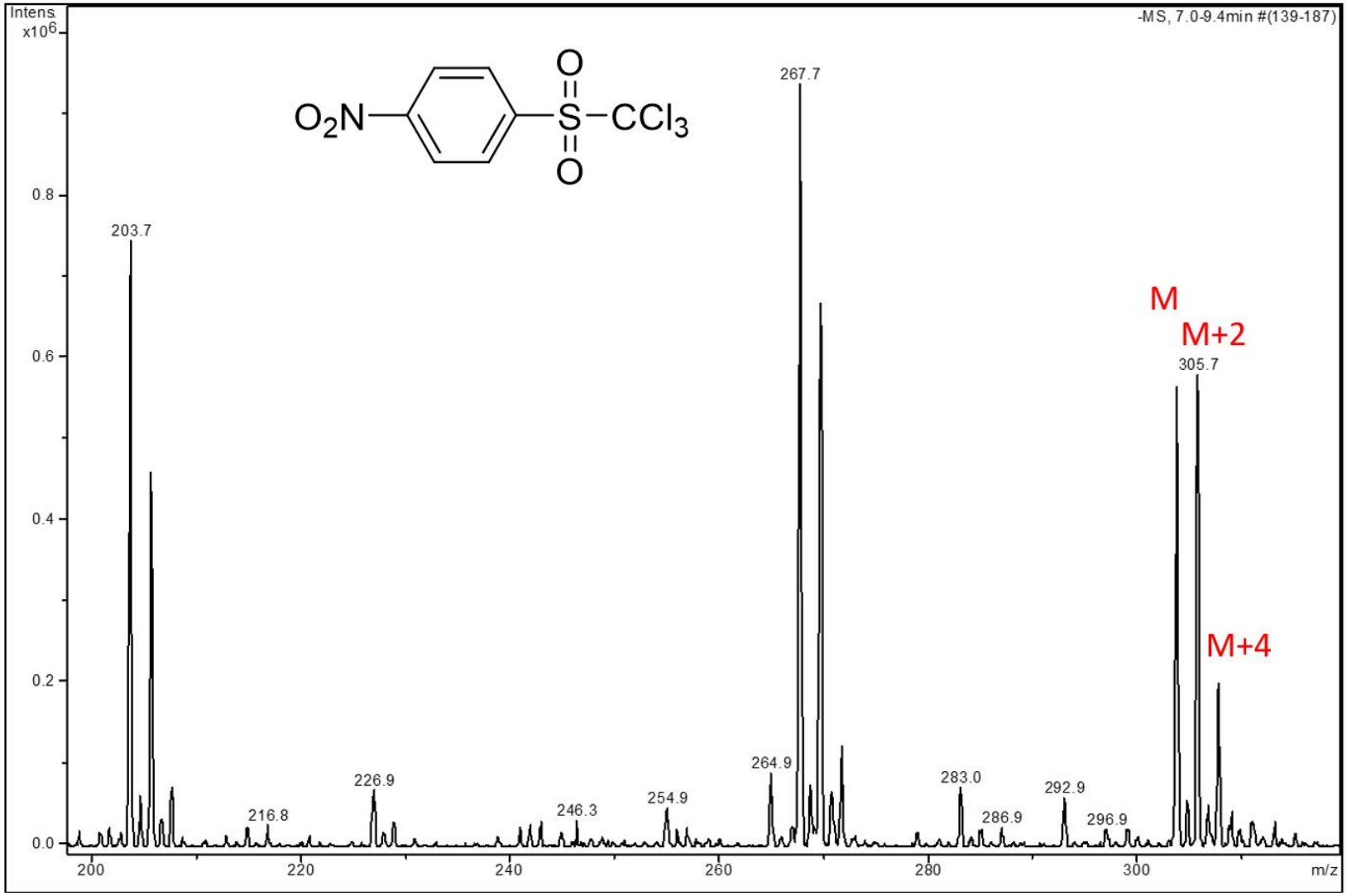
Intens.
x10^6
-MS, 7.0-9.4min #(139-187)
O2N
S
CCl3
O
O
267.7
203.7
M
M+2
305.7
M+4
0.8
0.6
0.4
0.2
0.0
216.8
226.9
246.3
254.9
264.9
283.0
286.9
292.9
296.9
200
220
240
260
280
300
m/z

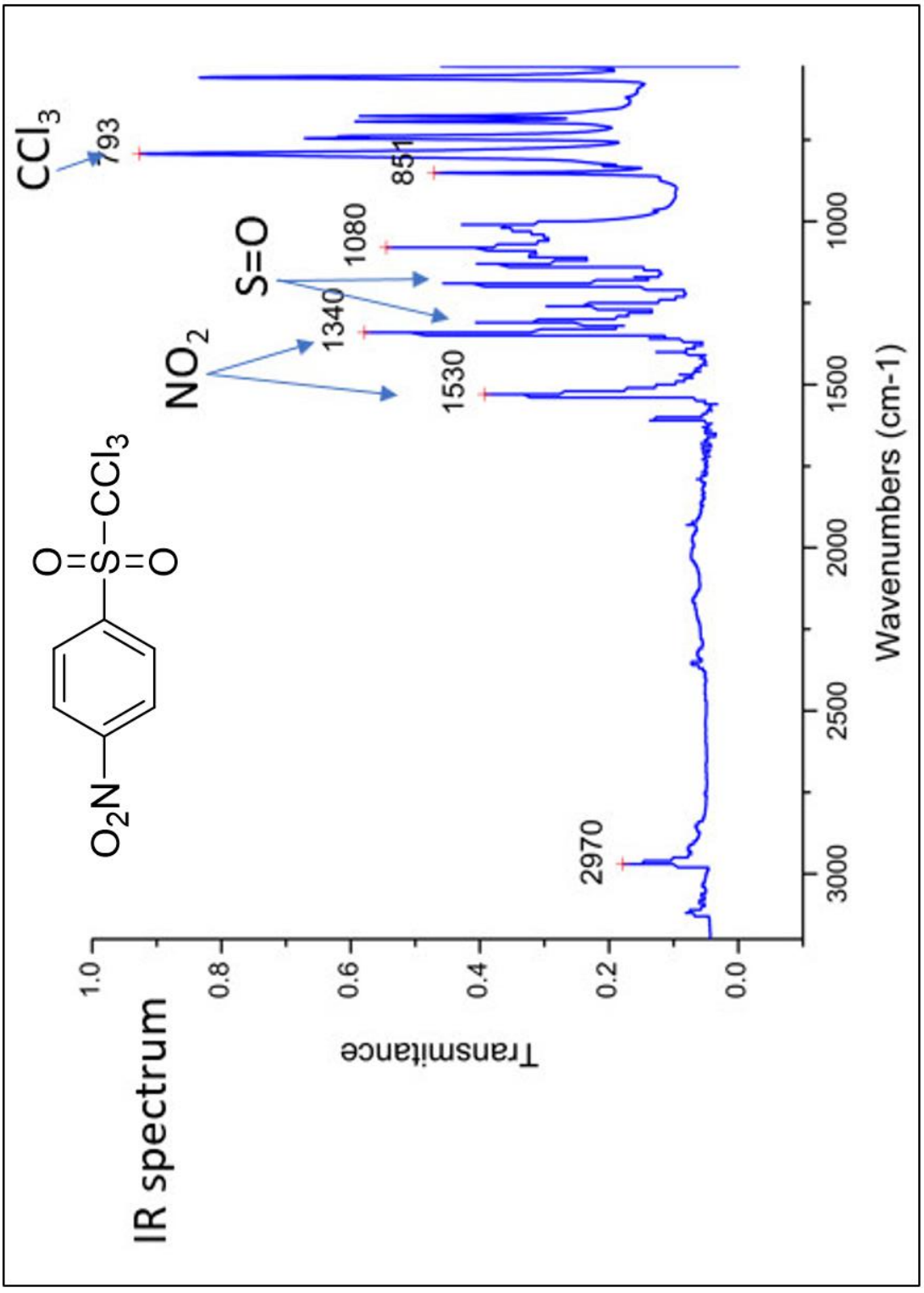
IR spectrum
Transmitance
Wavenumbers (cm-1)
1.0
0.8
0.6
0.4
0.2
0.0
3000
2500
2000
1500
1000
2970
1530
1340
1080
851
793
CCl_3
S=O
NO_2
O_2N
$S-CCl_3$
O
O

(4-Methylphenyl) boronic acid

^{1}H NMR (400 MHz, $CDCl_3$) δ 8.12 (d, *J* = 7.8 Hz, 2H), 7.31 (d, *J* = 7.7 Hz, 2H), 2.44 (s, 3H).

^{13}C NMR (101 MHz, $CDCl_3$) δ 142.97, 135.73, 133.53, 128.81, 21.97.

^{11}B NMR (128 MHz, $CDCl_3$) δ 29.47.

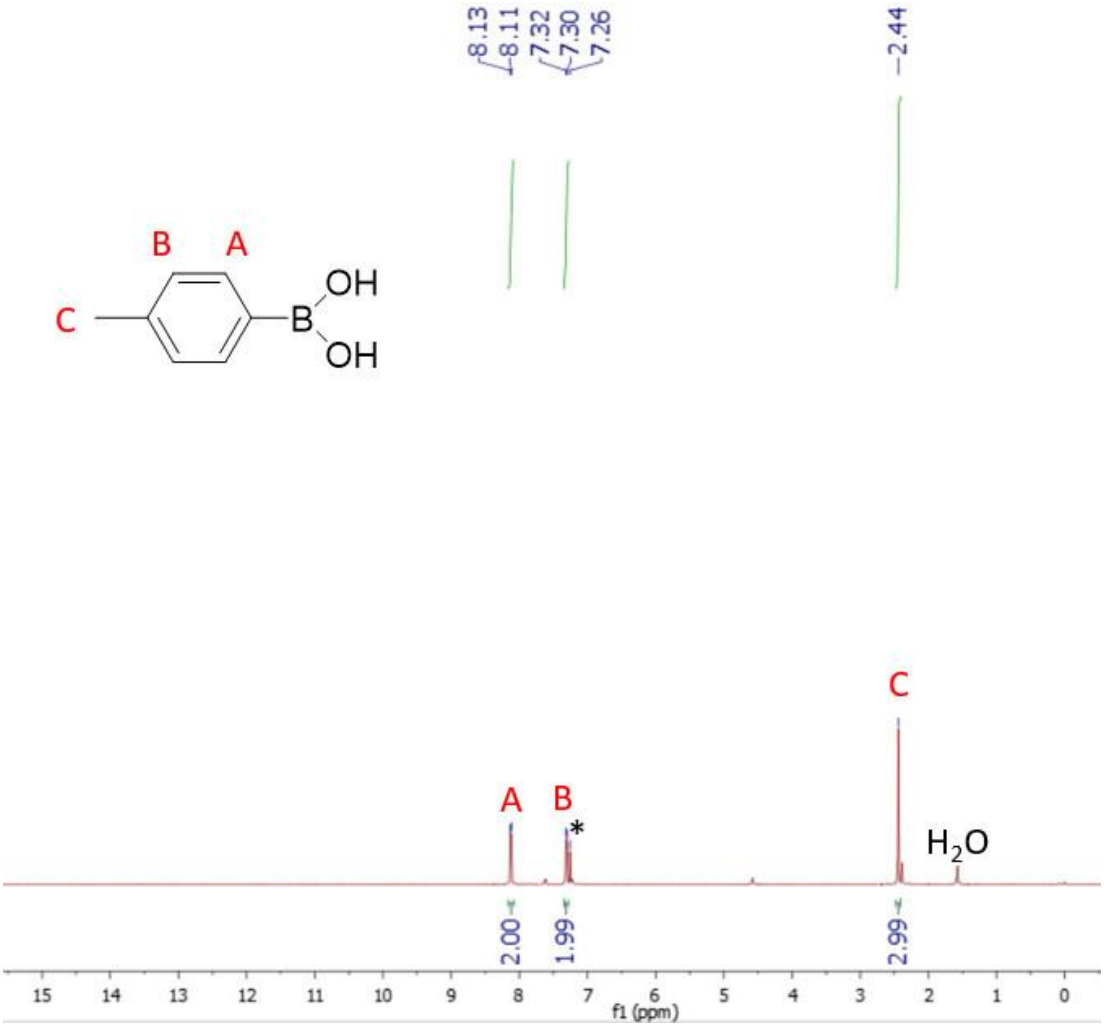

^{1}H NMR (400 MHz, $CDCl_3$, 298K) spectrum for **(4-Methylphenyl) boronic acid**

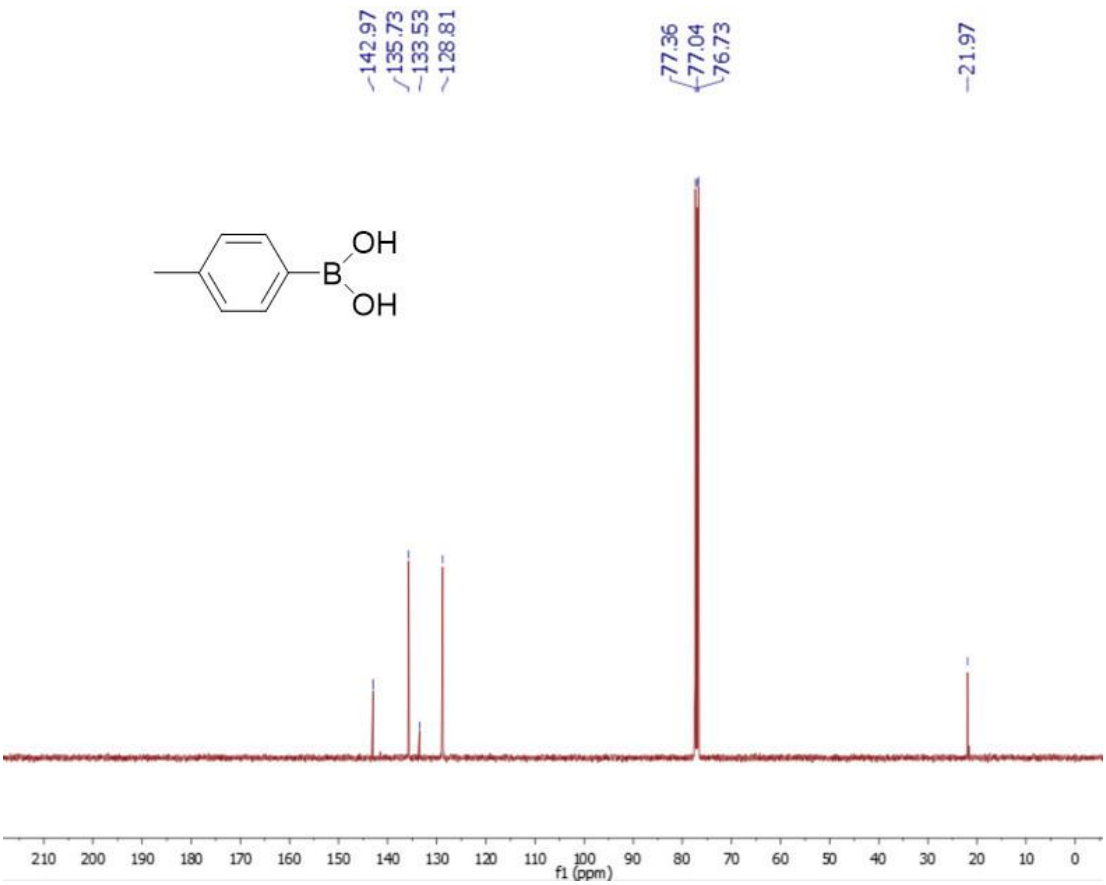

^{13}C NMR (101 MHz, $CDCl_3$, 298K) spectrum for **(4-Methylphenyl) boronic acid**

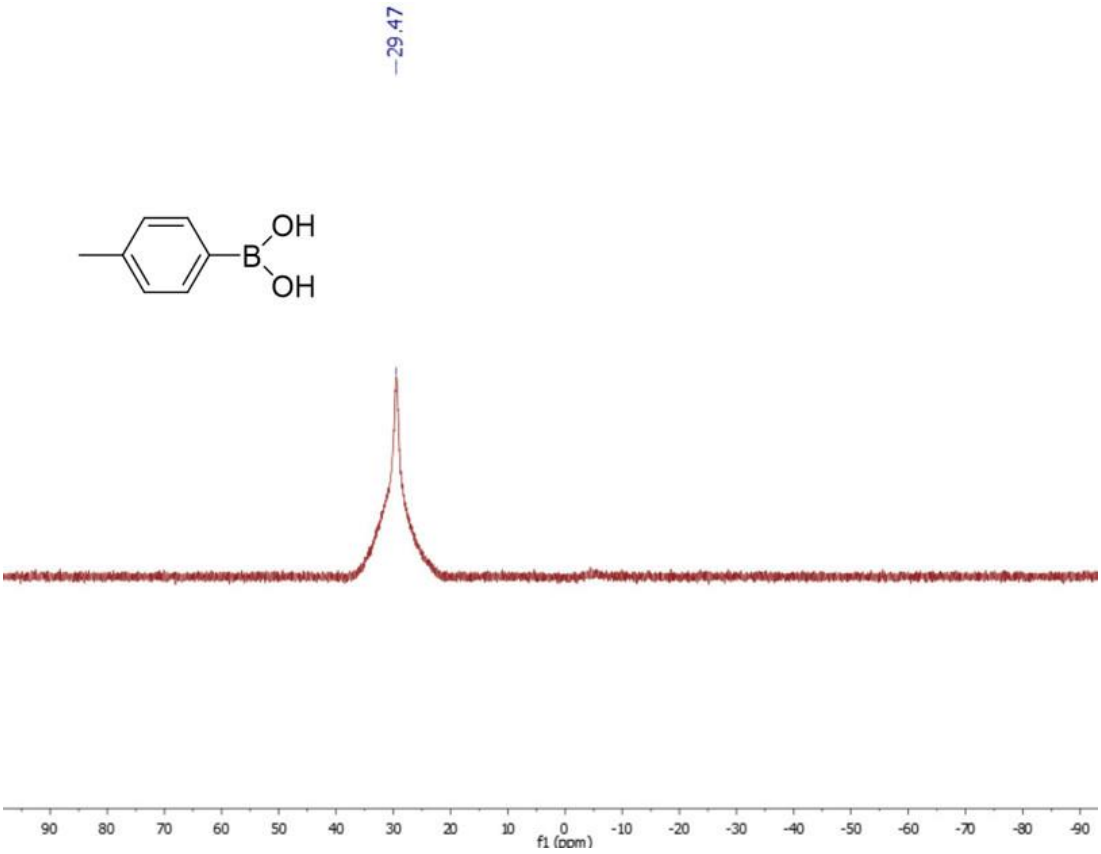

^{11}B NMR (128 MHz, $CDCl_3$, 298K) spectrum for **(4-Methylphenyl) boronic acid**

Potassium phenyl trifluoroborate

^{1}H NMR (400 MHz, DMSO-d6) δ 8.05 – 7.78 (m, 2H), 7.52 – 7.26 (m, 3H).

^{13}C NMR (101 MHz, DMSO-d6) δ 134.54, 133.91, 130.48, 129.92, 127.90, 127.82.

^{11}B NMR (128 MHz, DMSO-d6) δ -1.28.

^{19}F NMR (377 MHz, DMSO-d6) δ -148.23 (s).

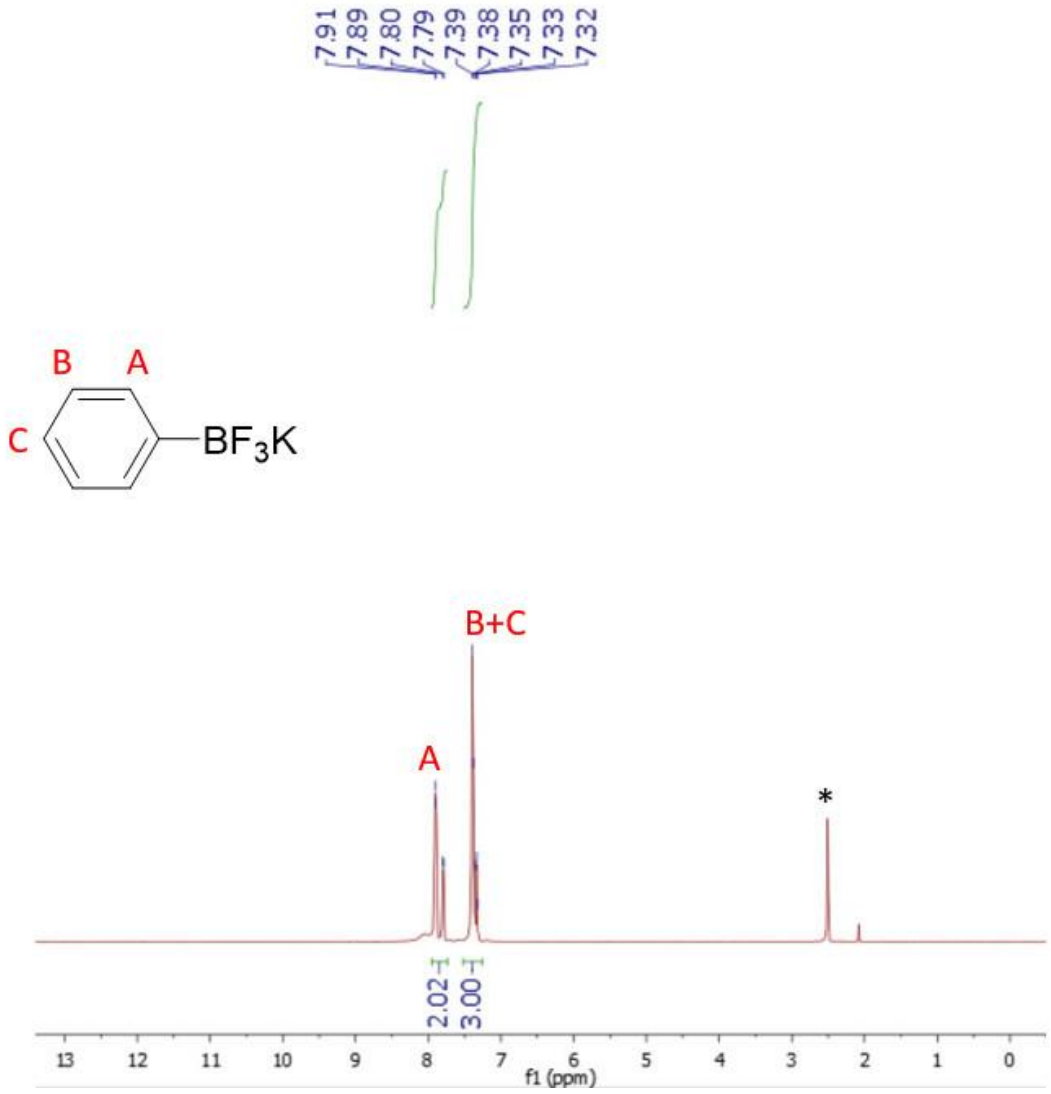

^{1}H NMR (400 MHz, DMSO-d6, 298K) spectrum for **potassium phenyl trifluoroborate**

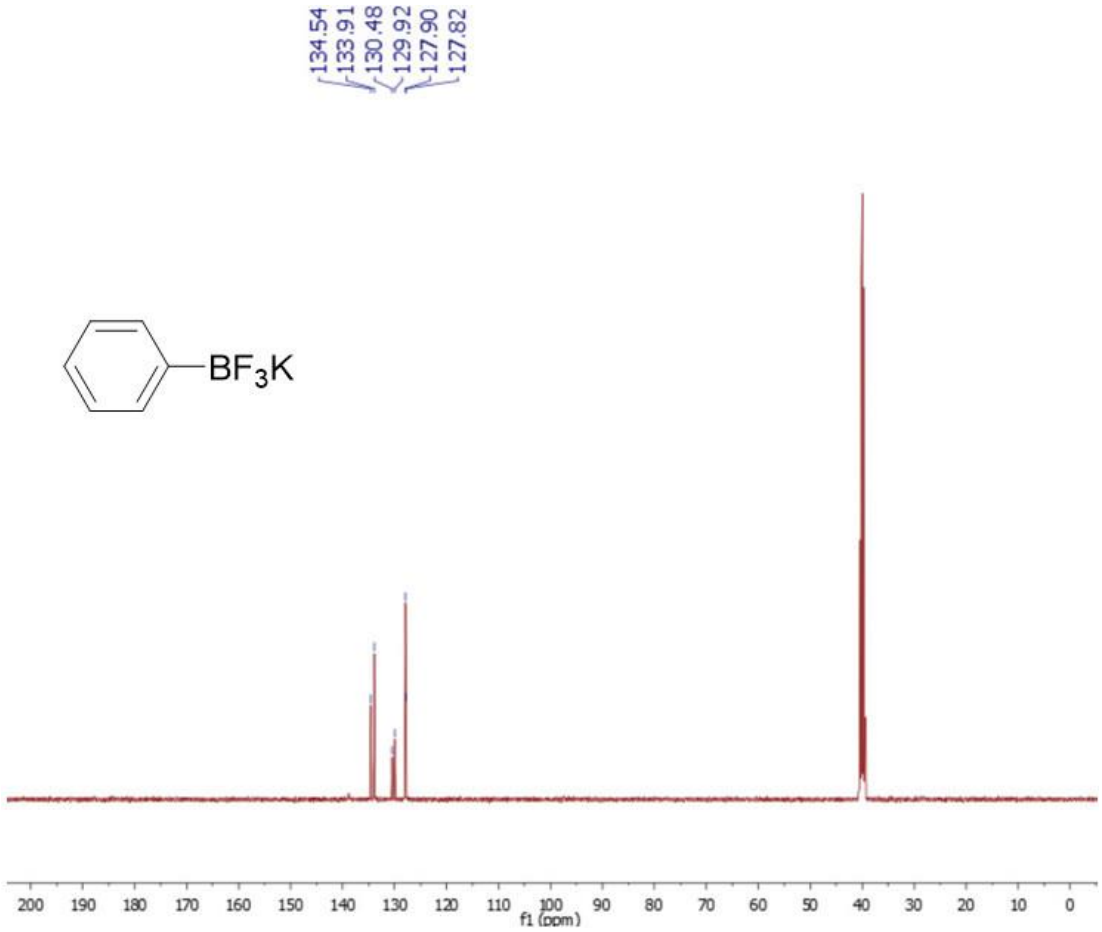

^{13}C NMR (101 MHz, DMSO-d6, 298K) spectrum for **potassium phenyl trifluoroborate**

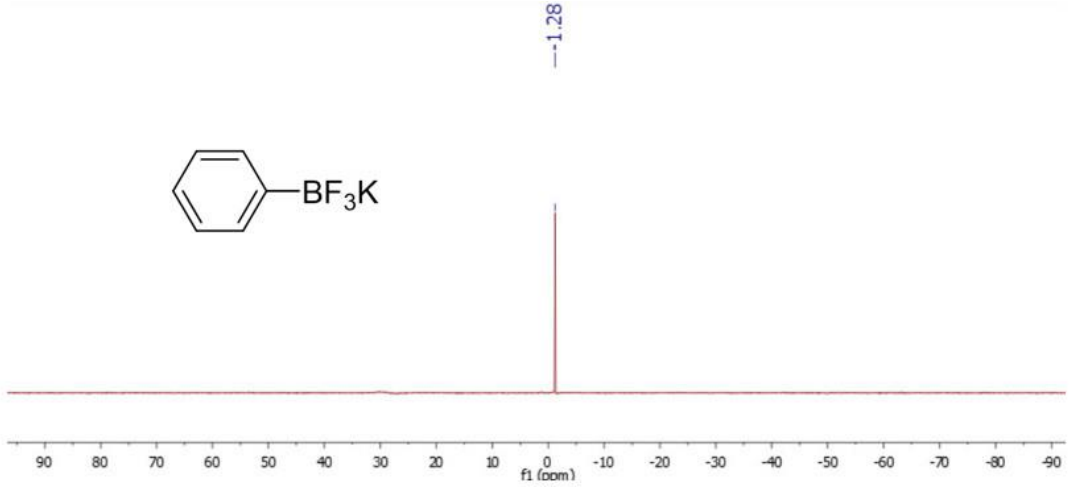

^{11}B NMR (128 MHz, DMSO-d6, 298K) spectrum for **potassium phenyl trifluoroborate**

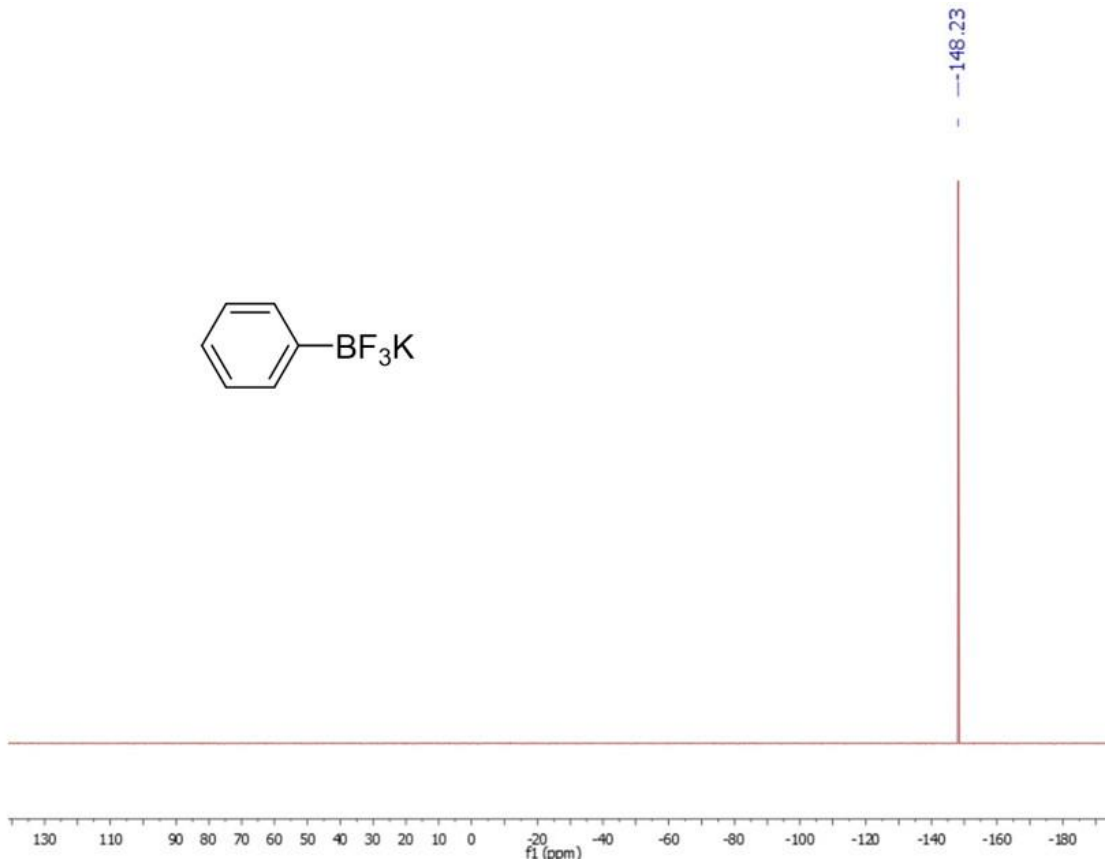

^{19}F NMR (377 MHz, DMSO-d6, 298K) spectrum for **potassium phenyl trifluoroborate**

Potassium 4-methylphenyl trifluoroborate

^{1}H NMR (400 MHz, DMSO-d6) δ 7.19 (d, *J* = 7.5 Hz, 2H), 6.89 (d, *J* = 7.4 Hz, 2H), 2.20 (s, 3H).

^{13}C NMR (101 MHz, DMSO-d6) δ 133.52, 131.81, 127.35, 21.47.

^{11}B NMR (128 MHz, DMSO-d6) δ 2.98.

^{19}F NMR (377 MHz, DMSO-d6) δ -138.56.

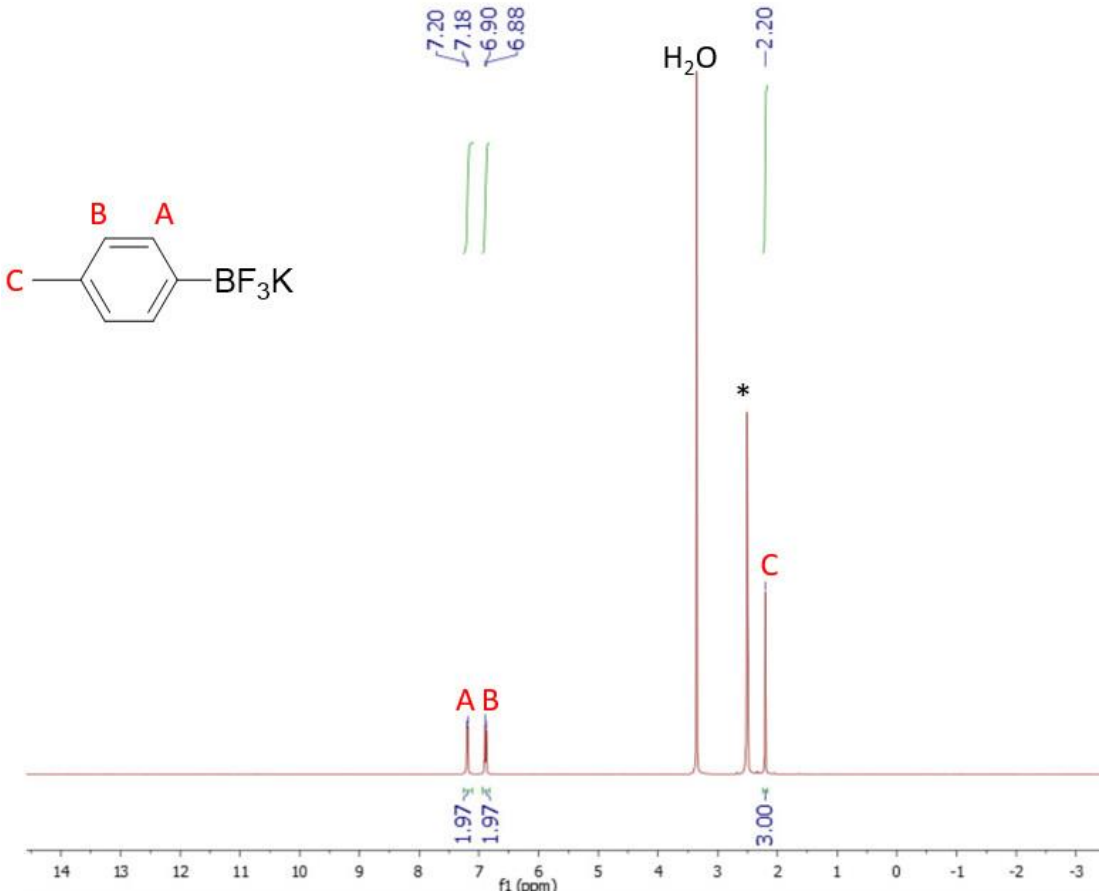

^{1}H NMR (400 MHz, DMSO-d6, 298K) spectrum for **potassium 4-methylphenyl trifluoroborate**

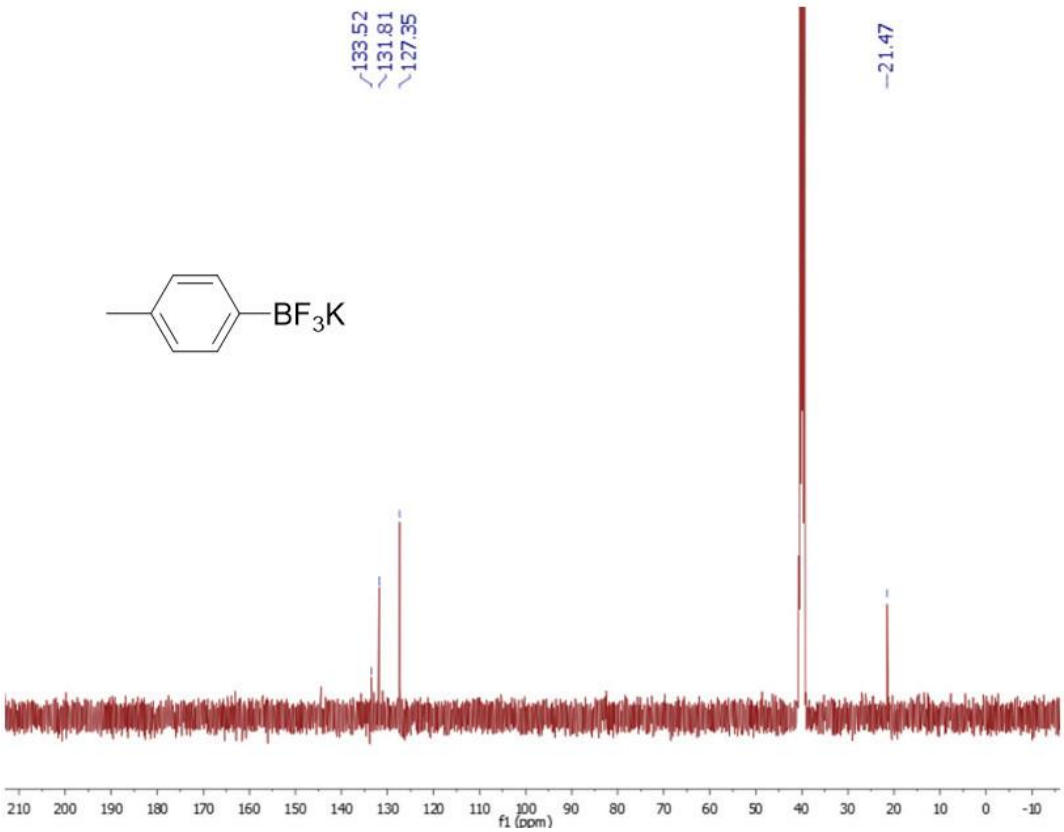

^{13}C NMR (101 MHz, DMSO-d6, 298K) spectrum for **potassium 4-methylphenyl trifluoroborate**

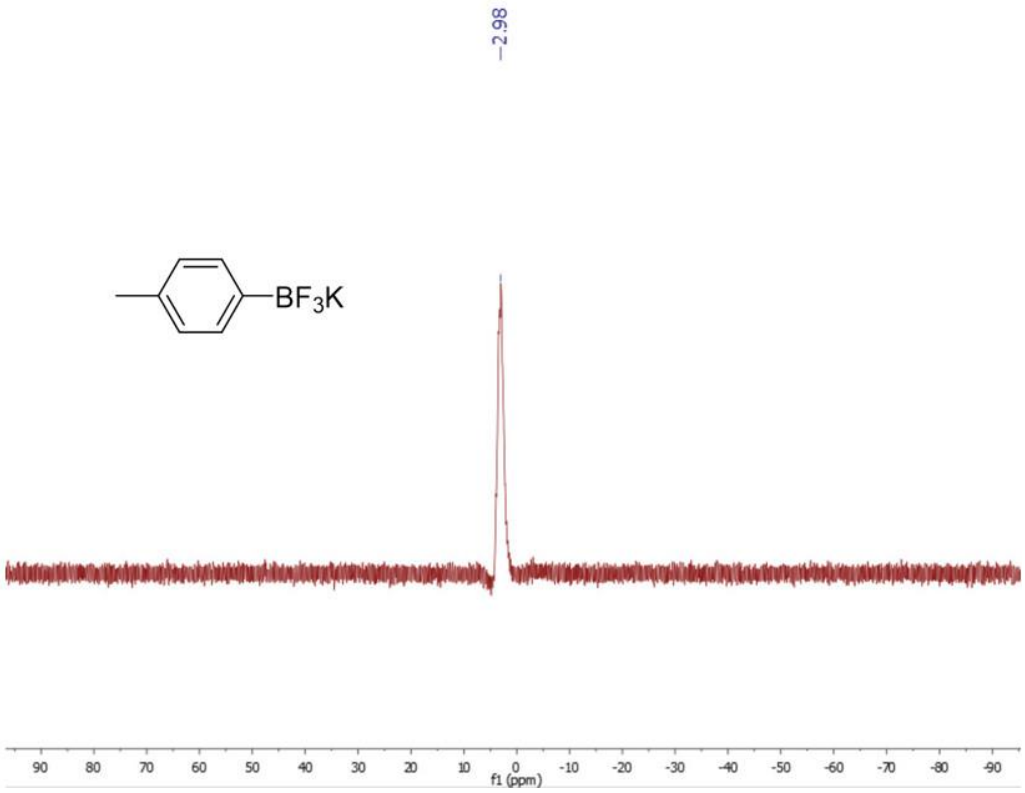

^{11}B NMR (128 MHz, DMSO-d6, 298K) spectrum for **potassium 4-methylphenyl trifluoroborate**

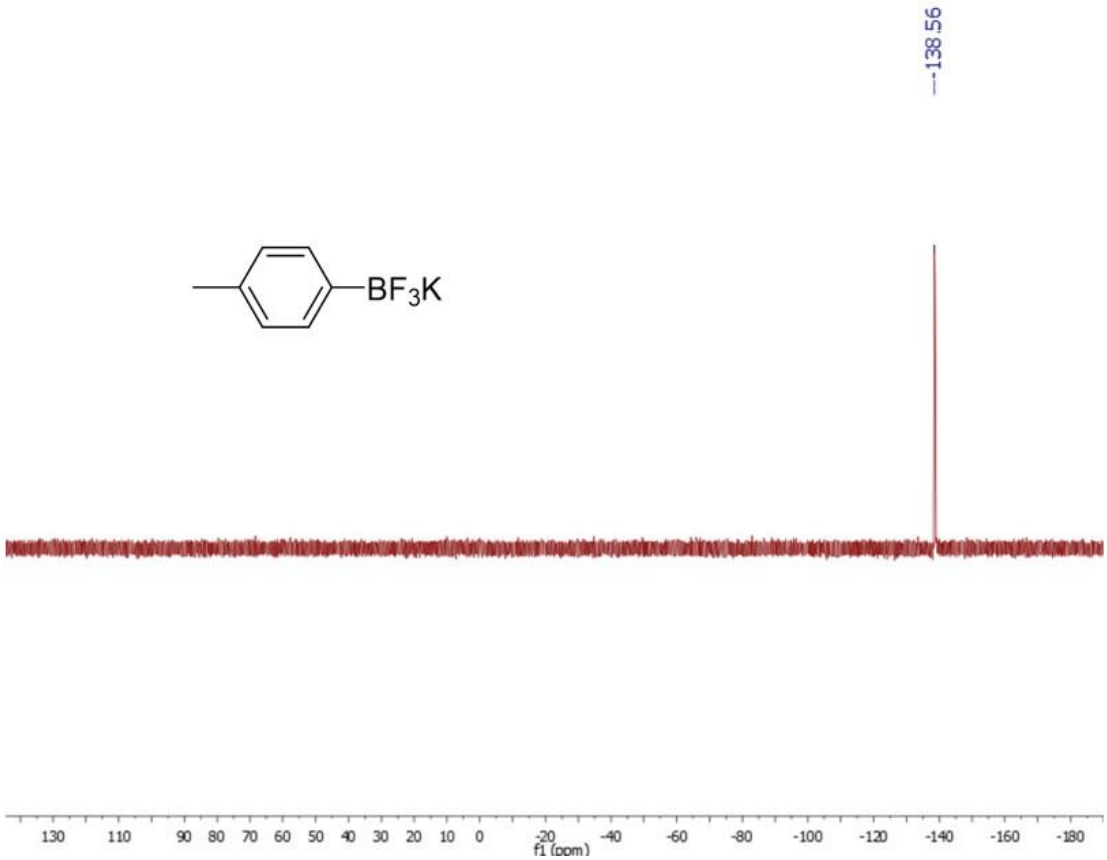

^{19}F NMR (377 MHz, DMSO-d6, 298K) spectrum for **potassium 4-methylphenyl trifluoroborate**

Dipotassium phenylene-1,4-bis(trifluoroborate)

^{1}H NMR (400 MHz, DMSO-d6) δ 6.86 (s, 4H).

^{13}C NMR (101 MHz, DMSO-d6) δ 130.09.

^{11}B NMR (128 MHz, DMSO-d6) δ 3.67.

^{19}F NMR (377 MHz, DMSO-d6) δ -137.96.

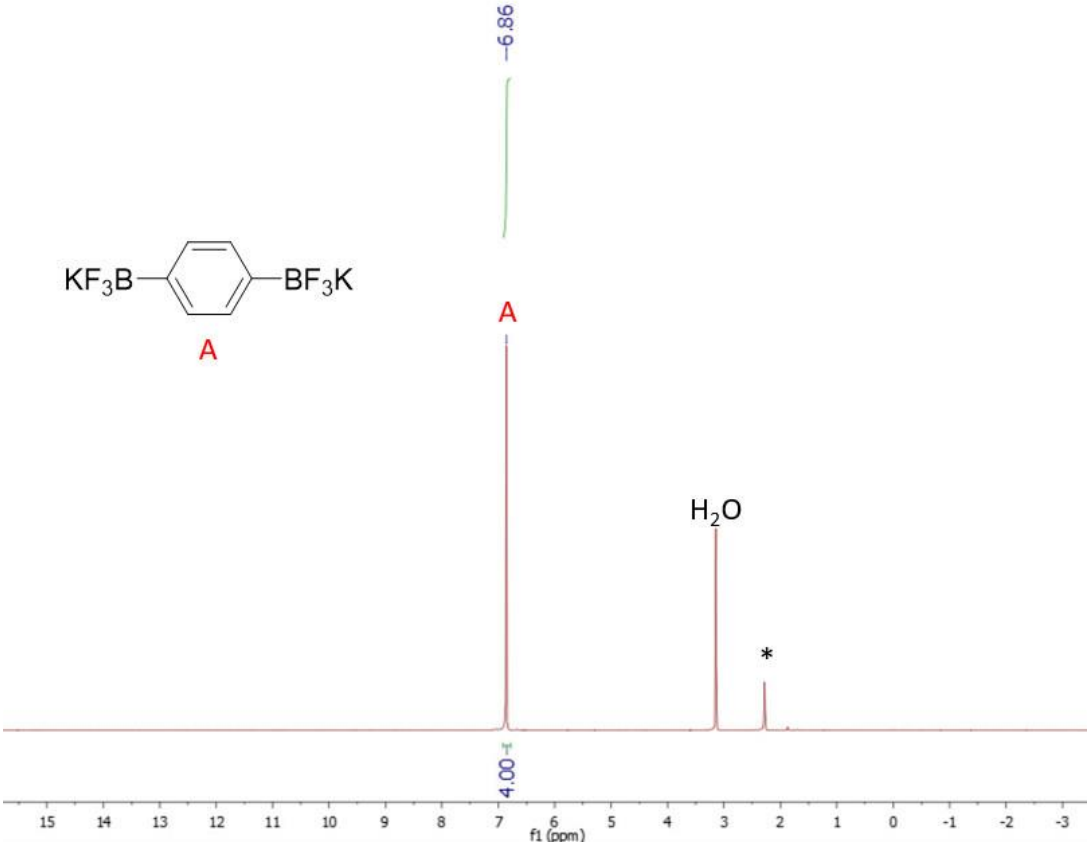

^{1}H NMR (400 MHz, DMSO-d6, 298K) spectrum for **dipotassium phenylene-1,4-bis(trifluoroborate)**

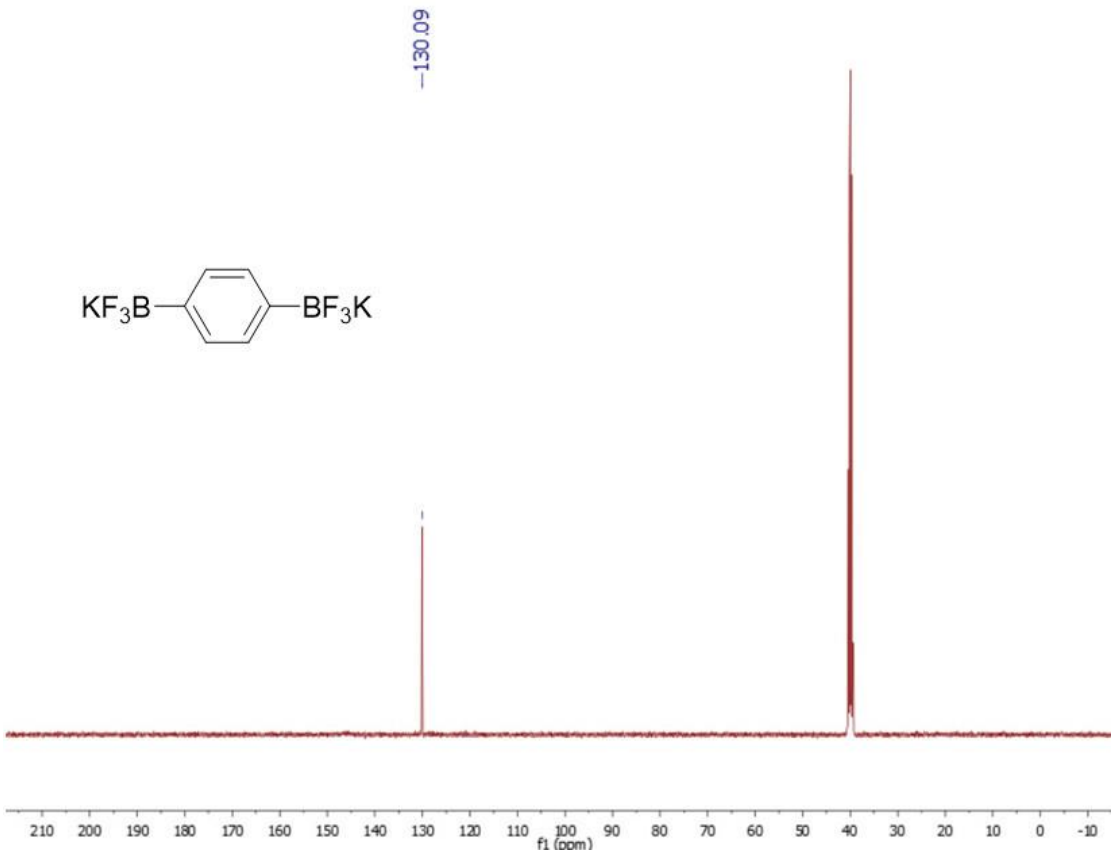

^{13}C NMR (101 MHz, DMSO-d6, 298K) spectrum for **dipotassium phenylene-1,4-bis(trifluoroborate)**

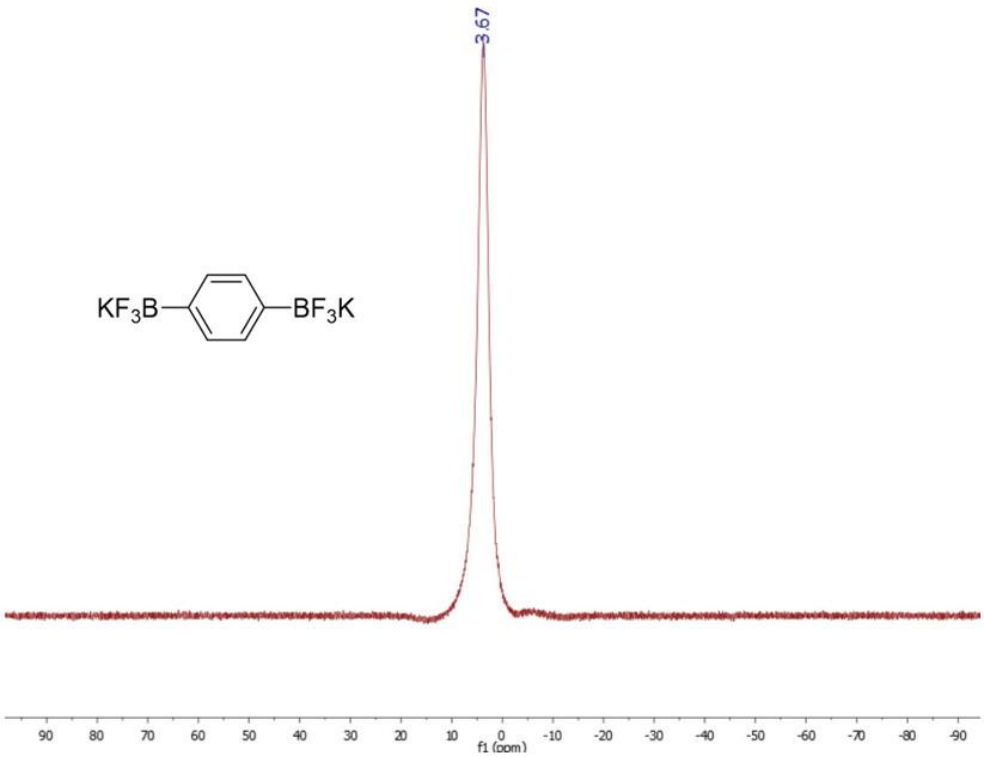

^{11}B NMR (128 MHz, DMSO-d6, 298K) spectrum for **dipotassium phenylene-1,4-bis(trifluoroborate)**

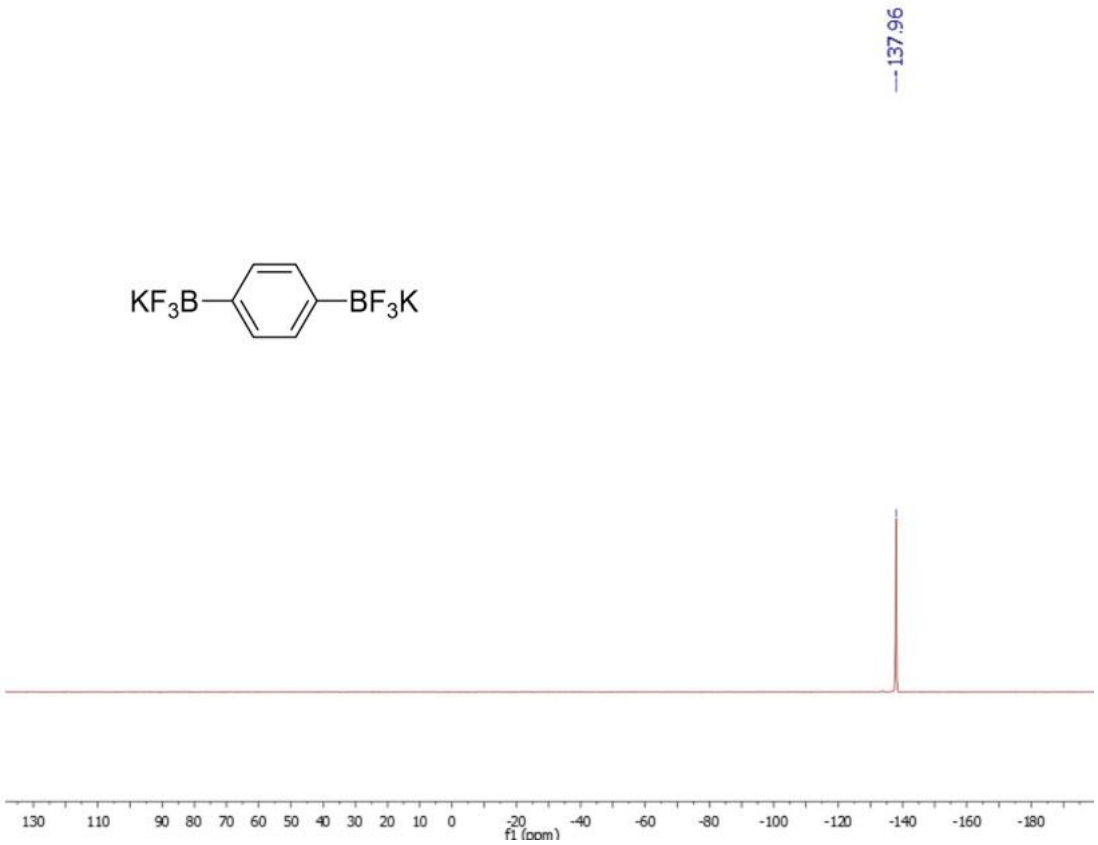

^{19}F NMR (377 MHz, DMSO-d6, 298K) spectrum for **dipotassium phenylene-1,4-bis(trifluoroborate)**

Phenylboronic acid pinacol ester: PhB(pin)

^{1}H NMR (400 MHz, $CDCl_3$) δ 7.81 (d, *J* = 6.7 Hz, 2H), 7.46 (t, *J* = 8.1 Hz, 1H), 7.37 (t, *J* = 7.3 Hz, 2H), 1.35 (s, 12H).

^{13}C NMR (101 MHz, $CDCl_3$) δ 134.76, 131.27, 127.72, 83.78, 78.30, 24.97.

^{11}B NMR (128 MHz, $CDCl_3$) δ 30.85.

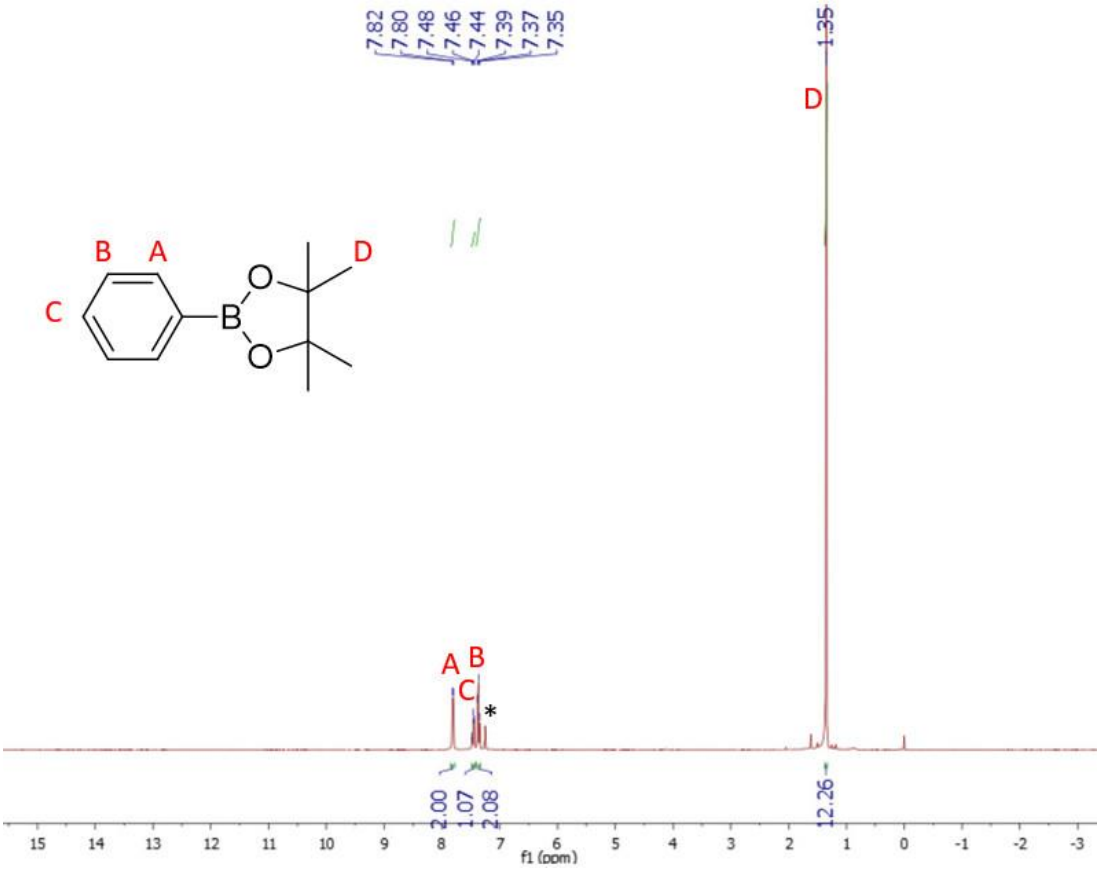

^{1}H NMR (400 MHz, $CDCl_3$, 298K) spectrum for **phenylboronic acid pinacol ester: PhB(pin)**

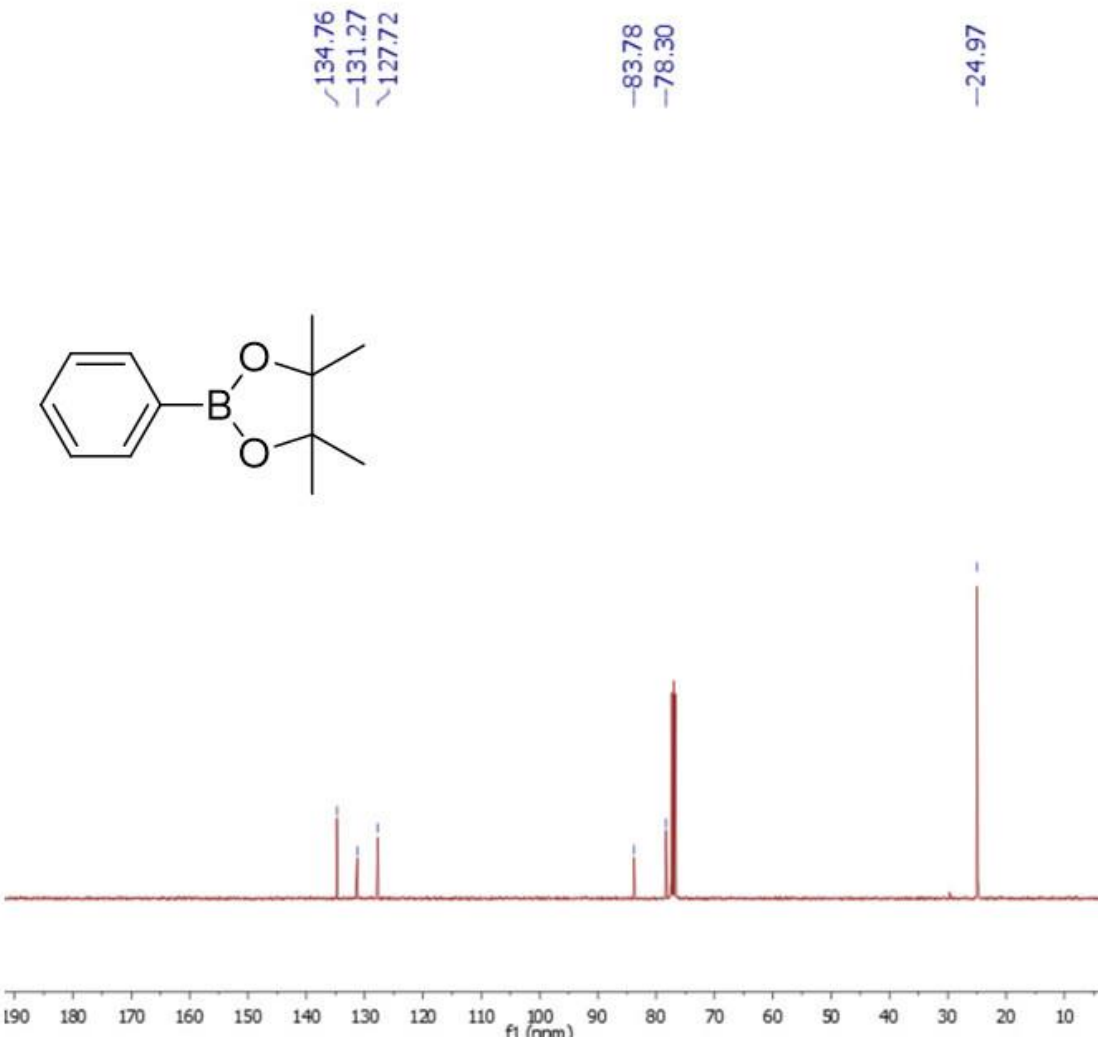

^{13}C NMR (101 MHz, $CDCl_3$, 298K) spectrum for **phenylboronic acid pinacol ester: PhB(pin)**

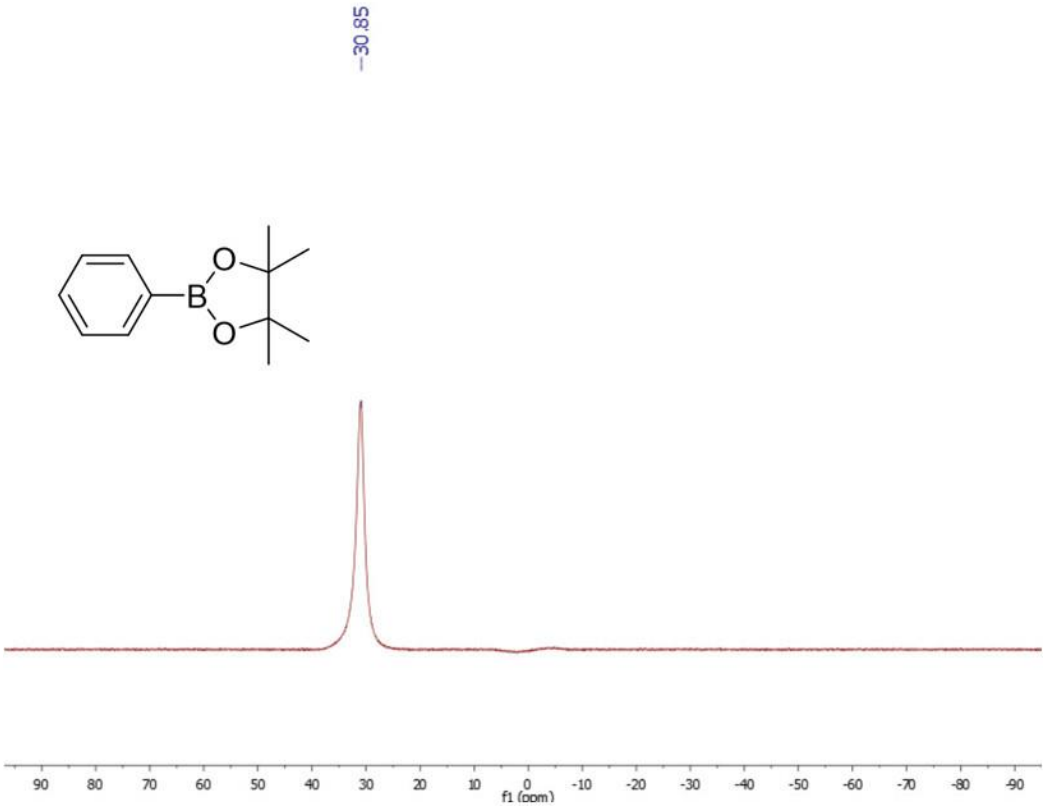

^{11}B NMR (128 MHz, $CDCl_3$, 298K) spectrum for **phenylboronic acid pinacol ester: PhB(pin)**

Phenylboronic acid neopentylglycol ester: PhB(neop)

^{1}H NMR (400 MHz, $CDCl_3$) δ 7.73 (d, *J* = 6.7 Hz, 2H), 7.36 (t, *J* = 7.3 Hz, 1H), 7.28 (t, *J* = 7.2 Hz, 2H), 3.70 (s, 4H), 0.95 (s, 6H).

^{13}C NMR (101 MHz, $CDCl_3$) δ 133.83, 130.71, 127.61, 72.32, 31.91, 21.94.

^{11}B NMR (128 MHz, $CDCl_3$) δ 26.79.

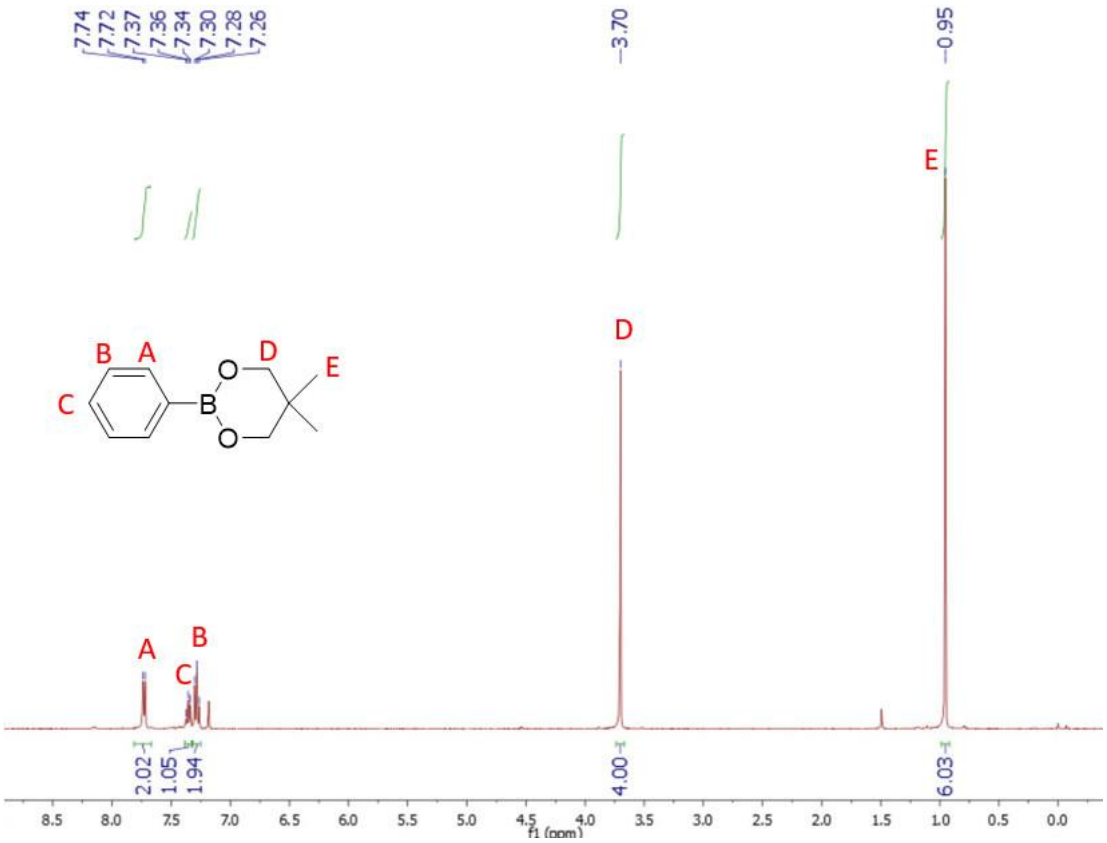

^{1}H NMR (400 MHz, $CDCl_3$, 298K) spectrum for **phenylboronic acid neopentylglycol ester: PhB(neop)**

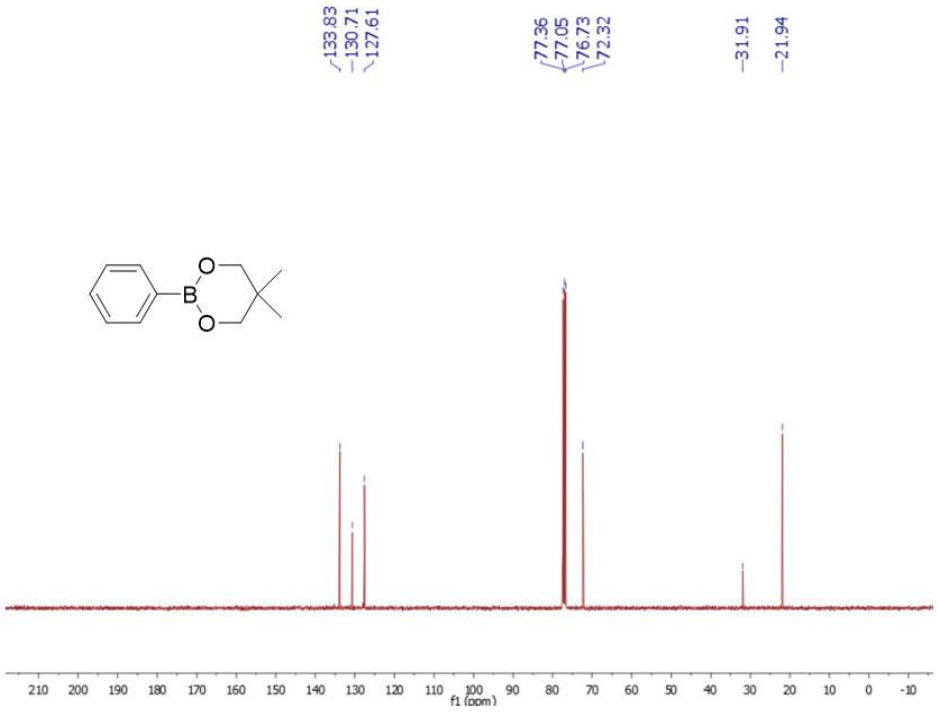

^{13}C NMR (101 MHz, $CDCl_3$, 298K) spectrum for **phenylboronic acid neopentylglycol ester: PhB(neop)**

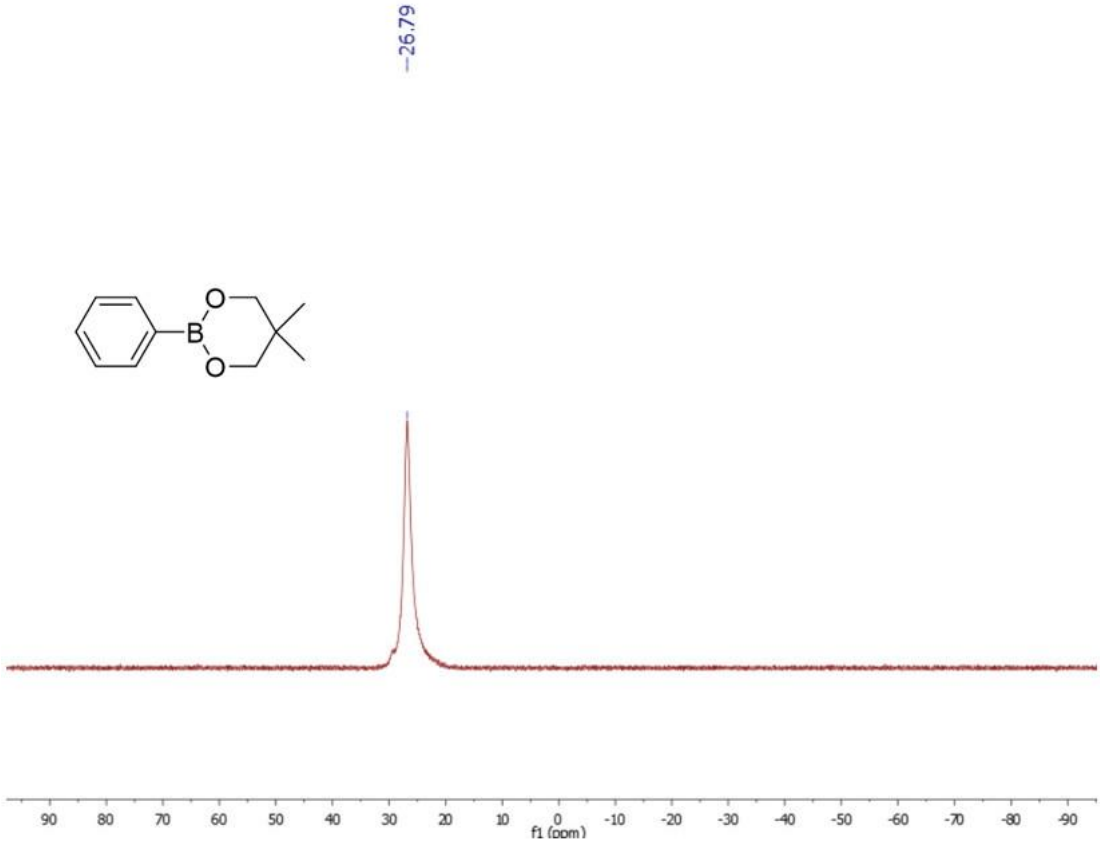

^{11}B NMR (128 MHz, $CDCl_3$, 298K) spectrum for **phenylboronic acid neopentylglycol ester: PhB(neop)**

1,4-Benzenediboronic acid bis(pinacol)ester: PhB(pin)$_2$

^{1}H NMR (400 MHz, $CDCl_3$) δ 7.73 (s, 4H), 1.27 (s, 24H).

^{13}C NMR (101 MHz, $CDCl_3$) δ 133.90, 83.87, 24.89.

^{11}B NMR (128 MHz, $CDCl_3$) δ 31.04.

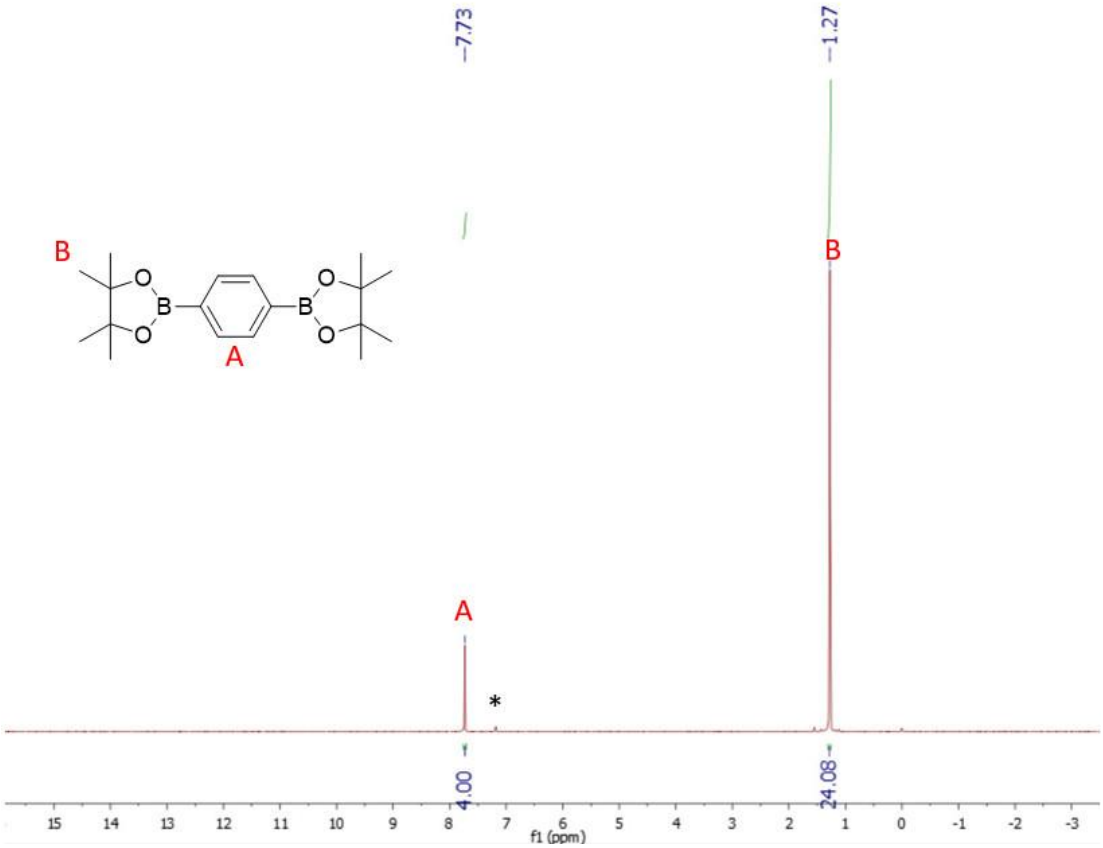

^{1}H NMR (400 MHz, $CDCl_3$, 298K) spectrum for **1,4-benzenediboronic acid bis(pinacol)ester**

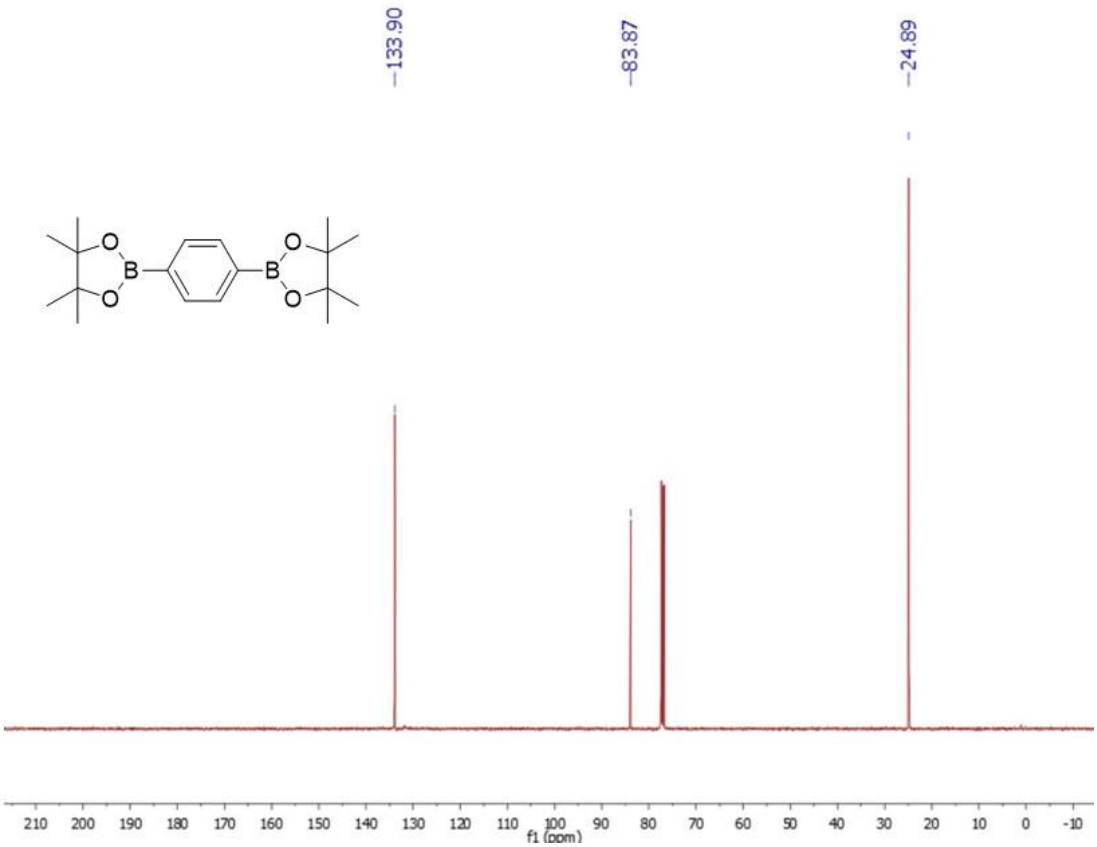

^{13}C NMR (101 MHz, $CDCl_3$, 298K) spectrum for **1,4-benzenediboronic acid bis(pinacol)ester**

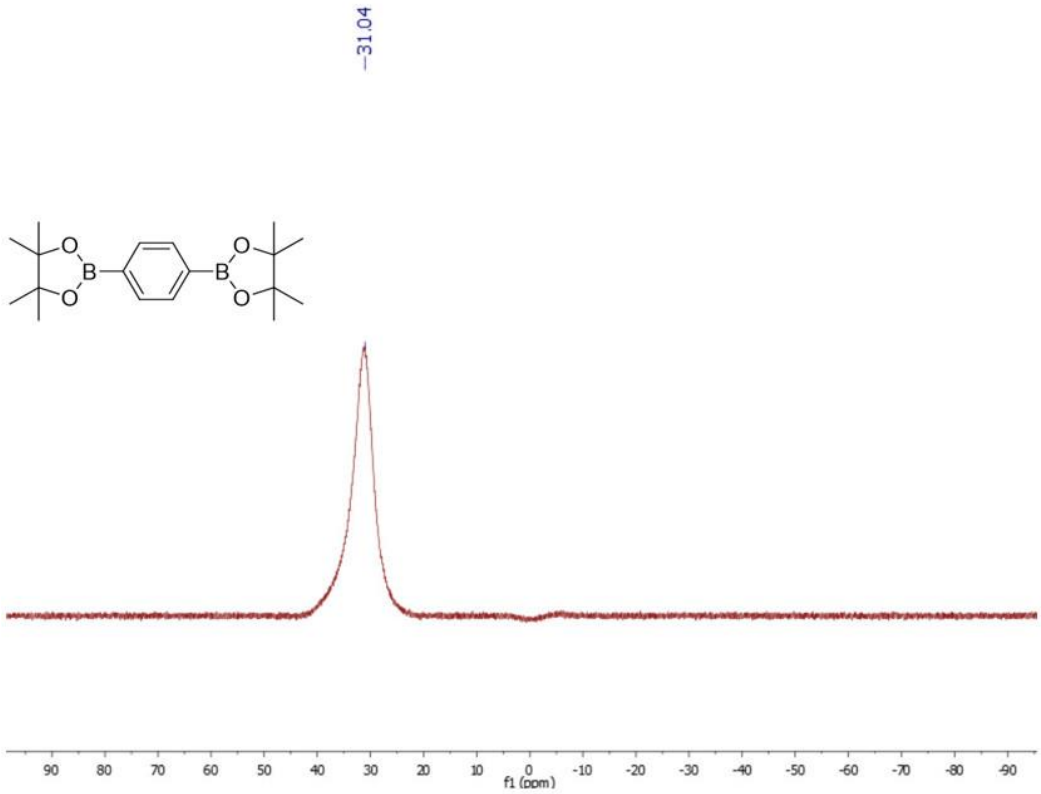

^{11}B NMR (128 MHz, $CDCl_3$, 298K) spectrum for **1,4-benzenediboronic acid bis(pinacol)ester**

1,4-benzenediboronic acid bis-2,2'-(methylimino)diethanol ester: PhB(MDEA)$_2$

^{1}H NMR (400 MHz, $CDCl_3$) δ 7.78 (s, 4H), 3.77 (s, 8H), 1.56 (s, 6H), 1.02 (s, 8H).

^{13}C NMR (101 MHz, $CDCl_3$) δ 132.92, 72.30, 31.88, 21.92.

^{11}B NMR (128 MHz, $CDCl_3$) δ 26.89.

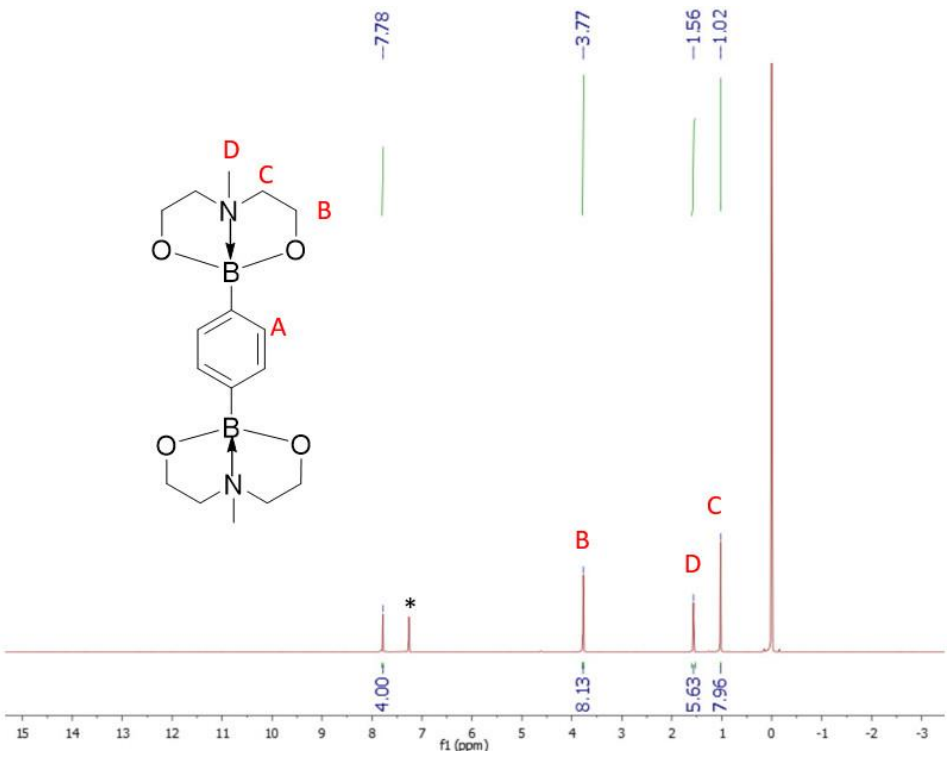

^{1}H NMR (400 MHz, $CDCl_3$, 298K) spectrum for **1,4-benzenediboronic acid bis-2,2'-(methylimino)diethanol ester**

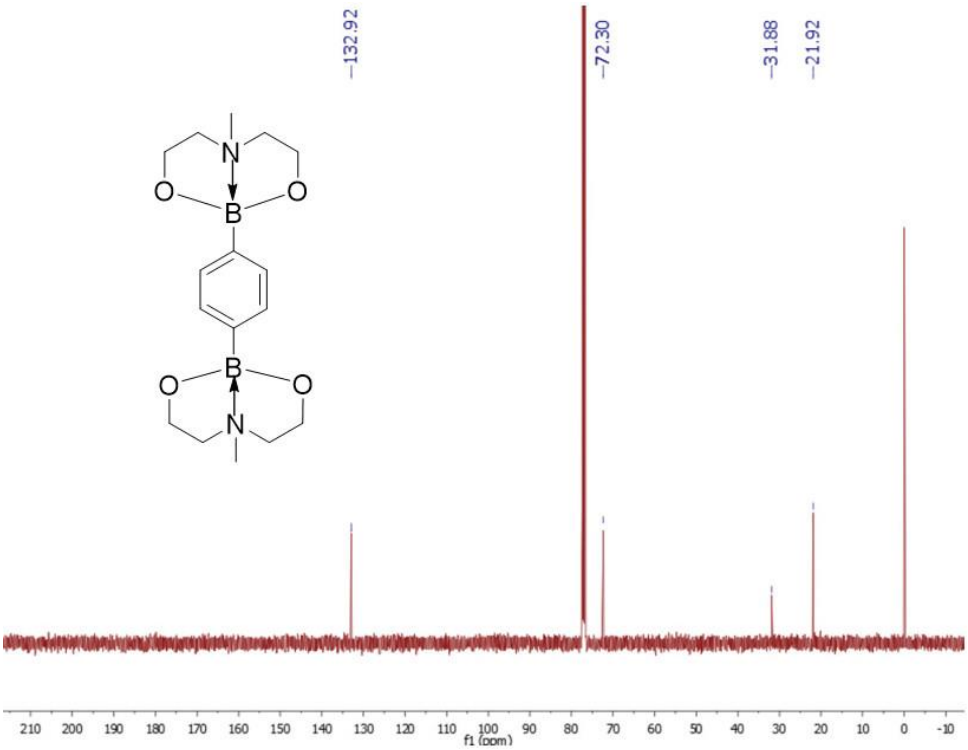

^{13}C NMR (101 MHz, $CDCl_3$, 298K) spectrum for **1,4-benzenediboronic acid bis-2,2'-(methylimino)diethanol ester**

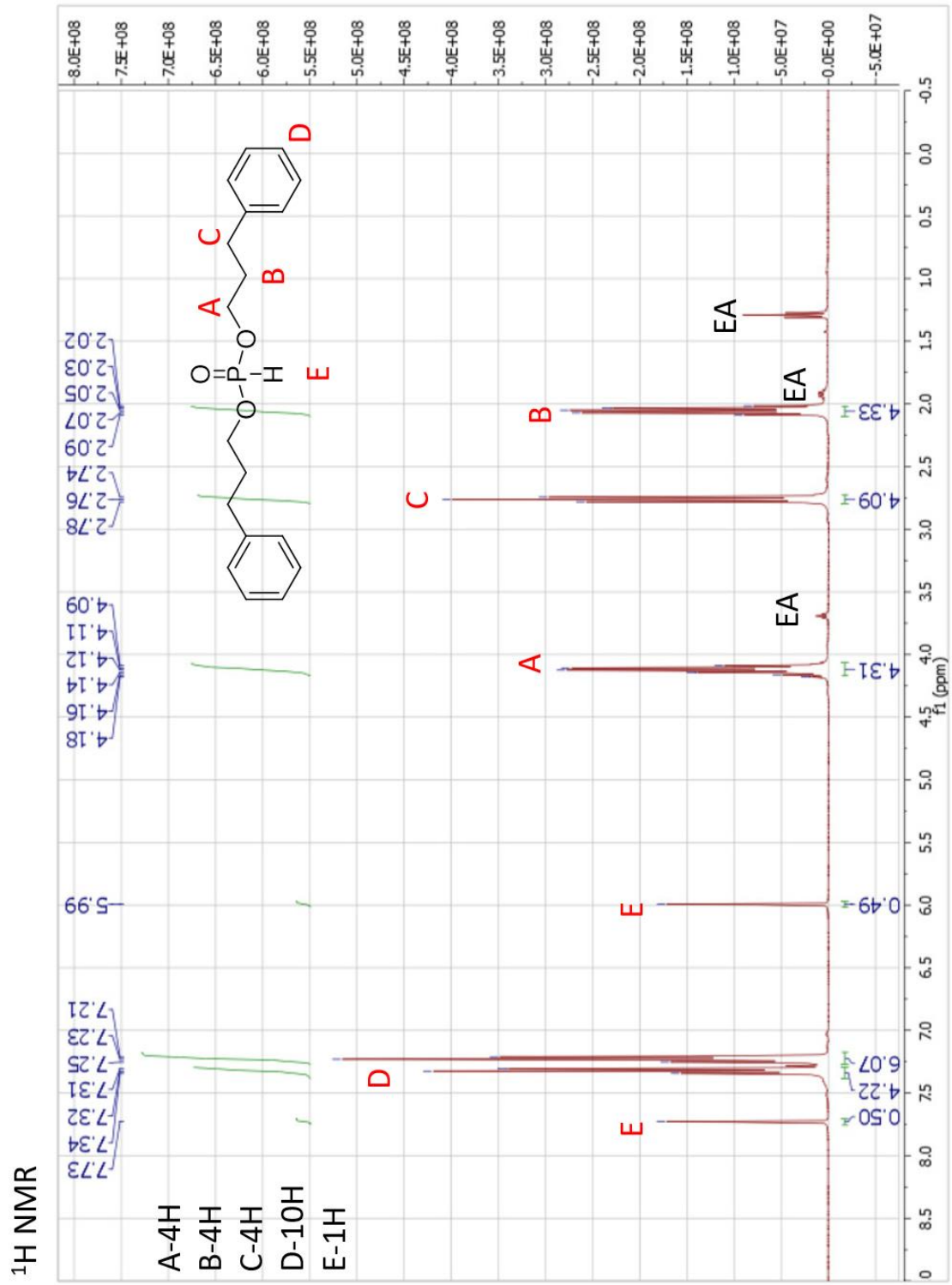
1H NMR
A-4H
B-4H
C-4H
D-10H
E-1H
7.73
7.34
7.32
7.31
7.25
7.23
7.21
5.99
4.18
4.16
4.14
4.12
4.11
4.09
2.78
2.76
2.74
2.09
2.07
2.05
2.03
2.02
A
B
C
D
E
EA
EA
EA
4.31
4.09
4.33
0.49
0.50
4.22
6.07
f1 (ppm)

^{31}P NMR

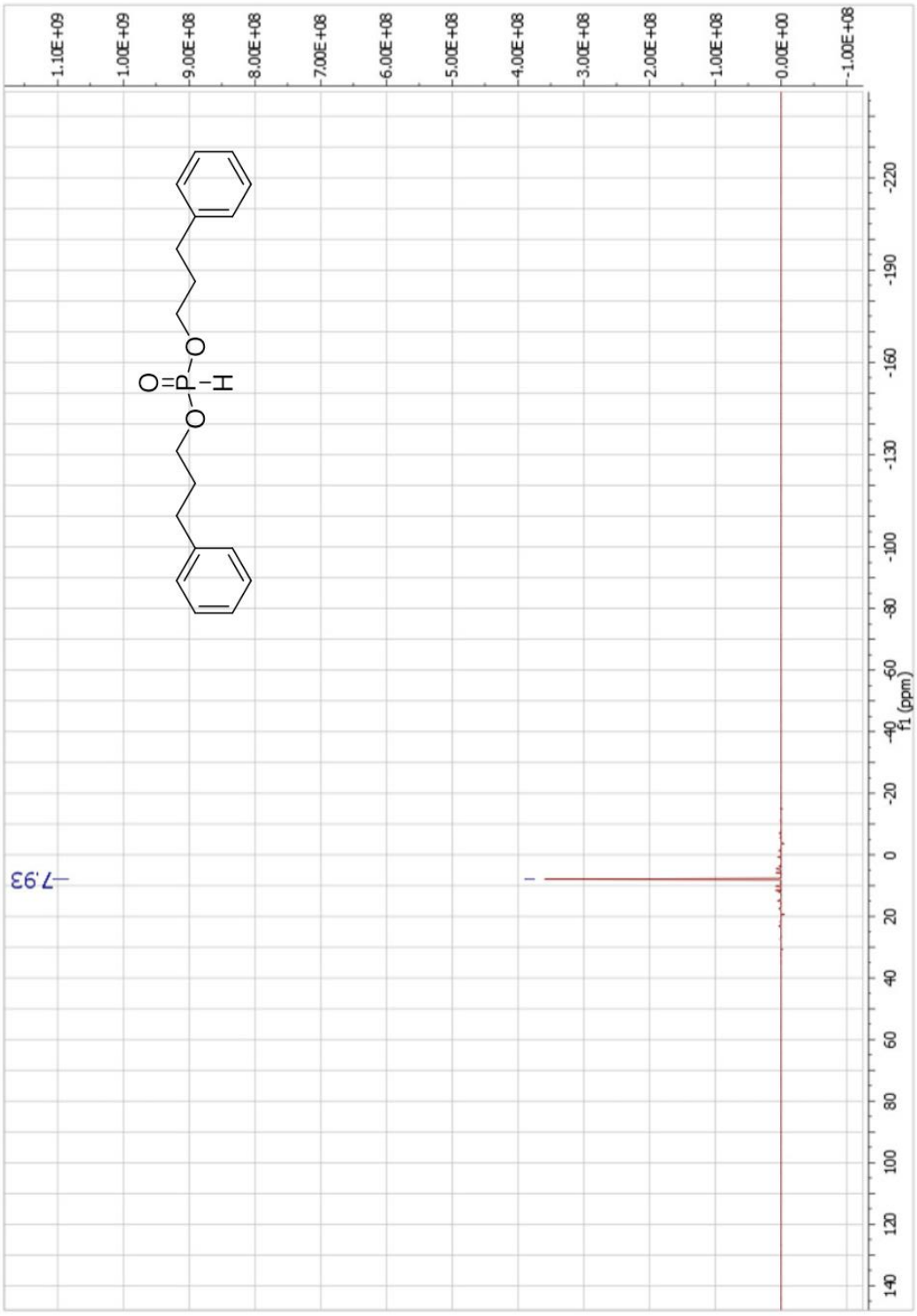

ESI-MS

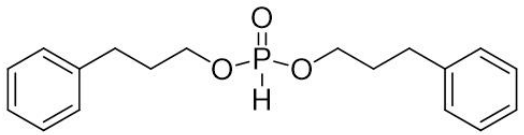

Mw=318.35
Mw(+Na)=341

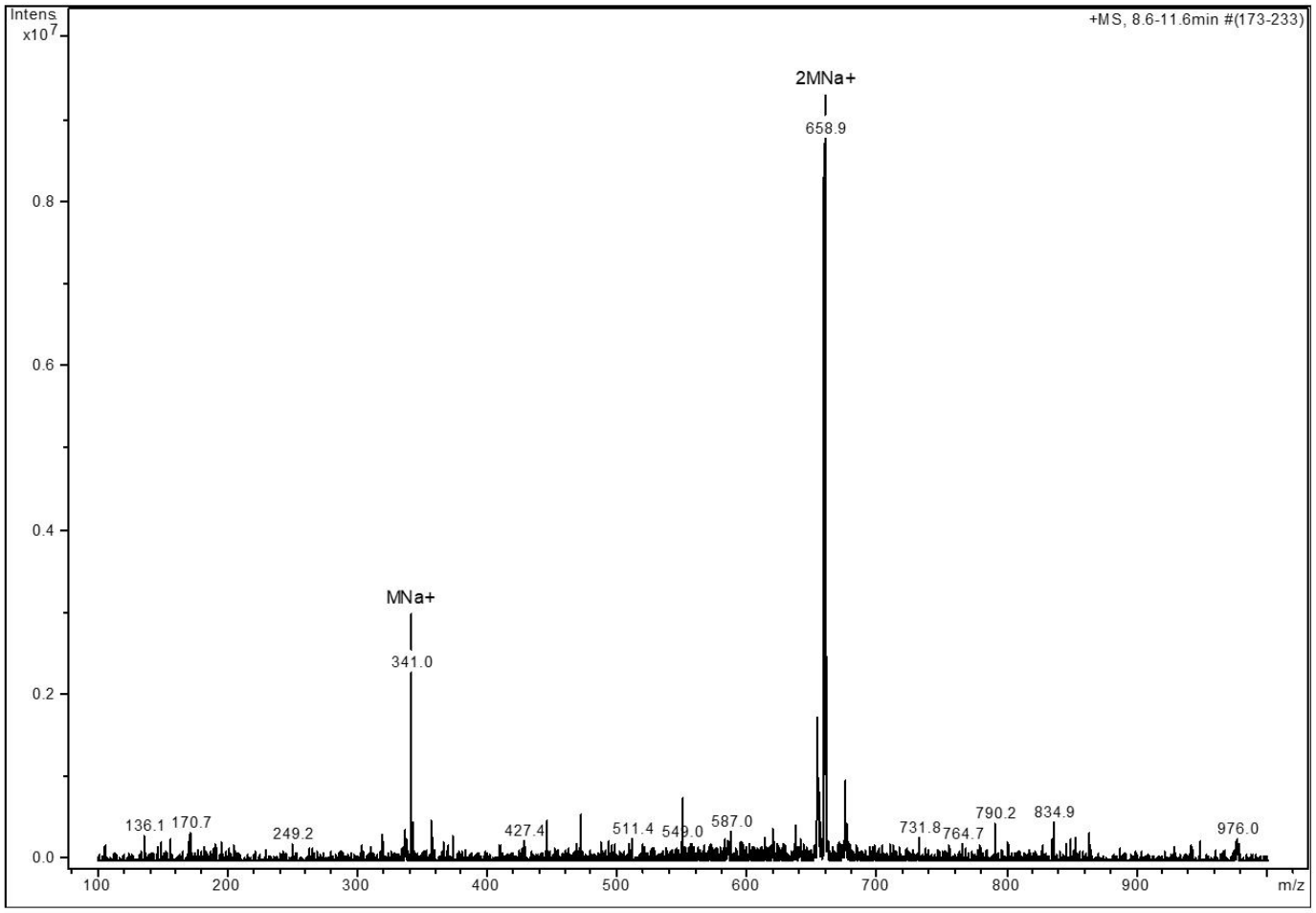

^{1}H NMR

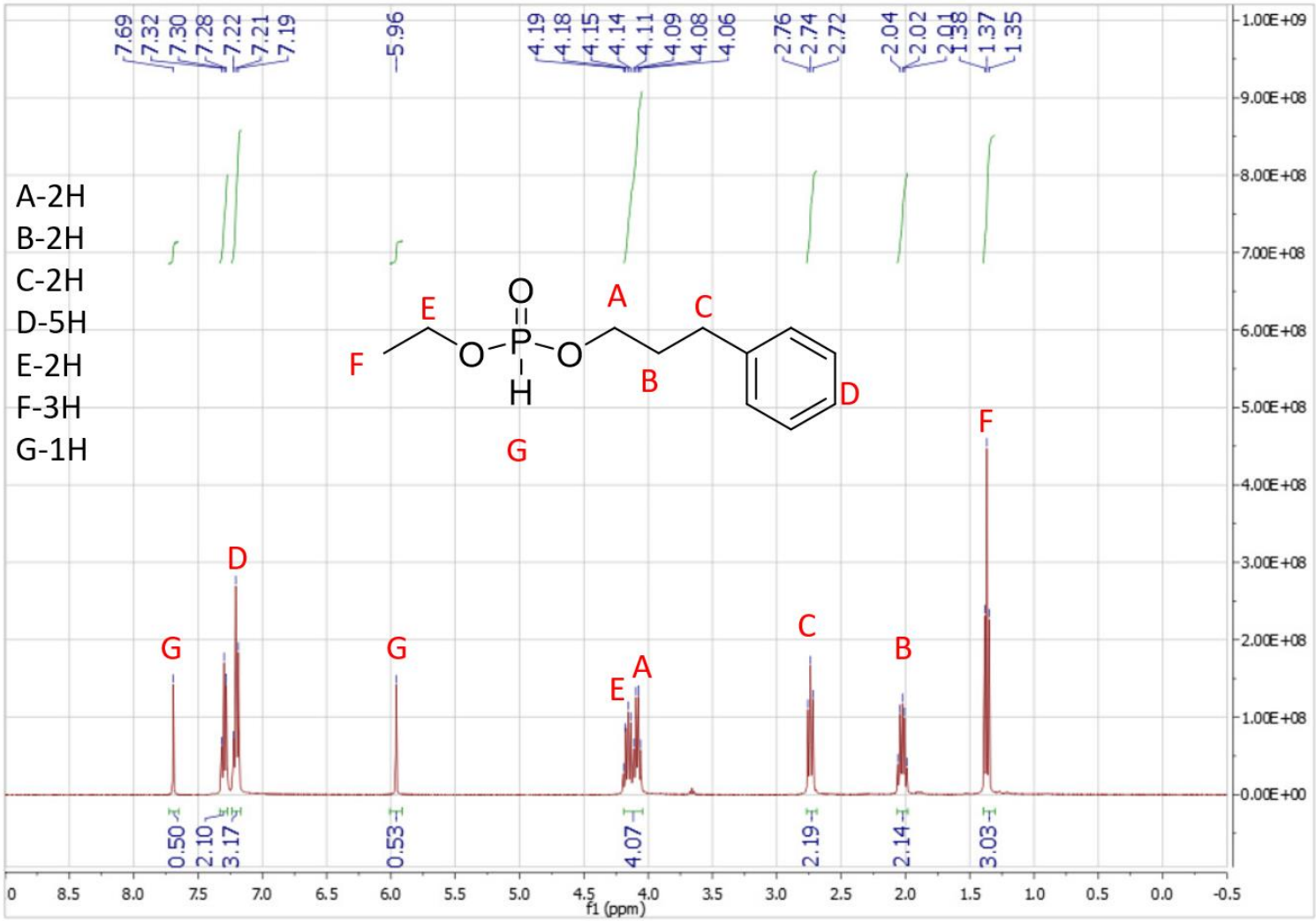
A-2H
B-2H
C-2H
D-5H
E-2H
F-3H
G-1H
7.69
7.32
7.30
7.28
7.22
7.21
7.19
5.96
4.19
4.18
4.15
4.14
4.11
4.09
4.08
4.06
2.76
2.74
2.72
2.04
2.02
2.01
1.38
1.37
1.35
f1 (ppm)

^{31}P NMR

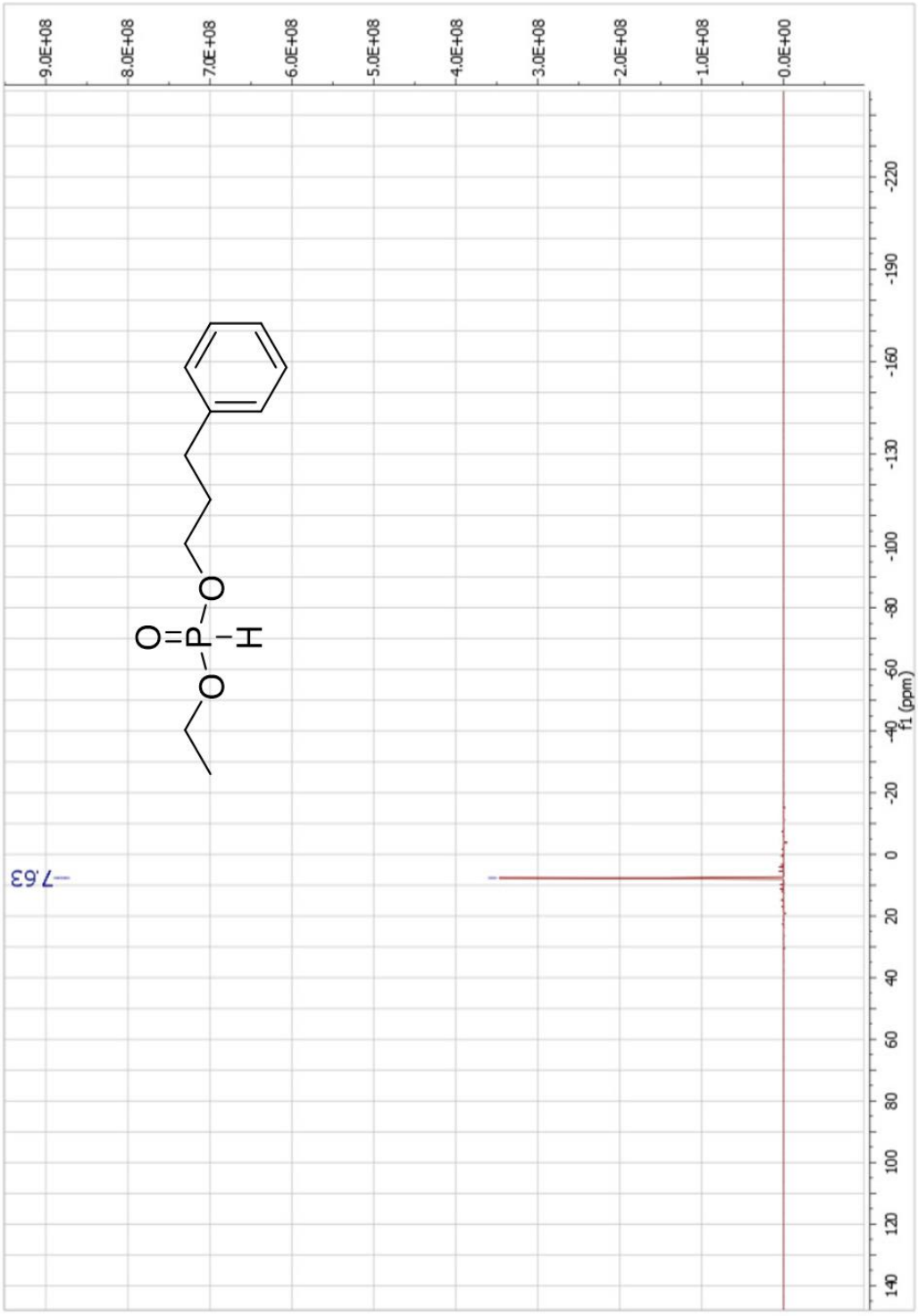

ESI-MS

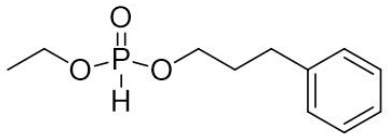

Mw=228.23
Mw(+H)=229